

SIMULATION OF STREAMFLOW USING HYDROLOGIC MODELING
SYSTEM HEC-HMS

A THESIS SUBMITTED TO
THE GRADUATE SCHOOL OF NATURAL AND APPLIED SCIENCES
OF
MIDDLE EAST TECHNICAL UNIVERSITY

BY

BERKAN ERŞAHİN

IN PARTIAL FULFILLMENT OF THE REQUIREMENTS
FOR
THE DEGREE OF MASTER OF SCIENCE
IN
EARTH SYSTEM SCIENCE

JANUARY 2020

Approval of the thesis:

**SIMULATION OF STREAMFLOW USING HYDROLOGIC MODELING
SYSTEM HEC-HMS**

submitted by **BERKAN ERŞAHİN** in partial fulfillment of the requirements for the degree of **Master of Science in Earth System Science Department, Middle East Technical University** by,

Prof. Dr. Halil Kalıpçılar
Dean, Graduate School of **Natural and Applied Sciences**

Prof. Dr. Bülent Akınoğlu
Head of Department, **Earth System Science**

Prof. Dr. Elçin Kentel Erdoğan
Supervisor, **Earth System Science, METU**

Prof. Dr. Zuhale Akyürek
Co-Supervisor, **Civil Engineering, METU**

Examining Committee Members:

Prof. Dr. İsmail Yücel
Civil Engineering, METU

Prof. Dr. Elçin Kentel Erdoğan
Earth System Science, METU

Prof. Dr. Zuhale Akyürek
Civil Engineering, METU

Prof. Dr. Ayşegül Aksoy
Environmental Engineering, METU

Assist. Prof. Dr. Meriç Yılmaz
Civil Engineering, Atılım University

Date: 30.01.2020

I hereby declare that all information in this document has been obtained and presented in accordance with academic rules and ethical conduct. I also declare that, as required by these rules and conduct, I have fully cited and referenced all material and results that are not original to this work.

Name, Surname: Berkan Erşahin

Signature:

ABSTRACT

SIMULATION OF STREAMFLOW USING HYDROLOGIC MODELING SYSTEM HEC-HMS

Erşahin, Berkan

Master of Science, Earth System Science

Supervisor: Prof. Dr. Elçin Kentel Erdoğan

Co-Supervisor: Prof. Dr. Zuhal Akyürek

January 2020, 132 pages

Basin models are fundamental for water resources assessment, analyzing quality and quantity of streamflow, managing water distribution systems, protecting and developing groundwater systems, flood protection, and water-supply forecasting. The integration of all hydrologic processes with their interconnections to each other at the basin scale is required for basin models. Mathematical basin models such as HEC-HMS are used for simulating hydrological processes in basin-scale to understand basin response to storm events. The goal of this study is to test the applicability of the HEC-HMS model for a basin located in Turkey and to demonstrate the importance of snowmelt especially for snow affected areas, such as Çakıt Basin which is the study area of this thesis. Requirements of event-based and continuous simulations are identified to guide future HEC-HMS applications in Turkey. Çakıt Basin, which is located in Niğde province has a drainage area of 518 km². Meteorological data, flow data, digital elevation model, land use/land cover map and soil properties are collected and used in building event-based and continuous models. The models are calibrated and validated with observation stations constructed within the scope of 115Y041 TUBITAK project. The results of this study showed that streamflow at Çakıt Stream Gage Station, both for event-based and continuous runs, can be estimated realistically

with NSE values higher than 0.6 for the validation periods using HEC-HMS. Furthermore, the importance of integration of the snowmelt into the hydrologic models is demonstrated.

Keywords: HEC-HMS, Çakıt Basin, Snowmelt, Event-based Model, Continuous Model

ÖZ

HİDROLOJİK MODELLEME SİSTEMİ HEC-HMS KULLANILARAK AKIŞ DEBİSİNİN SİMÜLASYONU

Erşahin, Berkan
Yüksek Lisans, Yer Sistem Bilimleri
Tez Danışmanı: Prof. Dr. Elçin Kentel Erdoğan
Ortak Tez Danışmanı: Prof. Dr. Zuhâl Akyürek

Ocak 2020, 132 sayfa

Havza modelleri su kaynaklarını değerlendirmek, su kalitesini ve miktarını analiz etmek, yer altı suyu sistemlerini korumak ve geliştirmek, su dağıtım sistemlerini yönetmek, taşkın koruması ve su temini tahminleri için oldukça önemlidir. Havza modelleri için, havza ölçeğinde bütün hidrolojik proseslerin ve birbirleriyle ilişkilerinin entegre edilmesi gereklidir. HEC-HMS gibi matematiksel havza modelleri havza ölçeğinde yağış olaylarına havzanın tepkisini simüle etmek için kullanılmaktadır. Yağış olaylarının havzada oluşan karşılığını havza ölçeğinde hidrolojik parametreleri entegre ederek anlamak için matematiksel havza modelleri kullanılır. Bu çalışmanın amacı HEC-HMS modelinin Türkiye'deki havzalarda uygulanabilirliğini test etmek ve özellikle bu tezinde çalışma alanı olarak seçilen, Çakıt Havzası gibi kar etkisi altında kalan alanlarda kar erimesi modelinin önemini göstermektedir. Olay eksenli ve kesintisiz modellerin gereksinimleri Türkiye'de HEC-HMS ile yapılacak çalışmalara yol göstermesi için tanımlanmıştır. Niğde ilinde bulunan Çakıt Havzası 518 km² drenaj alanına sahiptir. Olay eksenli ve kesintisiz modelleri oluşturmak için meteorolojik veriler, akış verileri, dijital yükseklik modeli (DEM), arazi kullanımı / arazi örtüsü (LULC) haritası ve toprak özellikleri bilgileri toplanmıştır. Oluşturulan modeller 115Y041 TÜBİTAK projesi kapsamında inşa

edilen gözlem istasyonları ile kalibre edilip doğrulanmıştır. Bu çalışmanın sonuçları Çakıt akım ölçüm istasyonunda ölçülen akım değerlerinin hem olay eksenli model hem de kesintisiz model için doğrulama sürecinde elde edilen 0.6 üstünde NSE değerleri ile gerçekçi bir şekilde tahmin edilebileceğini göstermiştir. Bunun yanında kar erimesinin de hidrolojik modele dahil edilmesinin önemi gösterilmiştir.

Anahtar Kelimeler: HEC-HMS, Çakıt Havzası, Kar Erimesi, Olay Eksenli Model, Kesintisiz Model

To my family

ACKNOWLEDGEMENTS

I would like to express my gratitude to a few people for their support and guidance during my thesis study. To begin with, I would like to thank to my advisors Prof. Dr. Elçin Kentel Erdoğan and Prof. Dr. Zuhale Akyürek for sharing their experiences with valuable feedbacks and suggestions on this thesis.

I would also like to express my gratitude to my family for their support. I would like to thank my dear wife Nilay Ercan Erşahin for supporting and motivating me for the whole time.

Finally, I gratefully acknowledge the financial support provided by the Scientific and Technological Research Council of Turkey (TÜBİTAK) through the project entitled 'Hydrological Cycle Parameter Estimation with Conceptual Hydrological Model' with project number 115Y041.

TABLE OF CONTENTS

ABSTRACT	v
ÖZ	vii
ACKNOWLEDGEMENTS	x
TABLE OF CONTENTS	xi
LIST OF TABLES	xiv
LIST OF FIGURES	xvi
LIST OF ABBREVIATIONS	xx
CHAPTERS	
1. INTRODUCTION	1
2. LITERATURE REVIEW	3
2.1. HEC-HMS	6
2.2. HEC-HMS Applications.....	8
2.3. Performance Evaluation	14
3. HEC-HMS MODELING	17
3.1. Preprocessing.....	20
3.2. Model Setup	22
3.2.1. Basin model	22
3.2.1.1. “Soil Conservation Service Curve Number” Loss Method	22
3.2.1.2. “Deficit and Constant” Loss Method	24
3.2.1.3. “Soil Conservation Service Unit Hydrograph” Runoff Transform Method	25
3.2.1.4. “Recession” Baseflow Method	26

3.2.1.5. “Muskingum” Routing Method	26
3.2.2. Meteorological Model	27
3.2.3. Data Input	29
3.2.4. Control Specifications	29
3.2.5. Model Calibration and Validation	29
4. CASE STUDIES	31
4.1. Study Area.....	31
4.1.1. Climate	33
4.1.1.1. Temperature	33
4.1.1.2. Precipitation	34
4.1.1.3. Relative Humidity and Wind	35
4.1.2. Topography, geology and soil information	36
4.1.3. Land Use.....	37
4.1.4. Soil Properties	38
4.2. Preprocessing	43
4.3. Case 1 - Event-based Model Setup	44
4.4. Case 2 - Continuous Model Setup.....	52
4.5. Case 3 - Continuous Model without Snowmelt Setup	56
5. RESULTS OF CALIBRATION AND VALIDATION OF CASE STUDIES ..	59
5.1. Case 1 - Event-based Model Results.....	59
5.2. Case 2 - Continuous Model Results	63
5.3. Case 3 - Continuous Model without Snowmelt Results	73
5.4. Comparison of Case 1 and Case 2	77
5.5. Comparison of Case 2 and Case 3	78

5.6. Comparison of Low and High Flows	85
5.7. Sensitivity Analysis	86
5.7.1. Event-based Model Sensitivity	86
5.7.2. Continuous Model Sensitivity	90
6. CONCLUSIONS	95
REFERENCES.....	97
APPENDICES	107
A. DATA USED IN GENERATING CN	107
B. SNOWMELT METHOD PARAMETER DEFINITIONS.....	113
C. PREPROCESSING STEPS	116

LIST OF TABLES

TABLES

Table 2.1. Selected event-based HEC-HMS applications	9
Table 2.2. Selected continuous HEC-HMS applications	12
Table 2.3. Performance evaluation criteria for basin-scale models (Moriassi, Gitau, Pai, & Daggupati, 2015)	16
Table 3.1. List of selected HEC-HMS methods	18
Table 3.2. List of selected meteorological model methods	19
Table 4.1. List of stream gauge stations in the study area	32
Table 4.2. List of weather stations in the study area	32
Table 4.3. Long term average monthly temperature (°C) (Akyürek, et al., 2019).....	34
Table 4.4. Long term average monthly precipitation (mm) (Akyürek, et al., 2019) .	35
Table 4.5. Long term average monthly relative humidity (Akyürek, et al., 2019)...	35
Table 4.6. List of great soil groups in the study area.....	39
Table 4.7. List of erosion degrees and depth levels (FAO, 2013)	40
Table 4.8. Hydrological soil group definition chart (Kızılkaya, 1983)	42
Table 4.9. Event-based model specifications	44
Table 4.10. Distributed curve numbers according to CORINE system.....	45
Table 4.11. Weighted curve numbers for each sub-basin.....	47
Table 4.12. Required inputs and calibrated parameters of used methods in event-based model	50
Table 4.13. Calibrated parameters used in the event-based model.....	51
Table 4.14. Calibrated routing parameters used in the event-based model	51
Table 4.15. Continuous model specifications.....	52
Table 4.16. Initial values used for snowmelt inputs of the continuous model	53
Table 4.17. Required inputs and calibrated parameters of used methods in the event-based model	54
Table 4.18. Calibrated parameters used in the continuous model	55

Table 4.19. Calibrated routing and snowmelt parameters used in the continuous model	56
Table 4.20. Continuous model without snowmelt specifications	56
Table 5.1. Result for comparison of low and high flows	85
Table 5.2. Results of sensitivity analysis for event-based model	88
Table 5.3. Results of sensitivity analysis for continuous model	91
Table A.1. Hydrological soil types (USDA, 2007).....	107
Table A.2. CORINE Land Cover (CLC) nomenclature (Büttner, Soukup, & Kosztra, 2012)	107
Table A.3. Runoff curve numbers for urban areas (USDA, 1986)	109
Table A.4. Runoff curve numbers for cultivated agricultural lands (USDA, 1986)	110
Table A.5. Runoff curve numbers for other agricultural lands (USDA, 1986)	111
Table A.6. Runoff curve numbers for arid and semiarid rangelands (USDA, 1986)	112

LIST OF FIGURES

FIGURES

Figure 2.1. A simplified diagram of the hydrological cycle (ESRI, 2015)	4
Figure 2.2. Overview of HEC-HMS simulation for hydrological processes (USACE, 2000).....	7
Figure 3.1. HEC-HMS model structure	19
Figure 3.2. Overview of the relation between HEC-GeoHMS and HEC-HMS (USACE, 2000).....	20
Figure 3.3. Flow chart of preprocessing with HEC-GeoHMS (USACE, 2013).....	21
Figure 3.4. “Deficit and Constant” method representation.....	25
Figure 3.5. Snowmelt algorithm of “Temperature Index” method (USACE, 2010).	28
Figure 3.6. Schematic of calibration procedure (USACE, 2000)	30
Figure 4.1. Location of gauging stations in the study area	33
Figure 4.2. The annual average temperature (°C) (Akyürek, et al., 2019)	34
Figure 4.3. The annual precipitation values (mm) (Akyürek, et al., 2019)	35
Figure 4.4. Upwind direction densities (Akyürek, et al., 2019)	36
Figure 4.5. The hypsometric curve of the study area	37
Figure 4.6. The hypsometric curve of the Darboğaz Basin	37
Figure 4.7. Land use in the study area (Corine, 2012)	38
Figure 4.8. Great soil types in the study area (National Soil Database, 2017).....	39
Figure 4.9. Erosion degrees of the soil in the study area (National Soil Database, 2017)	40
Figure 4.10. Depth levels of the soil in the study area (National Soil Database, 2017)	41
Figure 4.11. Hydrological soil groups in study area.....	42
Figure 4.12. The sub-basins of study area after preprocessing in HEC-GeoHMS....	44
Figure 4.13. Curve number map of the study area	46
Figure 4.14. Storm event observed in between 17 May 2018 and 23 May 2018	49
Figure 4.15. Storm events observed in between 1 March 2017 and 1 May 2017	49

Figure 5.1. Event-based model calibration for Çakıt SGS between 7 April, 2018 and 13 April, 2018	60
Figure 5.2. Event-based model validation for Çakıt SGS between 28 May, 2018 and 5 June, 2018	61
Figure 5.3. Scatter plot for event-based model calibration for Çakıt SGS in between 7 April, 2018 and 13 April, 2018	62
Figure 5.4. Scatter plot for event-based model validation for Çakıt SGS in between 28 May, 2018 and 5 June, 2018	62
Figure 5.5. Continuous model calibration for Çakıt SGS between 9 September, 2016 and 30 September, 2018.....	65
Figure 5.6. Continuous model calibration for Darboğaz SGS between 9 September, 2016 and 30 September, 2018.....	66
Figure 5.7. Continuous model validation for Çakıt SGS between 1 October, 2018 and 1 July, 2019.....	68
Figure 5.8. Continuous model validation for Darboğaz SGS between 1 October, 2018 and 1 July, 2019	69
Figure 5.9. Comparison of simulated and observed SWE	71
Figure 5.10. Observed temperature and precipitation values between 9 September, 2016 and 1 July, 2019	72
Figure 5.11. Results of continuous model without snowmelt for Çakıt SGS between 9 September, 2016 and 30 September, 2018.....	74
Figure 5.12. Results of continuous model without snowmelt for Çakıt SGS between 1 October, 2018 and 1 July, 2019	76
Figure 5.13. Daily total volume comparison of Case 1 and Case 2 between 7 April, 2018 and 13 April, 2018	77
Figure 5.14. Daily total volume comparison of Case 1 and Case 2 between 28 May, 2018 and 5 June, 2018.....	78
Figure 5.15. Percent errors in between 9 September, 2016 and 9 May, 2017	79
Figure 5.16. Percent errors in between 10 May, 2017 and 30 September, 2017	80
Figure 5.17. Percent errors in between 1 October, 2017 and 10 May, 2018.....	80

Figure 5.18. Percent errors in between 11 May, 2018 and 30 September, 2018.....	81
Figure 5.19. Percent errors in between 1 October, 2018 and 9 May, 2019	81
Figure 5.20. Percent errors in between 10 May, 2019 and 1 June, 2019.....	82
Figure 5.21. Comparison of Case 2 and Case 3 for Çakıt SGS between 9 September, 2016 and 30 September, 2018	83
Figure 5.22. Comparison of Case 2 and Case 3 for Çakıt SGS between 1 October, 2018 and 1 July, 2019.....	84
Figure 5.23. Nash-Sutcliffe Efficiency of sensitivity analysis for event-based model parameters.....	89
Figure 5.24. Nash-Sutcliffe Efficiency of sensitivity analysis for continuous model parameters.....	93
Figure C.1. Fill Sinks command in HEC-GeoHMS (USACE, 2013)	116
Figure C.2. DEM of the study area after applying the Fill Sinks command in HEC-GeoHMS.....	117
Figure C.3. Flow direction command in HEC-GeoHMS (USACE, 2013)	118
Figure C.4. The study area after applying the Flow Directions command in HEC-GeoHMS	119
Figure C.5. Flow accumulation command in HEC-GeoHMS (USACE, 2013)	120
Figure C.6. The study area after applying the Flow Accumulation command in HEC-GeoHMS	120
Figure C.7. Flow accumulation command in HEC-GeoHMS (USACE, 2013)	121
Figure C.8. Streams of the study area after applying the Stream Definition command in HEC-GeoHMS with a threshold of 25 km ²	122
Figure C.9. Stream Segmentation command in HEC-GeoHMS (USACE, 2013)...	123
Figure C.10. The study area after applying Stream Segmentation command in HEC-GeoHMS	123
Figure C.11. The study area after applying the Catchment Grid Delineation command in HEC-GeoHMS.....	124
Figure C.12. The study area after applying the Catchment Polygon Processing command in HEC-GeoHMS	125

Figure C.13. The study area after applying Drainage Line Processing command in HEC-GeoHMS	126
Figure C.14. The study area after applying Drainage Point Processing command in HEC-GeoHMS	127
Figure C.15. The study area after applying Slope command in HEC-GeoHMS	128
Figure C.16. The study area after applying Basin Processing commands in HEC-GeoHMS	129
Figure C.17. The study area after applying Characteristic commands in HEC-GeoHMS	130
Figure C.18. The study area after applying Parameter commands in HEC-GeoHMS	131
Figure C.19. The study area after preprocessing in HEC-GeoHMS	132

LIST OF ABBREVIATIONS

°C	Degrees Celsius
CN	Curve Number
CORINE	Copernicus Land Monitoring Service
DEM	Digital Elevation Model
DSİ	State Hydraulic Works
ESRI	Environmental Systems Research Institute
FAO	Food and Agriculture Organization of the United Nations
GIS	Geographic Information System
HEC	Hydrologic Engineering Center
LBRM	Large Basin Runoff Model
LULC	Land Use & Land Cover
LWASS	Liquid Water Available at The Soil Surface
NSE	Nash-Sutcliffe Efficiency
PBIAS	Percent Bias
PFR	Peak Rate Factor
RMSE	Root Mean Square Error
r	Correlation
R ²	Coefficient of Determination
SCS	Soil Conservation Service
SGS	Stream Gage Station
SMS	State Meteorological Service
SWE	Snow Water Equivalent
TUBITAK	The Scientific and Technological Research Council of Turkey
UH	Unit Hydrograph
USACE	US Army Corps of Engineers
USDA	United States Department of Agriculture
WS	Weather Station

CHAPTER 1

INTRODUCTION

Water resources management in basins becomes more critical with the increasing demand for limited water resources and due to the lack of ability to preserve and manage the available rainwater in a sustainable manner. It is essential to understand and qualify hydrological processes for a better understanding of rainfall-runoff relation. The amount of surface runoff is influenced by soil properties, land use, topography, vegetation, climate, storm properties such as rainfall duration, amount, and intensity and basin size. The integration of all hydrologic processes with their interconnections to each other at the basin scale is required in order to determine the basin response to rainfall. Mathematical basin models are tools used to accomplish this integrating.

Basin models are fundamental for water resources assessment, analyzing quality and quantity of streamflow, protecting and developing groundwater systems, managing water distribution systems, flood protection, and water-supply forecasting. Different techniques of hydrological modeling have been adopted through various software in different studies based on the purposes and data availability. HEC-HMS is one of that software which has become very popular and extensively used in hydrological studies in different parts of the world for estimating streamflow. This software is developed by the US Army Corps of Engineers Hydrologic Engineering Center (USACE, 2018) to simulate the streamflow with a graphical interface.

HEC-HMS has been tested and calibrated for many basins on a global scale, however, there are not many studies conducted in Turkey. Utilization and development of hydrological models for planning and management purposes are new for our country; thus, there are limited number of applications. This study is conducted to test the

applicability of the HEC-HMS model for a basin located in Turkey and to understand importance of snowmelt method for snow affected areas. Other goals of this study are to understand parameter selection for the HEC-HMS model setup and investigate requirements of event-based and continuous simulations. The study is expected to provide guidance for basin modeling with HEC-HMS software, both for event-based and continuous simulations. Data requirements are highlighted, so the findings of this study may shed light on development of hydrological models for other basins in Turkey.

The thesis is organized as follows. Chapter 2 presents a literature review for HEC-HMS software, HEC-HMS applications and performance evaluation for basin models. In Chapter 3, modeling methodology is provided, and mechanisms used for simulating hydrological processes are explained. In Chapter 4, the study area is introduced, and applied methodology for the model setup is given. Moreover, case studies, one for event-based, one for continuous simulations and one for continuous simulation without snowmelt, is demonstrated, and finally, results are given in Chapter 5. In Chapter 6, the conclusion of the study is presented with the major findings.

CHAPTER 2

LITERATURE REVIEW

The amount of freshwater available for the use of humans and other living things in the world is limited. Today, securing the quantity and quality of this natural asset has become essential due to climate change, increasing population, and urbanization. Additionally, the public has become more sensitive to water resources related problems while the water demand has been increasing parallel to the rapidly developing world. This sensitivity led to a systematic review of all activities related to the management of water resources. Management of water resources requires complementary hydrological studies for efficient management and for determining the amount of water that will be available in the following years.

It is essential to understand and qualify hydrological processes for a better understanding of rainfall-runoff correlation. Direct precipitation, runoff, and baseflow compose streamflow. A combination of saturation excess and infiltration excess mechanisms generates runoff. Saturation excess occurs when the soil becomes fully saturated with water, and infiltration excess occurs when rainfall intensity exceeds the maximum rate that water can infiltrate into the soil (Yang, Li, Sun, & Ni, 2015). Even when there is no runoff or precipitation baseflow exists in the stream channels. A simplified diagram of the hydrological cycle is presented in Figure 2.1.

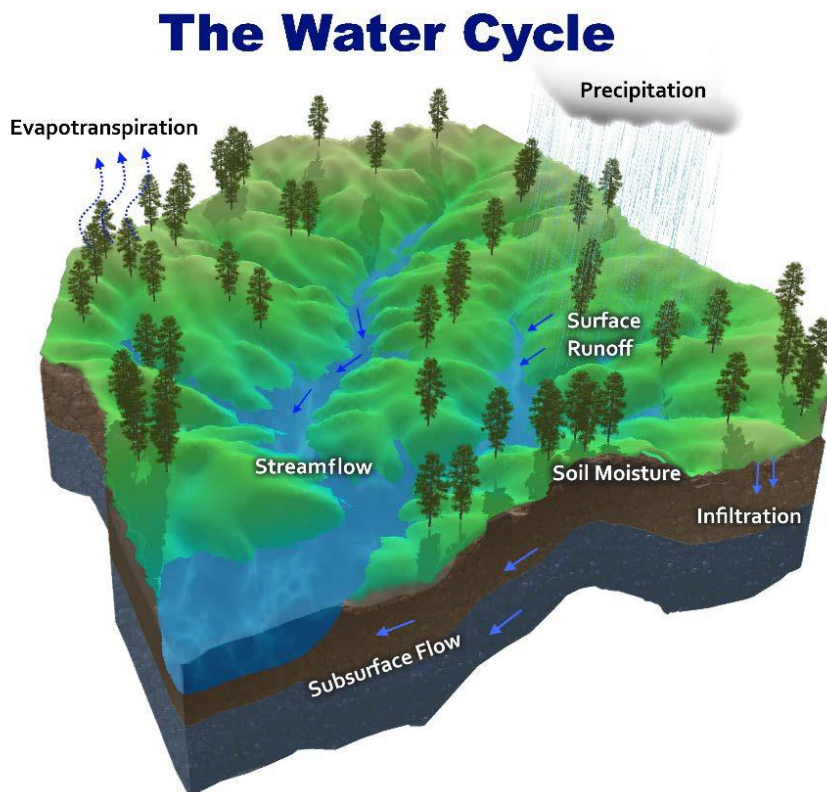


Figure 2.1. A simplified diagram of the hydrological cycle (ESRI, 2015)

A basin model simulates hydrologic processes of this cycle in a holistic approach. Therefore, basin-scaled modeling of waterbodies has great importance for a better understanding of the future of water resources and to create solutions for problems caused by changes in the amount of water. Various models are used to estimate the physical parameters of the basin and streamflow.

Numerous basin models are developed since the 1960s. Stanford Watershed Model-SWM by Crawford and Linsley (1966) was the first attempt to integrate multiple components of hydrological processes to create a virtual basin. Simultaneously, other models are developed by Dawdy and O'Donnell (1965) and HEC-1 Hydrologic Engineering Center (1968). In the following years, with revolutions of numerical simulation and statistical simulation and with developed computer technologies, the number of basin models rapidly increased. Today with the employment of GIS, remote

sensing techniques, and database management systems, basin models are much more powerful, and models continue to be developed and improved (Singh & Woolhiser, 2002).

Basin -scale models can be classified according to the modeling approaches used. One of the most critical classifications is based on the type: empirical models, conceptual models, and physically-based models (Sitterson, et al., 2017). Empirical models are data-driven models, and they involve mathematical equations that define the functional relationships between inputs and outputs by using regression and correlation models whereas conceptual models consist of linked reservoirs, which represent physical elements in a basin and hydrological processes by using semi-empirical equations. On the other hand, physical models are based on spatial distribution and evaluation of parameters describing physical characteristics (Devia, Ganasri, & Dwarakish, 2015). Basin-scale models can further be classified as lumped, semi-distributed, or distributed models. The lumped models simplify basin parameters into a single unit, whereas semi-distributed and distributed models include spatial variability of processes, boundaries, and characteristics of the basin (Daniel, et al., 2011).

Models can also be classified as deterministic or stochastic. The stochastic model can produce different outputs for a single set of inputs, whereas the deterministic model will give a single output. Deterministic models obtain outputs by known mathematical relations, whereas stochastic models obtain a range of outputs by inputs that are statistically distributed (Melone, et al., 2005). Another classification can be based on whether the model includes time or not. Sorooshian et al. (2007) had classified models as an event-based model in which output is produced for specific periods and as a continuous model in which output is produced for long term continuous periods. An event-based hydrological model focuses on revealing basins response to an individual storm event in a finer-scale, whereas a continuous hydrological model reveals both hydrological processes and the cumulative effect of several storm events over a more extended period with both wet and dry conditions (Chu & Steinman, 2009). The main

difference between these models is that evapotranspiration and groundwater seepage may be ignored in the event-based model, but the continuous model should include these processes for better reflection of soil drying (Scharffenberg, 2008). The coarse-scale continuous models will require bigger datasets when compared with the fine-scale event-based models (Chu & Steinman, 2009).

Software tool selection for basin modeling should be made according to the selected modeling approaches. Input and output requirements, model capabilities, spatial scales, and accuracy of the model should be considered (Singh & Frevert, 2006). The Hydrologic Engineering Center Hydrologic Modelling System (HEC-HMS) is selected for modeling applications that are presented in this study due to data availability, model capabilities, and ease of application.

2.1. HEC-HMS

The Hydrologic Modeling System (HEC-HMS) is a reliable model designed by the US Army Corps of Engineers in 1998 to simulate hydrological processes in basin systems (USACE, 2018). HEC-HMS is capable of simulating precipitation-runoff and routing hydrologic processes, and it can be classified as a deterministic, semi-distributed model that includes both conceptual and empirical methods. The program is a modeling system capable of representing different types of basins. HEC-HMS is a popular software among hydrological studies as it can simulate both short and longtime events and can be used within large or small, urban or natural basins (Halwatura & Najim, 2013; Verma, Jha, & Mahana, 2010). A model can be applied for the management of integrated water resources in basins and for estimating flood peaks in flood forecasting. It is also suitable for continuous analysis with capabilities for calculating evapotranspiration, snowmelt, and soil moisture accounting (USACE, 2010).

Moreover, the special extension of the HEC-HMS, which is called HEC-GeoHMS, can be used to import spatial data of the study area (Ali, Khan, Aslam, & Khan, 2011). Different methods can be selected based on existing data and study area

characteristics. Commonly, starting from the most upstream sub-catchments the sub-basin hydrographs are formed and routed. After the selection of methods, HEC-HMS creates consistent and reliable simulation results for runoff volume and peak values, which can be compared with observational data.

The development of the hydrological processes is critical in modeling applications. A considerable portion of the precipitation returns to the atmosphere through evapotranspiration. Evapotranspiration occurs from vegetation, land surface, and water bodies. On the other hand, some of the precipitation that falls on vegetation, before evaporating, falls through the leaves or runs down stems and branches, and reaches the soil. Moreover, some of the precipitation may infiltrate to the ground from land surfaces and water bodies. A model of the study area is developed by separating this complex hydrological cycle into manageable pieces. HEC-HMS represents any mass or flux with a mathematical model. HEC-HMS simulates the main mechanisms and connections between processes to calculate water balance (USACE, 2000). Figure 2.2 represents the hydrological processes used in HEC-HMS and inter-relations among them.

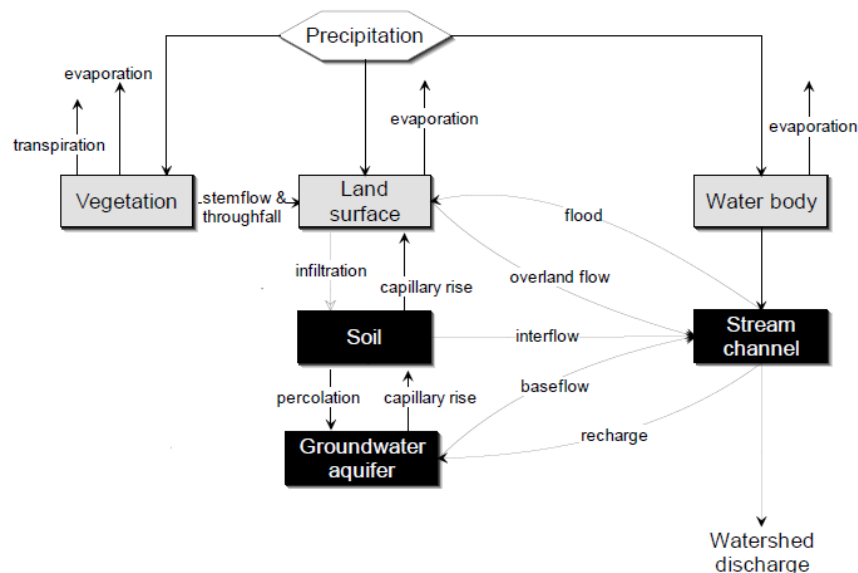


Figure 2.2. Overview of HEC-HMS simulation for hydrological processes (USACE, 2000)

HEC-HMS model provides optional methods for each of these process components, which can be categorized according to the modeling approach. Options for runoff-volume (loss) methods include Initial and Constant, SCS-CN, Gridded SCS-CN, etc. while direct-runoff (transform) methods include User-specified Unit Hydrograph, Clark's UH, Kinematic Wave, etc. Moreover, three different baseflow methods five different routing methods are provided in HEC-HMS. The details of these methods can be found in User's Manual of USACE (2018). A meteorological model to reflect precipitation, snowmelt, and evapotranspiration is also created in HEC-HMS. It is suggested in User's Manual of USACE (2018) that snowmelt can be optionally included according to the meteorological conditions of the study area, whereas evapotranspiration should be included if a continuous model is developed. For a short duration rainfall event evapotranspiration can be ignored (Knebl, Yang, Hutchison, & Maidment, 2005). HEC-HMS provides various options for meteorological processes. For example, Frequency Storm, Gage Weights and SCS Storm in addition to others are suggested for precipitation. For evapotranspiration, Annual Evaporation, Monthly Average, etc. are suggested; while for snowmelt, Temperature Index (TI) and Gridded TI are the alternatives.

2.2. HEC-HMS Applications

HEC-HMS models had been tested and calibrated for many basins all over the world. Studies are conducted to test the applicability of HEC-HMS models, which use different combinations of methods. Hydrological processes occur in basins such as precipitation, infiltration, and evapotranspiration, depending on land cover, size, topography, types of soils, and rocks (Deng, Zhang, Li, & Pan, 2015; Zare, Samani, & Mohammady, 2016; Chen, et al., 2016). Researchers who developed models in different areas with different methods obtained satisfactory results and used their models to study land-use changes, deforestation, climate change effects, flood risk assessment, future predictions, model comparison, and tool development. Some applications of the software, together with the methods used, are given for the event-based approach in Table 2.1.

Table 2.1. Selected event-based HEC-HMS applications

Source	Location	Study Area (km ²)	Runoff- Volume (Loss) Method	Direct- Runoff (Transform) Method	Baseflow Method	Routing Method
(Chu & Steinman, 2009)	USA	192	SCS CN	Clark's UH	Recession	Multiple
(Oleyiblo & Li, 2010)	China	797	Initial Constant	SCS UH	Exp. Recession	Muskingum-Cunge
(De Silva, Weerakoon, & Herath, 2014)	Sri Lanka	2,230	Green and Ampt	Clark's UH	Recession	None
(Choudhari, Panigrahi, & Paul, 2014)	India	16	SCS CN	SCS UH	Exp. Recession	Muskingum
(Derdour, Bouanani, & Babahamed, 2018)	Algeria	1,957	SCS CN	SCS UH	None	Muskingum
(Zeleeuw & Melesse, 2018)	Algeria	55	SCS CN	Multiple	Constant Monthly	Muskingum
(Moraes, Santos, Calijuri, & Torres, 2018)	Brazil	1,276	SCS CN	SCS UH	None	Muskingum-Cunge
(Zema, Labate, Martino, & Zimbone, 2016)	Italy	795	Multiple	SCS UH	Constant Monthly	None
(Jin, Liang, Wang, & Tumula, 2015)	China	270	Multiple	Multiple	None	Muskingum
(Tassew, Belete, & Miegel, 2019)	Ethiopia	1,609	SCS CN	SCS UH	None	Muskingum

Table 2.1. Selected event-based HEC-HMS applications (continued)

Source	Location	Study Area (km ²)	Runoff- Volume (Loss) Method	Direct- Runoff (Transform) Method	Baseflow Method	Routing Method
(Kaffas & Hrissanthou, 2014)	Greece	237	SCS CN	SCS UH	Recession	Muskingum-Cunge
(Fang, Yuan, Gao, Huang, & Guo, 2018)	China	2,631	SCS CN	SCS UH	Recession	Muskingum
(Adilah & Nuramirah, 2019)	Malaysia	1,630	SCS CN	Clark's UH	Recession	None
(Azam, Kim, & Maeng, 2017)	Korea	163	SCS CN	Multiple	Recession	Muskingum
(Koneti, Sunkara, & Roy, 2018)	Sri Lanka	300	SCS CN	SCS UH	Constant Monthly	Muskingum Cunge / Kinematic

For event-based studies, there are many successfully developed models with “SCS CN” infiltration method such as Choudhari et al. (2014), Derdour et al. (2018), Moraes et al. (2018), Tassew et al. (2019), Kaffas & Hrissanthou (2014), Fang et al. (2018), Adilah & Nuramirah (2019) and Koneti (2018). Chu & Steinman (2009) produced better results by applying “SCS CN” as the loss method and “Clark’s UH” method as the transform method with recession baseflow separation in the USA. In another study, Oleyibl & Li (2010) indicated that more credible results are obtained with “Initial and Constant” as the loss method and “SCS UH” as the transform method for a study area located in southern China. The study conducted by Jin et al. (2015) found that the “SCS CN” infiltration method performed better than “Initial and Constant” method in estimating runoff in semi-arid regions of northern China. Zema et al. (2016) compared “SCS CN,” “Initial and Constant,” and “Green and Ampt” methods, and results

indicated that “SCS CN” method demonstrated relatively better performance when compared with “Initial and Constant” method for the basin located at Italy. They also indicated that “Green and Ampt” method was not successful in calculating precipitation losses. On the other hand, the study by De Silva et al. (2014) indicated that the “Green and Ampt” method is applicable to basins located in Sri Lanka. In this study, for the event-based simulation, the SCS CN method is used due to its successful applications presented in the literature, and data availability.

Moreover, according to the study by Zelelew & Melesse (2018), “SCS CN” is used as the loss method with the option of “SCS UH” and “Clark’s UH” transform methods and results indicated that “SCS UH” method is more credible with “Initial and Constant” method for a study area located at northwest Ethiopia. Azam et al. (2017) compared the effectiveness of “Clark’s UH” and “Synder UH” in a flood risk study conducted in Korea, and they concluded that “Clark’s UH” simulated the flows better than “Synder UH.” Jin et al. (2015) compared “Kinematic Wave” and “SCS UH” transform methods and stated that the “Kinematic Wave” model is more successful for predicting the flood peak time for situations of long-lasting rainfall, whereas “SCS UH” performs relatively better with short rainfall duration. SCS UH transform method is selected for both event-based and continuous simulation in this study because it only requires the lag time as the input and previous studies reported that the method has excellent performance.

Studies also indicated that using a short time step for an event-based model decreases the possibility of missing transient storm events (Boughton & Droop, 2003). Most of the event-based applications given in Table 2.1 are conducted with hourly time steps, whereas some with daily and 15-minute time steps. Some applications of the software, together with the methods used, are given for the continuous approach in Table 2.2.

Table 2.2. Selected continuous HEC-HMS applications

Source	Location	Study Area (km ²)	Runoff-Volume (Loss) Method	Direct-Runoff (Transform) Method	Baseflow Method	Routing Method
(Chu & Steinman, 2009)	USA	192	SMA	Clark's UH	Recession	Multiple
(Fleming & Neary, 2004)	USA	22.83	SMA	Clark's UH	None	None
(Verdhen, Chahar, & Sharma, 2013)	India	350	Deficit and Constant	Clark's UH	Recession	Lag
(De Silva, Weerakoon, & Herath, 2014)	Sri Lanka	2,230	SMA	Clark's UH	Recession	None
(Azmat, Choi, Kim, & Liaqat, 2016)	Pakistan	33,867	Deficit and Constant	SCS UH	Constant Monthly	None
(Bhuiyan, McNairn, & Powers, 2017)	Canada	545	SMA	SCS UH	Recession	Muskingum
(Gebre, 2015)	Ethiopia	5,125	Deficit and Constant	Synder UH	Exp. Recession	None
(Gyawali & Watkins, 2013)	USA	5,273	SMA	None	None	None
(Gumindoga, Rwasoka, Nhapi, & Dube, 2017)	Zimbabwe	3600	Deficit and Constant	Synder UH	None	Muskingum
(Halwatura & Najim, 2013)	Sri Lanka	380	Deficit and Constant	Synder UH	Recession	None

For continuous models, studies implicitly proved that “SMA (Soil Moisture Accounting)” and “Deficit and Constant” methods are the only applicable loss methods for long term continuous simulations both for large and small basins (Halwatura & Najim, 2013; De Silva, Weerakoon, & Herath, 2014; Fleming & Neary, 2004; Chu & Steinman, 2009). There are many applications for both methods. For example, Chu & Steinman (2009), Fleming & Neary (2004), De Silva et al. (2014), Bhuiyan (2017), Gyawali & Watkins (2013) successfully developed models with “SMA” method and Verdhen et al. (2013), Azmat et al. (2016), Gebre (2015), Gumindoga et al. (2017), Halwatura & Najim (2013) with “Deficit and Constant” method. All the continuous model applications given in Table 2.2 are conducted using daily time steps because shorter time steps cause difficulties in the calculation for extended periods, and it will be redundant since the target of continuous simulations is to estimate the design flow (Boughton & Droop, 2003). For the continuous simulation in this study, the Deficit and Constant model is selected as the loss method because it requires less data when compared with the Soil Moisture Accounting method.

Azmat et al. (2016), Verdhen et al. (2013), De Silva et al. (2014), Bhuiyan et al. (2017), Gyawali & Watkins (2013) applied “Temperature Index” method to define snow content in the meteorological model of their studies. Gyawali & Watkins (2013) revealed the importance of using snow processes for continuous model calibration and a better description of the hydrological regime. Snowmelt is included for the continuous model that developed in this study.

Previous studies indicated that the results of the simulations are location-specific, and different method combinations may respond differently for a specific study area. Method selection for hydrological processes depends on data availability, study area, and engineering judgment (USACE, 2000). Loss, transformation, baseflow, and routing methods are the most critical components for the description of the hydrological processes in the study area. There are five different baseflow calculation methods provided in HEC-HMS. Based on literature review recession and constant

monthly methods are evaluated and recession base flow method is selected for event-based and continuous simulations. Moreover, the Muskingum routing method is selected due to its simplicity for both the event-based and continuous simulations.

There are several studies conducted in Turkey recently. Yılmaz et al. (2012) studied the applicability of HEC-HMS in the Upper Euphrates Basin by comparing it with LBRM models. “Initial and Constant” as the loss method, “Synder UH” as the transform method, “Constant Monthly” as the baseflow method, and “Lag” method as the routing method is used in the event-based simulation. They obtained acceptable results. Kocyigit et al. (2017) used HEC-HMS to estimate the hydrological parameters in Kocanaz Basin, which is a small basin in the Western Black Sea Region of Turkey. Both event-based and continuous simulation was developed with the “SCS CN” as the loss method, “Clark UH” as the transform method, the recession baseflow method, and their results were also acceptable. Akay and Kocyigit (2019) also studied with HEC-HMS for ungauged sub-basins for the Arac River located in the Western Black Sea Region of Turkey. The model developed with “SCS CN” with a specified unit hydrograph and helped to compare two different ungauged sub-basins. Özkaya & Akyürek (2019) evaluated the use of bias-corrected radar rainfall data in three flood events in Turkey. Radar rainfall data is used as input for event-based HEC-HMS model. The model developed with “SCS CN” loss method, “SCS UH” transform method and “Muskingum” flow routing model.

2.3. Performance Evaluation

Model calibration and validation require the examination of the accuracy of results to ensure valid representation of hydrological processes in basins. Use of model performance measures (PMs) and corresponding performance evaluation criteria (PEC) procure performance evaluation for a model. PM refers to the statistical and graphical methods for performance evaluation, and PEC refers to model performance qualitative ratings with the corresponding threshold for PM (Moriassi, Gitau, Pai, & Daggupati, 2015). Modelers have used different performance methods for basin

calibration and validation in the literature. For this study, most commonly used “Nash-Sutcliffe Efficiency”, “Percent Bias,” “Root Mean Square Error”, “Correlation” and “r squared” are used as performance measures.

$$NSE = 1 - \frac{\sum_{t=1}^{n_t} (Q_t^{\text{obs.}} - Q_t^{\text{calc.}})^2}{\sum_{t=1}^{n_t} (Q_t^{\text{calc.}} - \bar{Q}^{\text{obs.}})^2} \quad (1)$$

$$PBIAS = \frac{\sum_{t=1}^{n_t} (Q_t^{\text{obs.}} - Q_t^{\text{calc.}})}{\sum_{t=1}^{n_t} (Q_t^{\text{obs.}})} \times 100 \quad (2)$$

$$RMSE = \sqrt{\frac{1}{n_t} \sum_{t=1}^{n_t} (Q_t^{\text{obs.}} - Q_t^{\text{calc.}})^2} \quad (3)$$

$$r = \frac{\sum_{t=1}^{n_t} [(Q_t^{\text{obs.}} - \bar{Q}^{\text{obs.}}) \times (Q_t^{\text{calc.}} - \bar{Q}^{\text{calc.}})]}{\sqrt{\sum_{t=1}^{n_t} (Q_t^{\text{obs.}} - \bar{Q}^{\text{obs.}})^2 \times \sum_{t=1}^{n_t} (Q_t^{\text{calc.}} - \bar{Q}^{\text{calc.}})^2}} \quad (4)$$

$$R^2 = r^2 \quad (5)$$

where $Q_t^{\text{obs.}}$ is the observed flow at time t , $Q_t^{\text{calc.}}$ is the calculated flow at time t , n_t is the number of time steps, $\bar{Q}^{\text{obs.}}$ is the average of observed flows and $\bar{Q}^{\text{calc.}}$ is the average of estimated/modeled flows.

Moriasi et al. (2007) compiled studies related to performance evaluation of basin-scale models. Further, Moriasi et al. (2015) updated the previous study with emerged studies to recompose a list of performance methods and corresponding performance evaluation criteria. The recommended list for streamflow with “Nash-Sutcliffe Efficiency,” “Percent Bias,” and “R squared” methods are given in Table 2.3. Singh et al. (2004) emphasized that cases where the $RMSE$ value is less than half of the standard deviation of the observed flow can be regarded as low errors. Moreover, Santhi et al. (2001) and Van Liew et al. (2003) stated that “Correlation” values higher than 0.5 are satisfactory.

Table 2.3. Performance evaluation criteria for basin-scale models (Moriasi, Gitau, Pai, & Daggupati, 2015)

Method	<i>Very Good</i>	<i>Good</i>	<i>Satisfactory</i>	<i>Not Satisfactory</i>
R^2	$R^2 > 0.85$	$0.75 < R^2 \leq 0.85$	$0.60 < R^2 \leq 0.75$	$R^2 \leq 0.60$
NSE	$NSE > 0.80$	$0.70 < NSE \leq 0.80$	$0.50 < NSE \leq 0.70$	$NSE \leq 0.50$
$PBIAS$ (%)	$PBIAS < \pm 5$	$\pm 5 \leq PBIAS < \pm 10$	$\pm 10 \leq PBIAS < \pm 15$	$PBIAS \geq \pm 15$

CHAPTER 3

HEC-HMS MODELING

HEC-HMS is designed to simulate the precipitation-runoff processes of dendritic basin systems (USACE, 2018). The software can calculate and simulate hydrological processes with a system for storing and managing time variable data sets. It has a graphical user interface that illustrates hydrologic system components and the ability to display outputs (Halwatura & Najim, 2013). HEC-HMS has separate models to represent runoff volume, direct runoff, routing, baseflow, and it has separate tools to calculate hydrological processes. Similar to the classification done by Zema et al. (2016), model development can be simplified into four main components according to the USACE User's Manual (2018):

- Basin model. This component is for the basin physical description, which includes basin characteristics and representation of runoff processes such as loss, transform, baseflow, routing methods. Basin model also includes other elements such as reservoirs, sources, and sinks.
- Meteorological model. This component is for defining precipitation, evapotranspiration, and snowmelt.
- Data Input. This component allows a user to include required data for initial conditions, boundary conditions, or parameters as time-series data, gridded data, and paired data.
- Control specifications. This component is for controlling simulations.

The first step in the development of the HEC-HMS model is defining the characteristics of the basin and sub-basins of it. Basin model includes system connectivity and physical data, which describes the basin. Then precipitation, evapotranspiration, and snowmelt methods are defined in the meteorological model.

A model runs by combining the basin model, the meteorological model, and the control specifications to generate results.

Although physical basin description can be developed in HEC-HMS, there are geospatial hydrology tools for obtaining spatial data and basin characteristics, delineating sub-basins and streams and constructing inputs for hydrological models. One of these tools is the Watershed Modeling System (WMS), which is developed by the Environmental Modeling Research Laboratory of Brigham Young University in cooperation with the U.S. Army Corps of Engineers Waterways Experiment Station and is currently being developed by Aquaveo LLC (Aquaveo, 2019). Another tool is the HEC-GeoHMS, which was developed by the United States Army Corps of Engineers (USACE) in partnership with the Environmental System Research Institute (USACE, 2013). For this study, the basin and meteorological model are prepared by using HEC-GeoHMS, and this part of the study named as preprocessing. HEC-HMS model structure is represented in Figure 3.1.

In this study, both event-based and continuous models are developed. The list of the selected methods for both approaches is provided in Table 3.1, and the list of selected meteorological model methods is provided in Table 3.2. The main components of the model structure given in Figure 3.1 are explained in the following sections.

Table 3.1. List of selected HEC-HMS methods

Model Type	<i>Loss Method</i>	<i>Transform Method</i>	<i>Routing Method</i>	<i>Baseflow Method</i>
Event-based	SCS-CN	SCS Unit Hydrograph	Muskingum	Recession
Continuous	Deficit and Constant	SCS Unit Hydrograph	Muskingum	Recession

Table 3.2. List of selected meteorological model methods

	<i>Precipitation</i>	<i>Evapotranspiration</i>	<i>Snowmelt</i>
Event-based	Specified Hyetograph	Neglected	<i>Not used</i>
Continuous	Specified Hyetograph	Specified Evaporation	Temperature Index

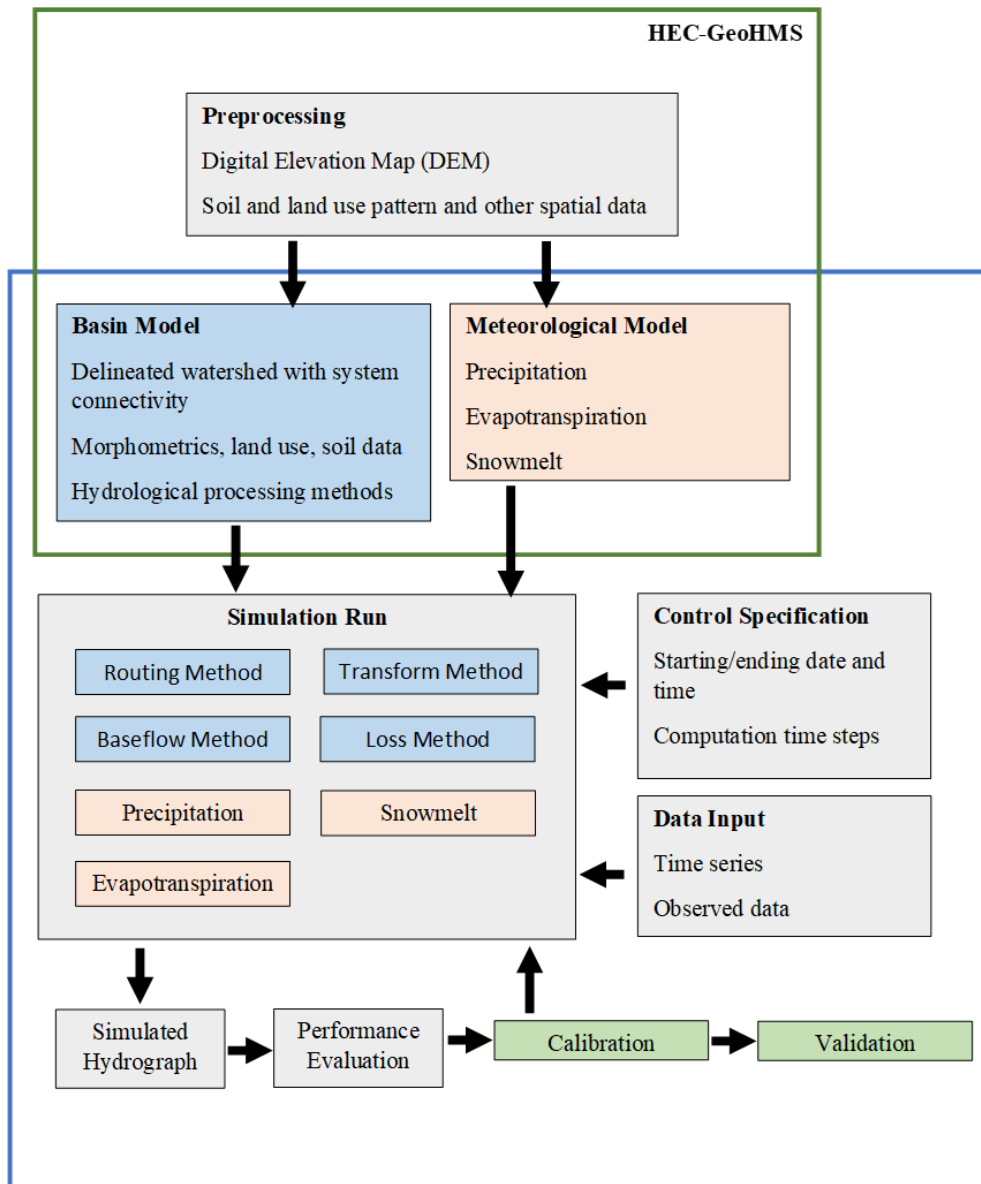


Figure 3.1. HEC-HMS model structure

3.1. Preprocessing

HEC-GeoHMS, which is a public-domain extension that works with ArcGIS 10.1 (ArcView-ESRI), is used for performing terrain preprocessing, basin processing, and hydrological parameters estimations. In case of using a preprocessing tool like the HEC-GeoHMS project will be created in this tool and will be transformed to HEC-HMS for the simulation process. Basics for basin model and meteorological model will be produced in this tool. Overview of the relation between HEC-GeoHMS and HEC-HMS is illustrated in Figure 3.2 (USACE, 2000).

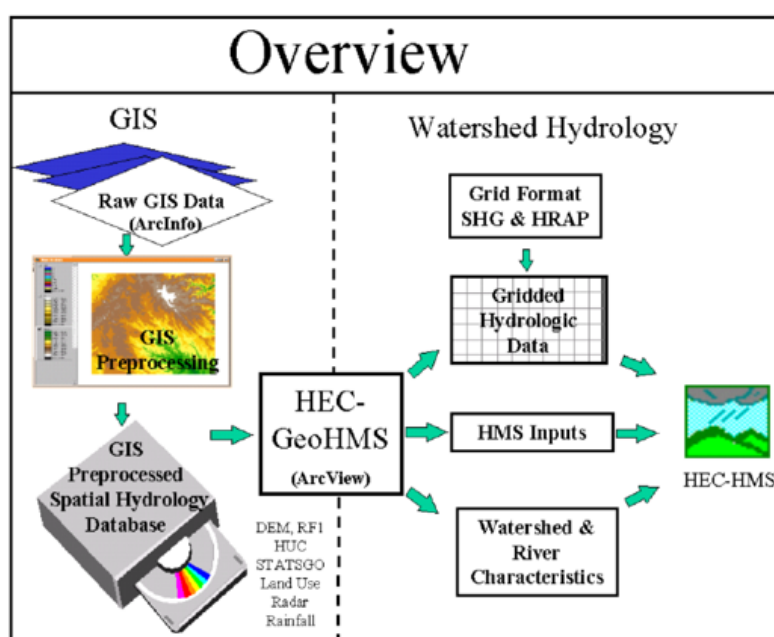


Figure 3.2. Overview of the relation between HEC-GeoHMS and HEC-HMS (USACE, 2000)

In this study, the basin model is initially generated using HEC-GeoHMS. Digital Elevation Model (DEM) of the study area is used to derive the stream network and to delineate the basin into interconnected sub-basins since each sub-basin has topographic attributes such as slope, area, and location (Ali, Khan, Aslam, & Khan, 2011). Moreover, HEC-GeoHMS enables the user to select hydrological process calculation methods. According to the selected methods, other inputs can be included,

such as land use information, hydrological soil group, and rainfall events that vary in space and time. Soil Conservation Service Curve Number, “SCS CN,” method (USDA, 1986), for example, requires both land use and hydrologic soil groups to generate curve numbers for each delineated sub-basin. Other processes that depend on spatial distribution can be performed using HEC-GeoHMS. Preprocessing can be grouped into six main steps with several sub-steps. These sub-steps are included in HEC-GeoHMS with commands (USACE, 2013). The flow chart of HEC-GeoHMS for preprocessing is provided in Figure 3.3. Application details of these tools are given in represented in case studies section.

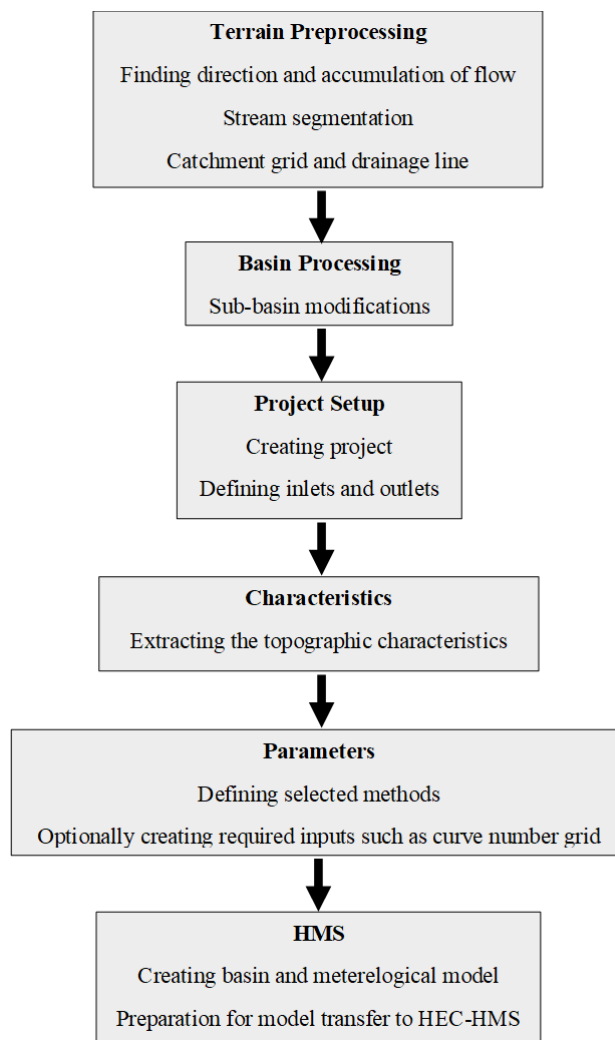


Figure 3.3. Flow chart of preprocessing with HEC-GeoHMS (USACE, 2013)

For this study, event-based and continuous models require different datasets and preprocessing steps according to the selected methods, while most of the development processes are the same. Basin and meteorological models are prepared for both approaches, but there is one more step required for the event-based model, which is the generation of the curve numbers required by the selected loss method (i.e., “SCS CN”).

3.2. Model Setup

The Model Setup in HEC-HMS (i.e., the blue box is shown in Figure 3.1) is composed of Basin and Meteorological Models, which are necessary to run simulations. The main components of the Model Setup are explained in the following sections.

3.2.1. Basin model

HEC-GeoHMS delineates basin by using spatial data and creates a basin model. Basin model will be transformed to HEC-HMS from HEC-GeoHMS with defined components such as sub-basins, reaches, junctions, sources, sinks, reservoirs, and diversions. Except for the stream and topography of the study area, basin model includes the realization of hydrological processes such as the loss method. As stated before, this study, both event-based and continuous approaches are implemented. As the loss method, the “SCS CN” method for event-based model and “Deficit and Constant” method for the continuous model are selected, whereas “SCS UH,” “Muskingum,” and “Recession” methods are selected for both approaches. Mechanisms and formulations of the selected methods are explained in the following sections.

3.2.1.1. “Soil Conservation Service Curve Number” Loss Method

Incremental losses for each sub-basin are calculated using corresponding curve numbers in the Soil Conservation Service Curve Number method. The program computes incremental precipitation excess during a storm event by estimating the infiltration volume at the end of each time interval. Infiltration during each time

interval is calculated by taking the difference in volume at the end of two adjacent time intervals. The “SCS CN” values calculate precipitation excess as a function of cumulative precipitation, soil cover, land use, and antecedent moisture. The infiltration loss is derived from empirical equations (USACE, 2018).

$$P_e = \frac{(P - I_a)^2}{P - I_a + S} \quad (6)$$

where P_e is accumulated precipitation excess at time t , P is the accumulated rainfall depth at time t , I_a is the initial abstraction (initial loss), and S is the potential maximum retention, a measure of the ability of a basin to abstract and retain storm precipitation.

According to this formulation, the accumulated precipitation excess and consequently the runoff are zero until the accumulated rainfall exceeds the initial abstraction. The relationship between the initial abstraction and potential maximum retention is given as follows:

$$I_a = 0.2 \times S \quad (7)$$

Therefore, cumulative excess at time t is estimated using:

$$P_e = \frac{(P - 0.2 \times S)^2}{P + 0.8 \times S} \quad (8)$$

The maximum retention, S , and basin characters are related to the curve number as:

$$S = \frac{25400 - 254 \text{ CN}}{\text{CN}} \quad (\text{in SI units}) \quad (9)$$

The curve numbers are calculated using hydrological soil groups, and land uses. The hydrological soil group, which is defined according to USDA (2007) with land-use types defined according to the Corine System (Corine, 2012) are processed with respect to the chart defined by the United States Department of Agriculture (1986) to create curve numbers. Hydrological Soil Types, according to USDA, are given in Appendix A.

Deep sand, deep loess, and aggregated silts belong to Hydrologic Soil Group A and they have the lowest runoff potential. Hydrologic Soil Group B has low runoff potential as well and include soils like shallow loess and sandy loam. Soils that are low in organic content and usually high in clay such as clay loams and shallow sandy loam belong to Hydrologic Soil Group C and they have higher runoff potential. Finally, Hydrologic Soil Group D has the highest runoff potential. These types of soils are such as heavy plastic clays, and certain saline swell considerably when wet.

Hydrologic soil type is used together with land-use types in determining the CN. In this study the Corine System, which is developed by the European Topic Center on Urban land and soil systems is used to identify land-use types in the study area. The Corine Land Cover nomenclature updated by Büttner et al. (2012) based on the technical guide created by Bossard et al. (2000) is given in Appendix A.

Vector maps with a scale of 1:100000, a minimum cartographic unit (MCU) of 25 ha, and a geometric accuracy better than 100 m are provided in the CORINE system. Maps reflect more than 75% of the pattern within given nomenclature (Corine, 2012). Chart provided by United States Department of Agriculture (1986) to create curve numbers according to the land use and hydrologic soil groups for urban areas, cultivated agricultural lands, other agricultural lands, and arid and semiarid rangelands are given in Appendix A.

3.2.1.2. “Deficit and Constant” Loss Method

The “Deficit and Constant” is a quasi-continuous model for calculating precipitation loss. In this method the initial loss recovers after a long dry period where there was no rainfall. A single layer is used to account for continuous changes in moisture content. According to HEC-HMS User’s Manuel (2018) “Deficit and Constant” method is suggested to be used together with the “Canopy” method which uses potential evapotranspiration calculated in the meteorological model to extract water from the soil. Canopy model represents the presence of plants in the landscape. The soil layer will dry out between storm events as the canopy extracts water. However, unless a

canopy method is used there will be no soil water extraction. Moreover, the “Surface” method where water is accumulated as the depression surface storage can be used as well. In the “Deficit and Constant” method, percolation occurs when the soil layer is saturated.

The basic parameters that are used in this method are the initial deficit (mm/day), the maximum deficit (mm/day), the constant rate (mm/day), and the imperviousness (%). Initial deficit defines the amount of water required to fill the soil layer to the maximum storage, whereas the maximum deficit, represented as depth, specifies the amount of water the soil layer can hold. The constant rate defines the percolation rate when the soil layer is saturated. Impervious area is excluded from the loss calculations by specifying the percent of impervious area. Parameters of the “Deficit and Constant” method are illustrated in Figure 3.4. “Deficit and Constant” method representation. All precipitation becomes excess and subject to surface storage or direct runoff according to the percentage (USACE, 2018; Scharffenberg, 2008).

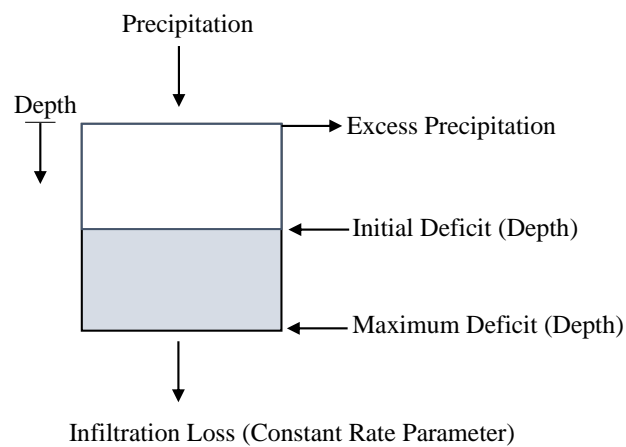


Figure 3.4. “Deficit and Constant” method representation

3.2.1.3. “Soil Conservation Service Unit Hydrograph” Runoff Transform Method

The calculation of the surface runoff transform is realized using the “Soil Conservation Unit Hydrograph (SCS UH)” method for both event-based and

continuous studies. In this method a curvilinear unit hydrograph is generated by first setting the percentage of the unit runoff that occurs before the peak flow. The only input required for the “SCS-UH” method is the lag time for each sub-basin. The lag time is defined as the time between the centroid of the precipitation mass and the peak flow of the resulting hydrograph, which can be calculated as the duration of unit precipitation divided by two, plus 60% of the time of concentration (USACE, 2018).

Additionally, the percentage of unit runoff occurring before the peak flow (peak rate factor, PFR) may need to be selected according to the requirements of basins with varying topographies and other characteristics. The default unit hydrograph has a PFR of 484. Studies indicated that flat basins typically have a lower PFR of about 100, whereas steeper basins may range up to 600 (USDA, 2007).

3.2.1.4. “Recession” Baseflow Method

For basins where channel flow recedes exponentially after a storm, the “Recession” baseflow method can be used. The method is intended for both event-based and continuous simulations. There are three parameters to select in this method as the “initial type,” the “recession constant,” and the “threshold type.” These two initial types are initial discharge and initial discharge per area. When observed flow records are available, the initial discharge method can be used. Otherwise initial discharge per area is used. In this case, general guidelines used in estimating the basin yield can be used to estimate the initial flow. The rate of baseflow recession (i.e. the ratio of the baseflow at day t to the base flow at $t-1$) is described by the recession constant. Either the ratio to peak or threshold flow methods can be used to reset the baseflow.

3.2.1.5. “Muskingum” Routing Method

Flow is routed along the stream reach using mass balance in the “Muskingum” routing method. This mathematical formulation developed by McCarthy (1938). It assumes linear method accounts increased and decreased storage during flood wave by adding a travel time for the reach and weighting between the influence of inflow and outflow

(USACE, 2018). The derivation of the mathematical formulation of the method is given in Equations (10 and (11).

$$\frac{dS}{dt} = I - Q \quad (10)$$

$$S = K[xI + (1 - x)Q] \quad (11)$$

where S is the water storage, t is time (hr), I is the inflow (m^3/sec), Q is the outflow (m^3/sec), K is the storage constant (hr), and x is the weighting factor.

Equations (10) and (11) represent the mass balance and channel storage volume, respectively. The storage volume is the simple linear combination of the inflow of the upstream and outflow of the downstream. Parameter K reflects the wave travel time, and parameter x reflects the flood peak attenuation and hydrograph shape flattening of a diffusion wave in motion. Two model parameters, K , and x , can be determined from observations (Song, Kong, & Zhu, 2011).

3.2.2. Meteorological Model

The meteorological model requires the inclusion of the climatic data into the model to prepare meteorological boundary conditions for sub-basins. Precipitation, evapotranspiration, and snowmelt are the main components of the meteorological model. The software provides various methods to integrate these components. For this study, precipitation and evapotranspiration will be included as specific values since times series values of these variables are available from the observation stations located in the study area. Evapotranspiration values are taken from study of Akyürek et al. (2019) in which evapotranspiration is calculated by Penman-Monteith method.

HEC-HMS has two methods for snowmelt calculations, which are the temperature index for a lumped model and the gridded temperature index for a distributed model. A snowpack can be modeled by the temperature index method. This is an approach obtained by modification of the degree-day approach. In the degree day approach, for each degree above freezing a fixed amount of snowmelt is assumed. As the internal

snowpack conditions and atmospheric conditions change, the melt coefficient also changes (USACE, 2018).

Snowmelt model calculates the volume of snow water equivalent, the timing and magnitude of snowmelt with impacts on the soil moisture and the streamflow. The method uses the precipitation computed by the precipitation method. On the other hand, the air temperature is used to select if the calculated precipitation was in the liquid rain or frozen snow form. Atmospheric condition is used to determine the accumulation and melt of the snowpack. The output of the method is water available at the soil surface, which becomes the hyetograph for the sub-basin (Gyawali & Watkins, 2013). The schematic of the snowmelt algorithm is provided in Figure 3.5.

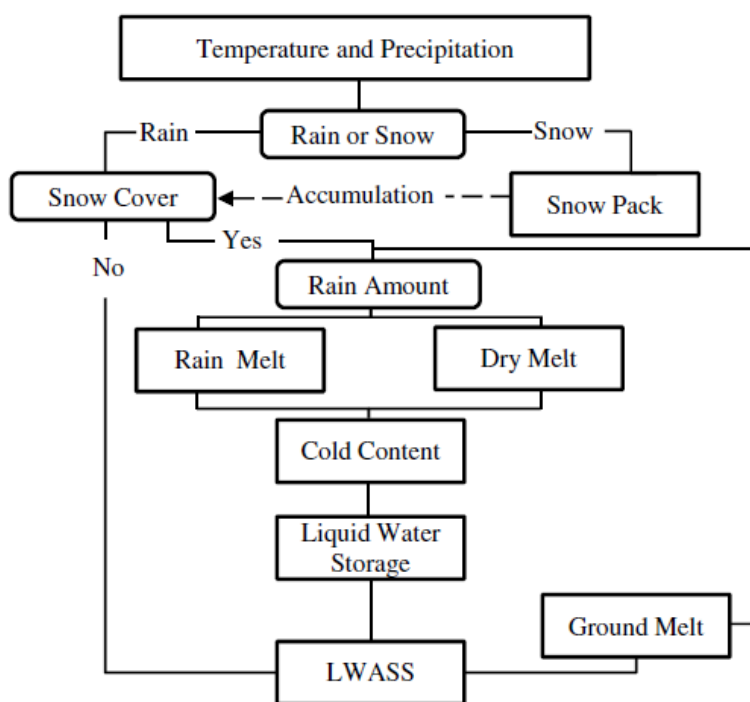


Figure 3.5. Snowmelt algorithm of “Temperature Index” method (USACE, 2010)

The temperature index method has various input requirements for parameters (e.g. base temperature, wet meltrate, rain rate limit, etc.) to be used in snowmelt

calculations, which can be calibrated using observed values. These parameters and their definition according to USACE manual (2018) are given in in Appendix B.

3.2.3. Data Input

Data types include time-series data, paired data, and grid data required by basin and meteorological models according to selected methods for the realization of hydrological processes. For example, precipitation observations are required for the meteorological model, and a storage-discharge relationship is required for the flow calculation with the “Modified-Puls routing” method (USACE, 2018).

3.2.4. Control Specifications

Control specification is for defining when the simulation starts and stops, and intervals of simulation. Different control specifications can be used according to the modeling approach. Mathematical calculations are based on defined time windows and time intervals (USACE, 2018).

3.2.5. Model Calibration and Validation

Calibration is the process of adjusting the parameters of the model within reasonable ranges until the simulated results are close enough to the observed values (Zeckoski, Smolen, Moriasi, Frankenberger, & Feyereisen, 2015). Validation is the process for ensuring that the calibrated model is capable of reproducing a set of observations or predicting future conditions without any further adjustment to the parameters (Zheng, Hill, Cao, & Ma, 2012).

HEC-HMS has a module to search the best parameter values. By comparing the generated hydrograph to the measured hydrograph, the software computes the index of goodness-of-fit. Algorithm searches for the model parameters that yield the best value of the index, also known as the objective function (USACE, 2000). This search can be done according to several objective functions, such as maximum of absolute residuals, the sum of absolute residuals, peak-weighted RMSE, etc.

If the fit of observed and calculated parameters is not acceptable, the parameters further adjusted and the calibration continues. When a satisfactory fit is obtained the best parameter, values are reported. The schematic of the calibration procedure is provided in Figure 3.6.

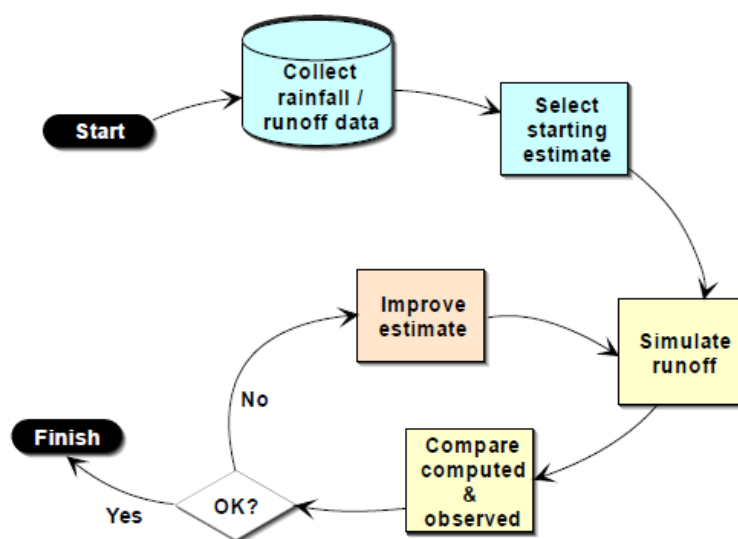


Figure 3.6. Schematic of calibration procedure (USACE, 2000)

In HEC-HMS, two auto-calibration methods, namely “Univariate-Gradient” and “Nelder-Mead” is used to search for the best (optimal) parameter values. “Univariate-Gradient” algorithm searches for the optimal value using gradients. On the other hand, “Nelder-Mead” algorithm do not use derivatives in its search algorithm. Two auto-calibration methods provided by HEC-HMS are either inefficient or time-consuming and challenging to use, especially when using a snowmelt module in a continuous model (Dariane, Javadianzadeh, & James, 2016; Dariane, Bagheri, Karami, & Javadianzadeh, 2019). Therefore auto-calibration is not used for the continuous model. For the event-based model, first auto-calibration is carried out then fine tuning is applied by manual calibration.

CHAPTER 4

CASE STUDIES

In this chapter, the selected study area is introduced, and case studies are presented. The first case is event-based model development for the study area, the second case is continuous model development and the third case is continuous model without snowmelt.

4.1. Study Area

Çakıt tributary of the Çakıt Basin is selected as the study area which has a drainage area of 518 km². Çakıt and Alihoca tributaries meet and run as Çakıt River. There is one stream gage station on each tributary just before they meet. Çakıt Basin has a drainage area of 421 km² and Alihoca has 97 km². Moreover, there is a Darboğaz basin which is sub-basin of Çakıt Basin and it has a drainage area of 179 km². Alihoca tributary is excluded from study area therefore it has a total of 421 km². Within the scope of the TUBITAK project, three stream gauge stations and three weather stations were installed in the study area. List of stream gauge stations in the study area is provided in Table 4.1.

Moreover, the General Directorate of State Hydraulic Works of Turkey has two stream gauging station, namely D18A043 and D18A044, in the study area, which measured daily streamflow for the period of 1997-2002. There is also a weather station of the Turkish State Meteorological Service named Ulukışla Weather Station. The list of SGSs in the study area is given in Table 4.1, and the list of WSs in the study area in Table 4.2. Locations of SGS and WS stations are represented in Figure 4.1.

Table 4.1. List of stream gauge stations in the study area

Station	Established by	Latitude	Longitude	Drainage Area (km ²)	Altitude (m)	Observation years	Data Time Steps
Darboğaz SGS	TUBITAK Project 115Y041	37° 30' 31.94"	34° 34' 13.92"	179	1286	2016-2019	15 min.
Alihoca SGS	TUBITAK Project 115Y041	37° 30' 48.06"	34° 44' 43.98"	97	983	2016-2019	15 min.
Çakıt SGS	TUBITAK Project 115Y041	37° 30' 49.10"	34° 44' 43.59"	421	974	2016-2019	15 min.
D18A044	DSI	37° 50' 80.40"	34° 56' 97.30"	121	1250	1997-2002	1 day
D18A043	DSI	37° 47' 49.50"	34° 56' 50.90"	43	1382	1997-2002	1 day

Table 4.2. List of weather stations in the study area

Station	Established by	Latitude	Longitude	Altitude (m)	Observation years	Data Time Steps
Darboğaz WS	TUBITAK Project 115Y041	37° 28' 40.99"	34° 33' 0.72"	1580	2016-2019	15 min.
Madenköy WS	TUBITAK Project 115Y041	37° 26' 56.50"	34° 37' 8.23"	1790	2016-2019	15 min.
Hasangazi WS	TUBITAK Project 115Y041	37° 31' 2.23"	34° 37' 10.36"	1246	2016-2019	15 min.
Ulukışla WS	SMS	37° 54' 64.00"	34° 48' 63.40"	974	1929-2019	1 day

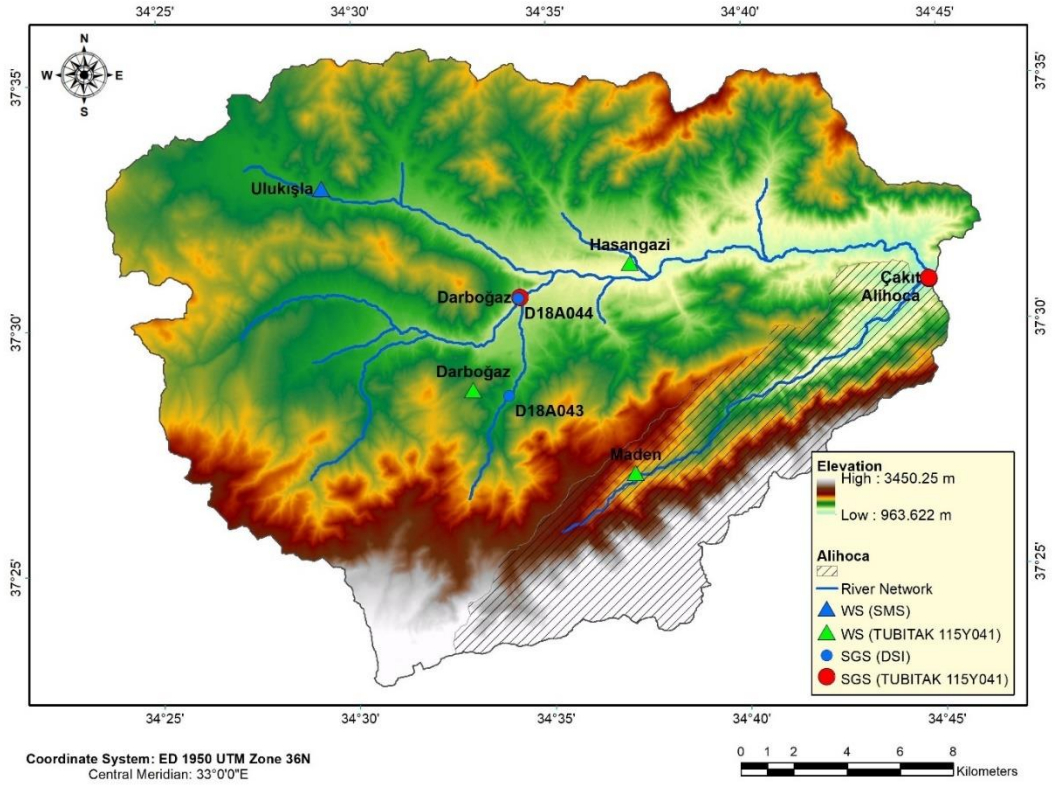


Figure 4.1. Location of gauging stations in the study area

4.1.1. Climate

Ulukışla Weather Station (Station number: 17906) of the Turkish State Meteorological Service collects meteorological data in the study area.

4.1.1.1. Temperature

According to the average temperature recorded between 1937 and 2016, the lowest average temperature of the study area was $-8.3\text{ }^{\circ}\text{C}$, while the highest average temperature was $25.3\text{ }^{\circ}\text{C}$; the coldest month is January with an average temperature of $-1.7\text{ }^{\circ}\text{C}$ and the hottest month is July with an average of $21.6\text{ }^{\circ}\text{C}$ (Akyürek, et al., 2019). After the 1990s, an increasing trend is observed in temperatures. The average annual temperatures observed at the Ulukışla WS is presented in Figure 4.2 and long term average monthly temperature values are given in Table 4.3.

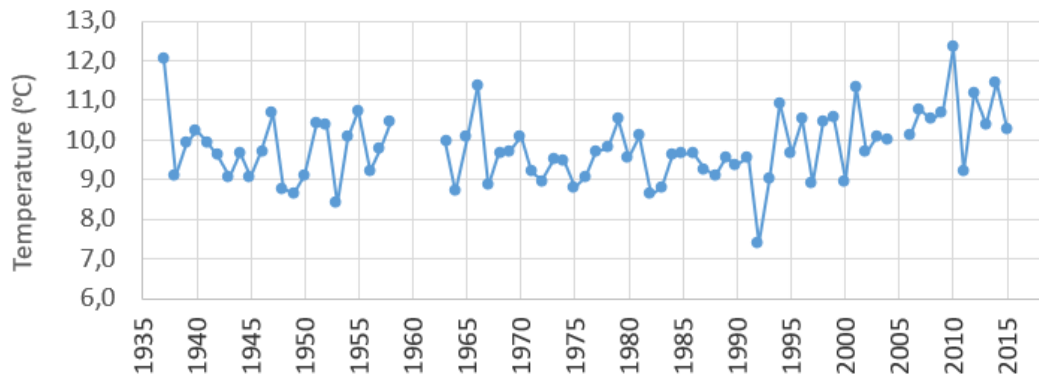


Figure 4.2. The annual average temperature (°C) (Akyürek, et al., 2019)

Table 4.3. Long term average monthly temperature (°C) (Akyürek, et al., 2019)

January	February	March	April	May	June	July	August	September	October	November	December	Yearly
-1.7	-0.3	3.5	8.9	13.5	18.1	21.6	21.3	16.7	10.9	5.0	0.4	9.80

4.1.1.2. Precipitation

According to the measurements obtained from Ulukışla Meteorology Station between 1929 and 2016, the average annual precipitation at Çakıt Basin was determined as 338 mm (Akyürek, et al., 2019). There is a downward trend in total annual rainfall in recent years. The total annual precipitation values obtained between 1929 and 2016 are presented in Figure 4.3 and long term average monthly precipitation values are given in Table 4.4.

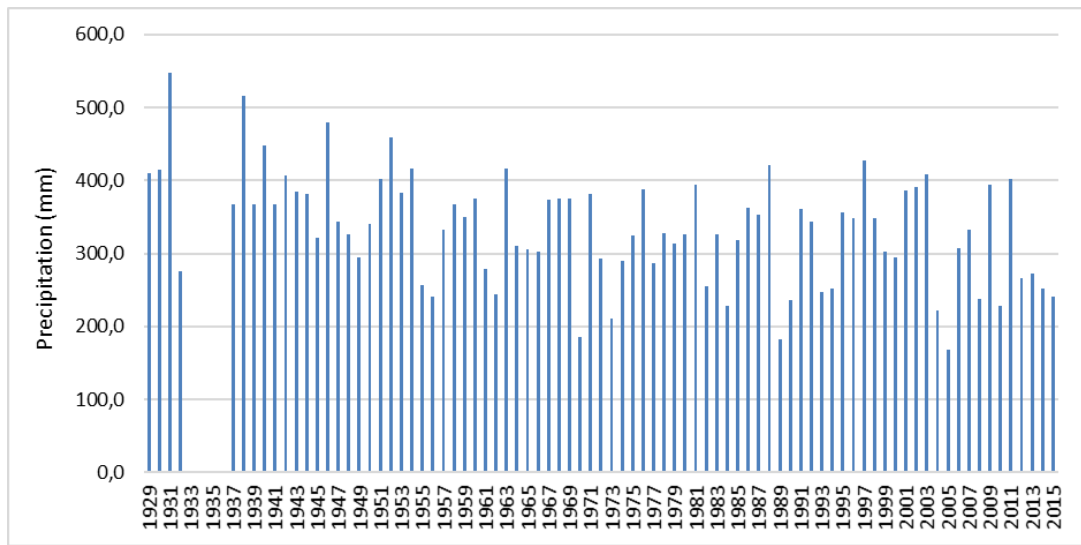


Figure 4.3. The annual precipitation values (mm) (Akyürek, et al., 2019)

Table 4.4. Long term average monthly precipitation (mm) (Akyürek, et al., 2019)

January	February	March	April	May	June	July	August	September	October	November	December	Yearly
31.6	30.6	36.8	48.9	51.3	27.3	8.1	8.0	10.8	24.3	30.5	37.9	338.3

4.1.1.3. Relative Humidity and Wind

According to the data obtained from Ulukışla meteorology station between 1975 and 2016, long term average monthly relative humidity is given in Table 4.5. Upwind direction densities of the study area are represented in Figure 4.4. (Akyürek, et al., 2019)

Table 4.5. Long term average monthly relative humidity (Akyürek, et al., 2019)

January	February	March	April	May	June	July	August	September	October	November	December
76.8	74.3	67.7	62.8	60.9	53.8	46.7	47.2	51.9	63.3	69.4	75.9

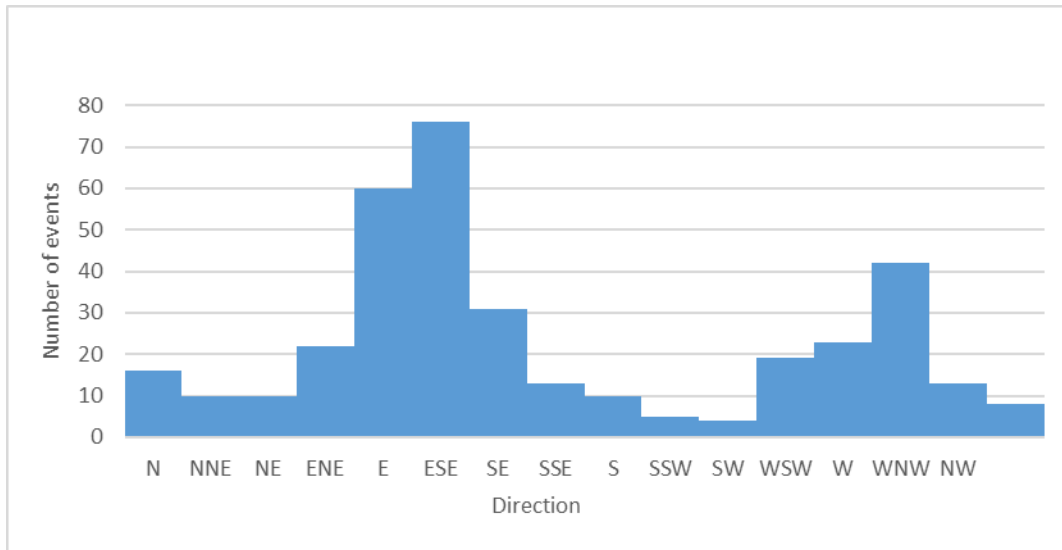


Figure 4.4. Upwind direction densities (Akyürek, et al., 2019)

4.1.2. Topography, geology and soil information

There is generally brown forest soil in the basin, and alluvial soil is observed along the river line (Akyürek, et al., 2019). The south of the basin consists of bare mountainous areas. The basin is covered with natural vegetation, farmlands, and fruit trees. The geological formation of the basin consists of gradual transitions of conglomerate, sandstone, claystone, and limestone rocks (Akyürek, et al., 2019).

The maximum elevation within the basin is around 3450 meters, while the lowest elevation is around 963 meters (Figure 4.1). The basin has a scattered elevation and average elevation is around 1727 meters. The median elevation value of the basin is close to 1600 meters which is presented on the hypsometric curve (Figure 4.5). The median elevation value for Darboğaz Basin is close to 2314 meters which is presented on the hypsometric curve in Figure 4.6. Darboğaz WS is located at an elevation of 1580 m.

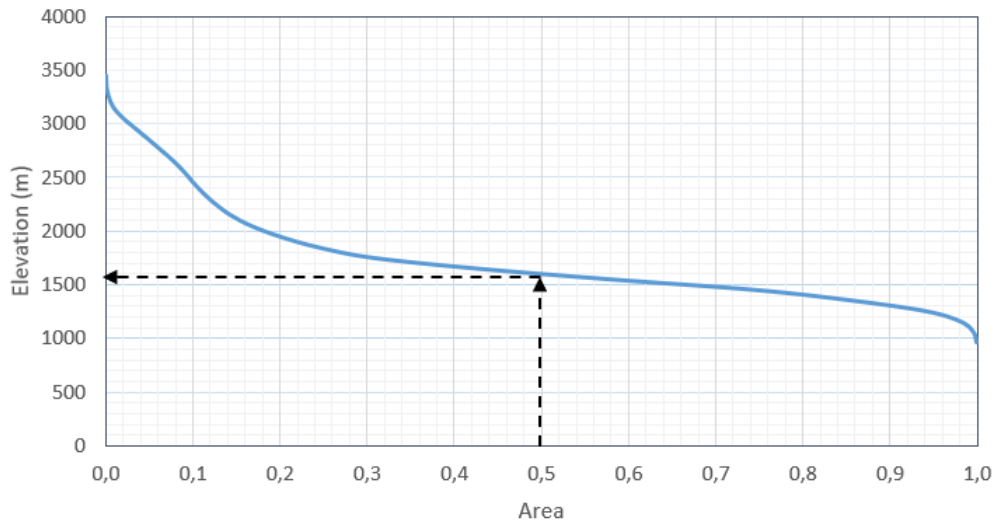


Figure 4.5. The hypsometric curve of the study area

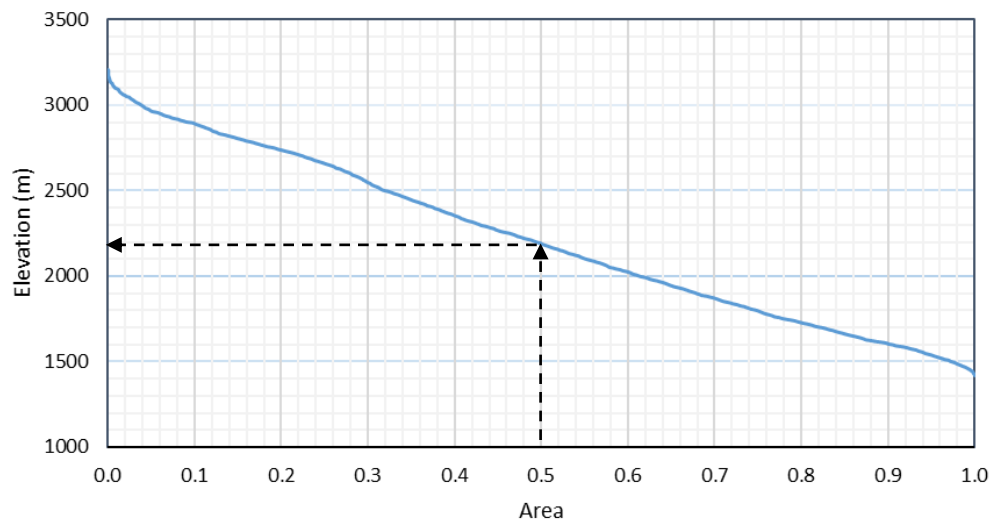


Figure 4.6. The hypsometric curve of the Darboğaz Basin

4.1.3. Land Use

Çakıt Basin mainly consists of agricultural areas, forest, and semi-natural areas. Also, there is a small amount of urban area. Land use map of the study area is given in Figure 4.7. Land use in the study area according to land cover nomenclature list provided in technical guideline prepared by European Environment Agency (Büttner, Soukup, & Kosztra, 2012) includes 16 different types. The main land use types in the study area

with land cover code are natural grasslands (321), bare rocks (332), sparsely vegetated areas (333) and transitional woodland-shrub (324) and they represent around 78% of the total area.

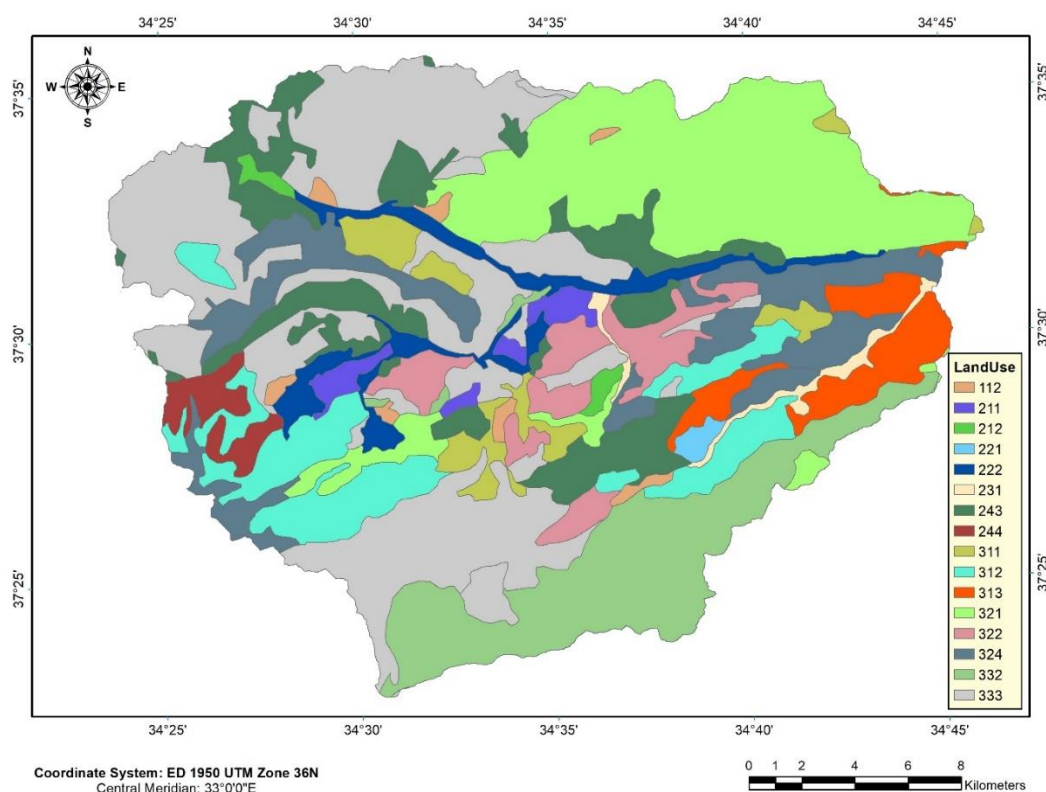


Figure 4.7. Land use in the study area (Corine, 2012)

4.1.4. Soil Properties

There is no data for hydrological soil groups for the study area. However, great soil groups, water erosion degrees, and depth of soil data are obtained from the 1/25,000 scale map prepared by the General Directorate of Agricultural Reform of Republic of Turkey Ministry of Agriculture and Forestry (National Soil Database, 2017) and the chart created by Kızılkaya (1983) are used to define the hydrological soil groups. The list of great soil groups in the study area and their permeability classes are presented in Table 4.6. The map of the great soil groups in the region is given in Figure 4.8.

Table 4.6. List of great soil groups in the study area

Great Soil Type		<i>Permeability Class</i>
Brown Earth	(B)	1
Colluvial Soils	(K)	2
Brown Forest Soil	(M)	1
Lime-free Brown Forest Soil	(N)	1

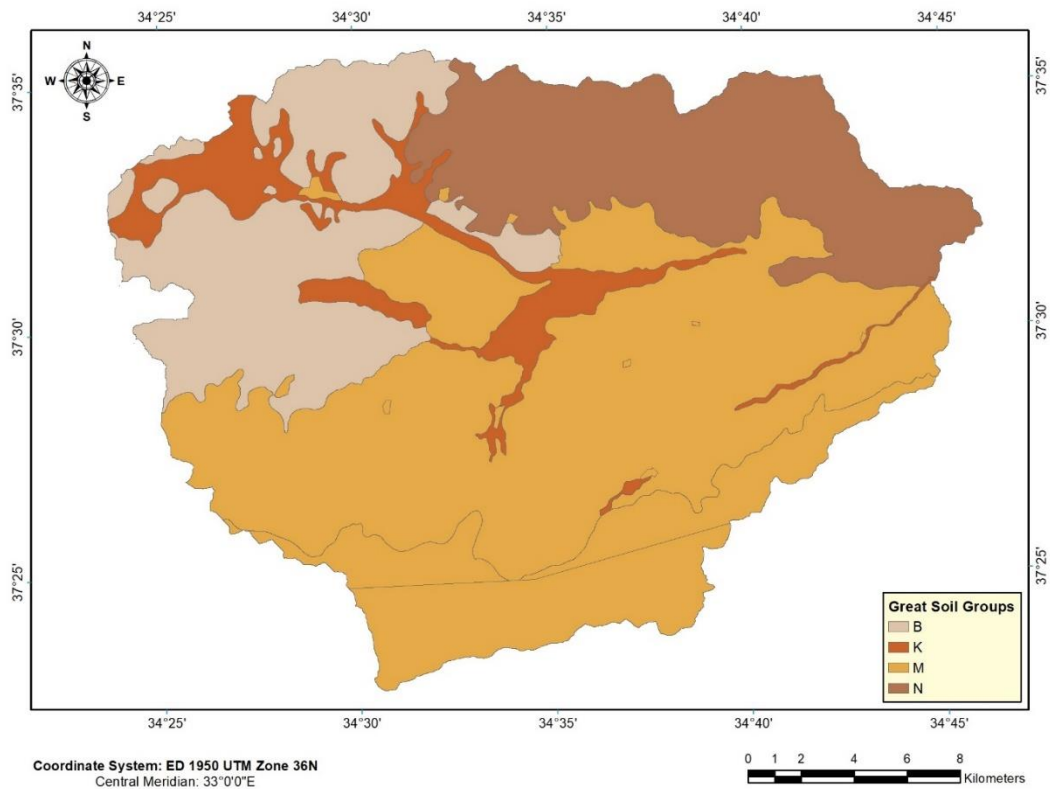


Figure 4.8. Great soil types in the study area (National Soil Database, 2017)

Water erosion occurs in four degrees according to severity (FAO, 2013). The depth of soil profile from the top to bedrock is classified in four main levels by FAO (2006). Erosion degrees and depth levels are represented in Table 4.7. Erosion degrees of the study area is illustrated in Figure 4.9 and the depth levels are shown in Figure 4.10.

Table 4.7. List of erosion degrees and depth levels (FAO, 2013)

<i>Level of Erosion</i>	<i>Severity of Erosion</i>	<i>Level of Depth</i>	<i>Description</i>
1	Weak	A	Deep ($D > 90$ cm)
2	Moderate	B	Moderate Deep ($90 > D > 50$ cm)
3	Severe	C	Shallow ($50 > D > 20$ cm)
4	Very Severe	D	Very Shallow ($20 > D > 0$ cm)

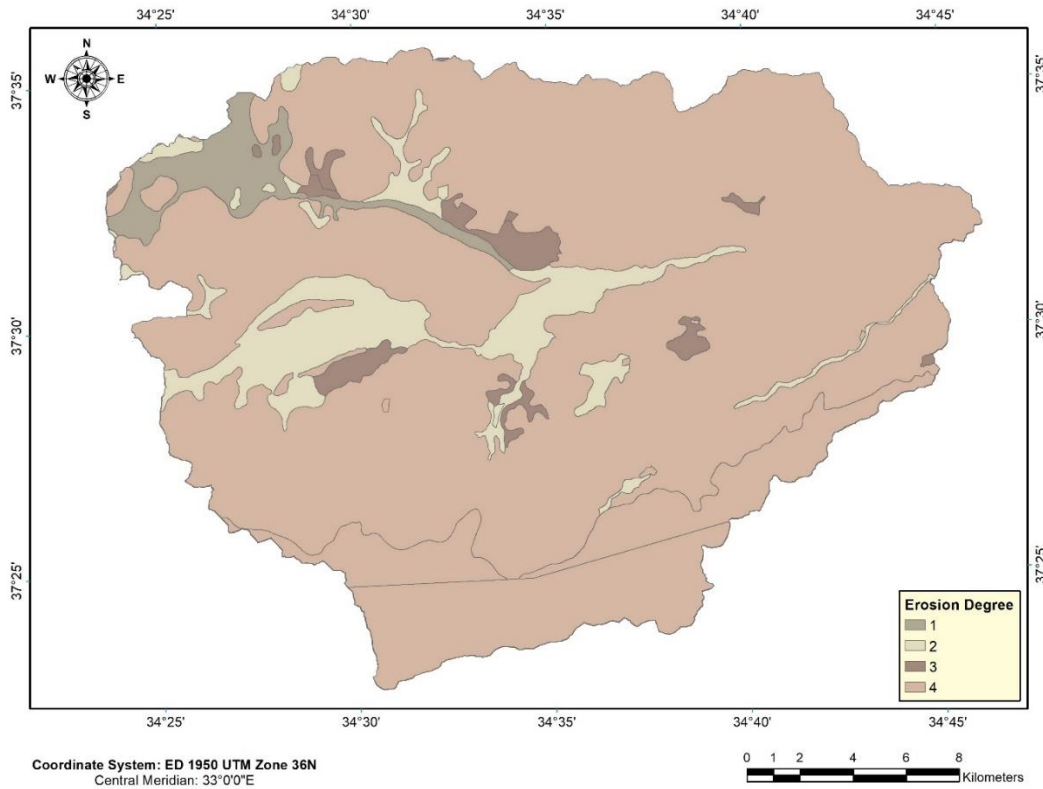


Figure 4.9. Erosion degrees of the soil in the study area (National Soil Database, 2017)

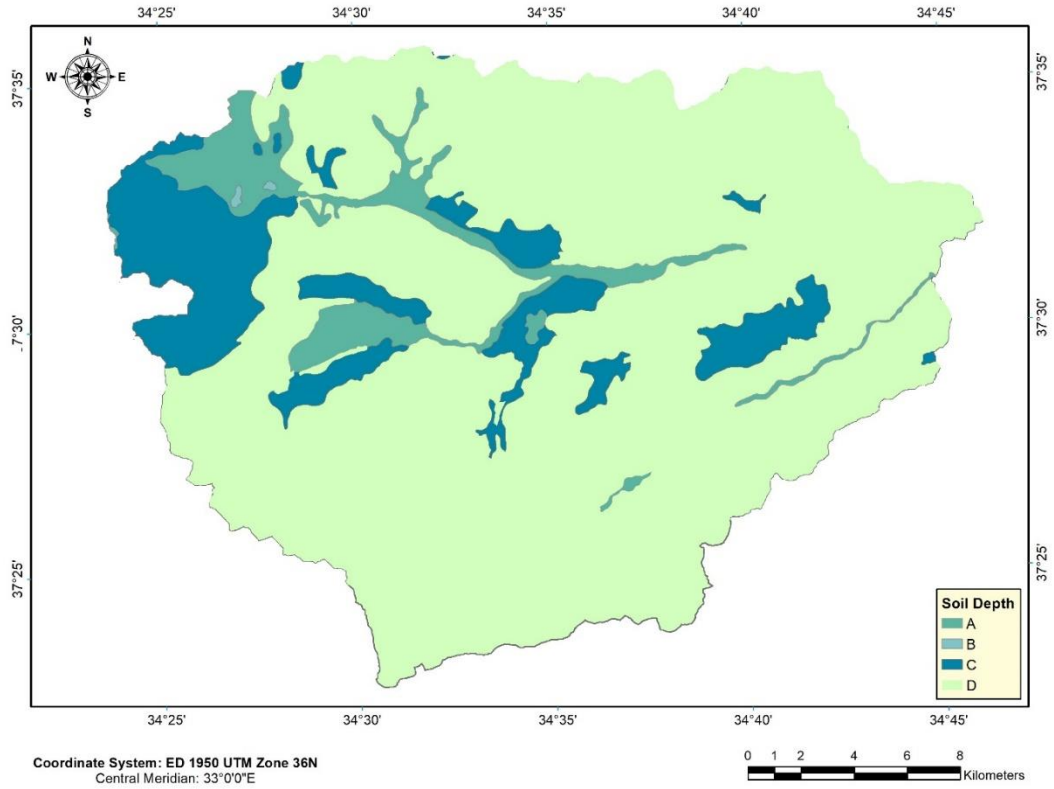


Figure 4.10. Depth levels of the soil in the study area (National Soil Database, 2017)

Kızılkaya (1983) created a chart to define the hydrological soil group from great soil groups, erosion and depth. Hydrological soil group definitions provided by Kızılkaya (1983) is given in Table 4.8. The map of the hydrological soil groups is obtained by using this chart in the ArcGIS environment, and it is provided in Figure 4.11.

Table 4.8. Hydrological soil group definition chart (Kızılkaya, 1983)

Great Soil Type	Erosion	Depth	Hydrological Soil Group
1	1/2	1	B
		2	B
		3	C
		4	C
		5	C
2	3/4		D
2		A	
2	1/2		D

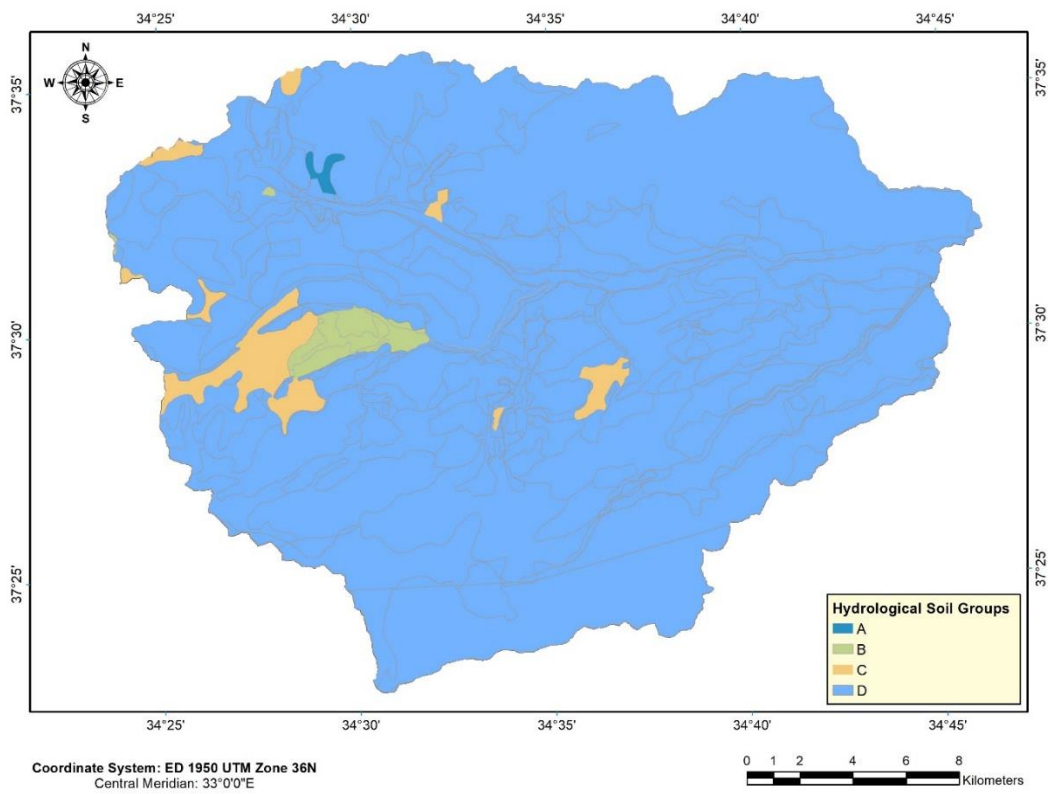


Figure 4.11. Hydrological soil groups in study area

4.2. Preprocessing

Model setups for both event-based and continuous models require some preprocessing in the HEC-GeoHMS tool, and the event-based model requires further calculations for curve number estimation, as explained in HEC-HMS modelling section. The step-by-step procedure is followed in HEC-GeoHMS in order to delineate the basin. Procedures provided in HEC-GeoHMS User's Manual (2013) and studies done by Merwade (2019), Baumbach et al. (2015), and Singh et al. (2019) are followed in this study. Preprocessing steps consist of six main groups:

- Terrain preprocessing
- Project Setup
- Basin Processing
- Characteristics
- Parameters
- HEC-HMS Transfer

Terrain preprocessing includes fill sinks, flow direction, flow accumulation, stream definition, stream segmentation catchment grid delineation, catchment polygon processing, drainage line processing, adjoint catchment and drainage point processing and slope steps to delineate basin. Project setup is for project definition whereas basin processing for modifying sub-basin, characteristics are for defining terrain properties to the software and parameters are for introducing selected methods. In the end created basin and meteorological models are transferred to HEC-HMS. Detailed explanation of these steps is given in Appendix C.

As a result of these preprocessing steps study area is represented in software. This representation includes river network with junctions, reaches, diversions, sources and sinks. Also, sub-basins are presented with unique characteristics according to terrain. Model has 13 sub-basins, 9 reaches, 9 junctions and 1 sink. The study area after preprocessing in HEC-GeoHMS is illustrated in Figure 4.12.

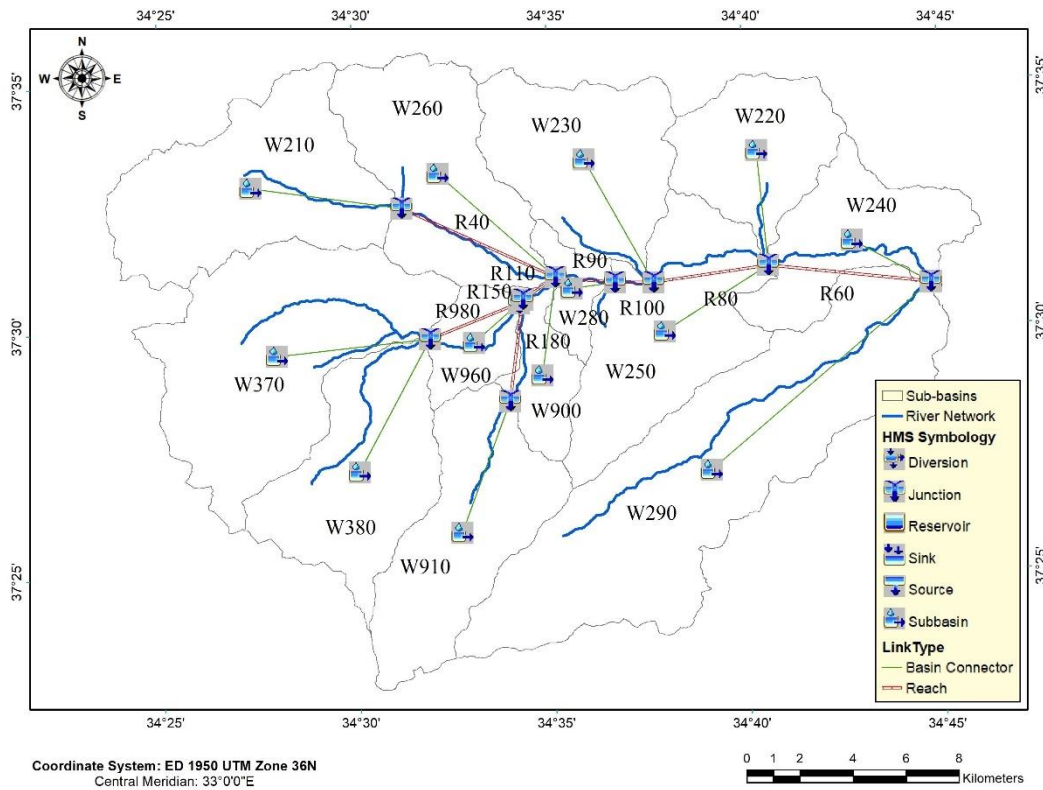


Figure 4.12. The sub-basins of study area after preprocessing in HEC-GeoHMS

4.3. Case 1 - Event-based Model Setup

An event-based model is developed for simulating an individual storm event for Çakıt Basin. Specifications of event-based model simulation of Çakıt Basin are provided in Table 4.9.

Table 4.9. Event-based model specifications

<i>Basin Model Parameters</i>		<i>Meteorological Model Parameters</i>	
Loss Method	SCS-CN	Precipitation	Specified Hyetograph
Transform Method	SCS UH	Evapotranspiration	Neglected
Routing Method	Muskingum	Snowmelt	Not used
Baseflow Method	Recession	Control Specification	1 hour

The curve numbers are calculated according to the hydrological soil group and land use. The hydrological soil groups (Figure 4.11) and the land-use pattern (Figure 4.7) of the study area are processed together according to the chart provided by the United States Department of Agriculture (1986) in the HEC-GeoHMS tool. Distributed curve numbers calculated using the land-uses identified according to CORINE in the study area are provided in Table 4.10. Created curve number grid of the study area is provided in Figure 4.13.

Table 4.10. Distributed curve numbers according to CORINE system

<i>Corine Code/ Hydrological soil group</i>	<i>A</i>	<i>B</i>	<i>C</i>	<i>D</i>
112	83	89	92	93
211	77	86	91	94
212	77	86	91	94
221	39	61	74	80
222	66	77	85	89
231	49	69	79	84
243	63	75	83	87
244	63	75	83	87
311	36	60	73	79
312	36	60	73	79
313	36	60	73	79
321	49	69	79	84
322	30	58	71	78
324	43	65	76	82
332	98	98	98	98
333	68	79	86	89

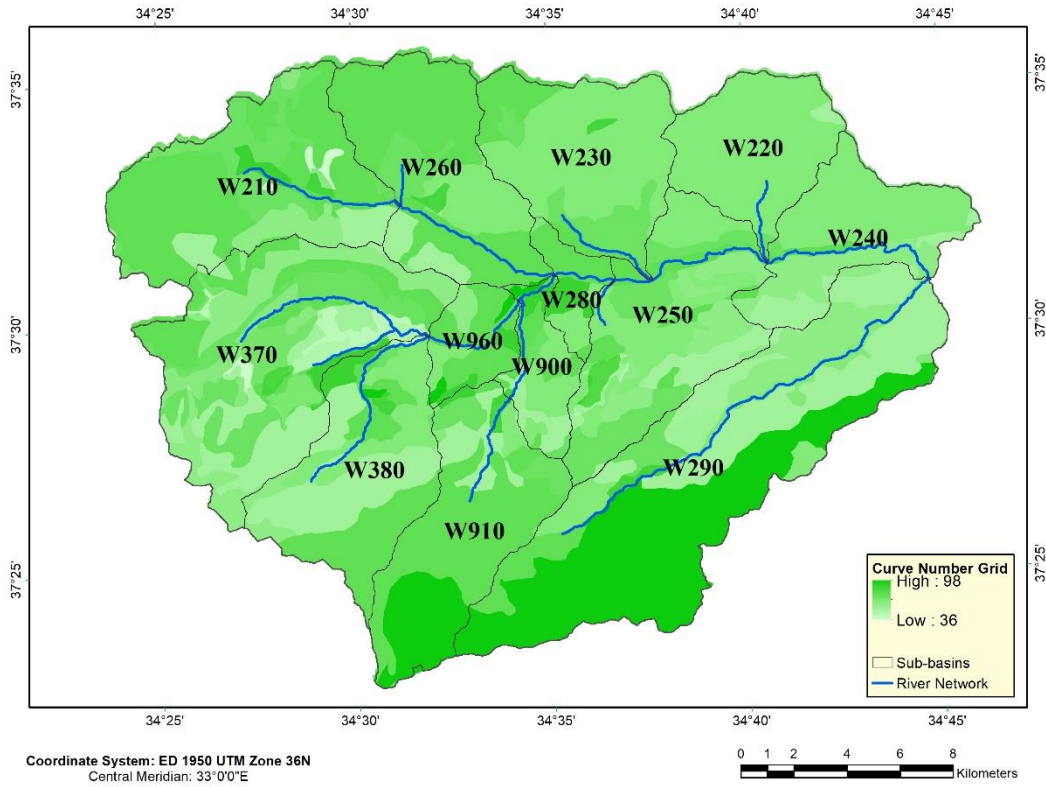


Figure 4.13. Curve number map of the study area

The calculated curve numbers for each sub-basin are given in Table 4.11. The weighted curve numbers for each sub-basin are calculated according to the weighted percent of the sub-basin area per hydrologic soil group and land use pattern:

$$w_i = \frac{A_i}{\sum A_i} \quad (12)$$

$$\text{Weighted CN} = \sum_{i=1}^n w_i CN_i \quad (13)$$

where i is the index for curve numbers according to the land use and hydrological soil group, A_i is area corresponding to curve number i and n is the total number of curve numbers.

Table 4.11. Weighted curve numbers for each sub-basin

<i>Sub-basin Code</i>	<i>Sub-basin Area (km²)</i>	<i>Curve Number</i>
W370	67	83.7
W380	43	84.3
W960	13	88.6
W910	43	89.7
W210	53	86.9
W260	42	87.2
W900	13	85.6
W280	7	88.7
W230	38	85.3
W250	45	84.5
W220	27	83.9
W290	97	89.3
W240	30	83.1

The basin model of the study area is first prepared in HEC-GeoHMS and created database is transferred to HEC-HMS. Later, required parameter inputs are entered in HEC-HMS for each sub-basin. The curve numbers calculated according to the land use and soil types in the preprocessing steps are transferred to HEC-HMS. For the “SCS CN” method, initial abstraction and impervious area percent are required as inputs with curve numbers. Some initial values are assigned to these inputs according to range provided in User’s Manual of HEC-HMS (2018) and similar studies conducted with “SCS CN” method. For the “SCS-UH” method, lag time is required as the input. The initial value is entered according to similar studies and the manual. The default unit hydrograph PFR of 484 is selected for peak rate factor. For the “Recession” baseflow method, the ratio to the peak value, recession constant is required as inputs. Moreover, for the “Muskingum” routing method the storage constant (K) and weighting factor (x) is required as input. Initial values are entered for all the inputs based on similar studies and the manual. Initial abstraction values are entered as 50 mm, while impervious areas as 1%, lag times as 150 minutes, recession

constants as 0.9 and ratio to peaks as 0.5 for all the sub-basins. Moreover, storage constant (K) parameters are entered as 2 and weighting factor (x) as 0.15 for all sub-basins.

The meteorological model of the study area is prepared in HEC-GeoHMS, and a database which is transferred to HEC-HMS is created. Evapotranspiration is ignored for the event-based model since the effect of this process to runoff is negligible for short storm events. Also, snowmelt is not included due to the fact that selected events occurred when there is no snow. For meteorological model, the “Specified Hyetograph” method is used for precipitation calculations, which only requires observed precipitation as the input.

As explained in the Literature Review section of this study, event-based models should be created with hourly time steps or shorter for better accuracy, whereas daily time steps are enough for continuous models. Therefore, the hourly time step is used for the event-based model simulation. The event-based model is developed for the Çakıt SGS. Hourly flow data which is obtained from the Çakıt SGS are used in the event-based models. Moreover, hourly precipitation data obtained from Ulukışla WS are used. Simulation starts at 00:00 on 7 April 2018 and ends at 23:00 on 13 April 2018 for calibration and starts at 00:00 on 28 May 2018, and ends at 23:00 on 4 June 2018 for validation. The time interval of mathematical calculations is defined as 1 hour.

Calibration and validation periods for event-based runs are selected by evaluating the relations between precipitations and recorded streamflow. During the calibration period, it is observed that precipitations and corresponding runoffs are not in agreement for many of the studied events. Hydrographs of two storm events those are observed in Çakıt Basin are given in Figure 4.14 and Figure 4.15 to demonstrate these events.

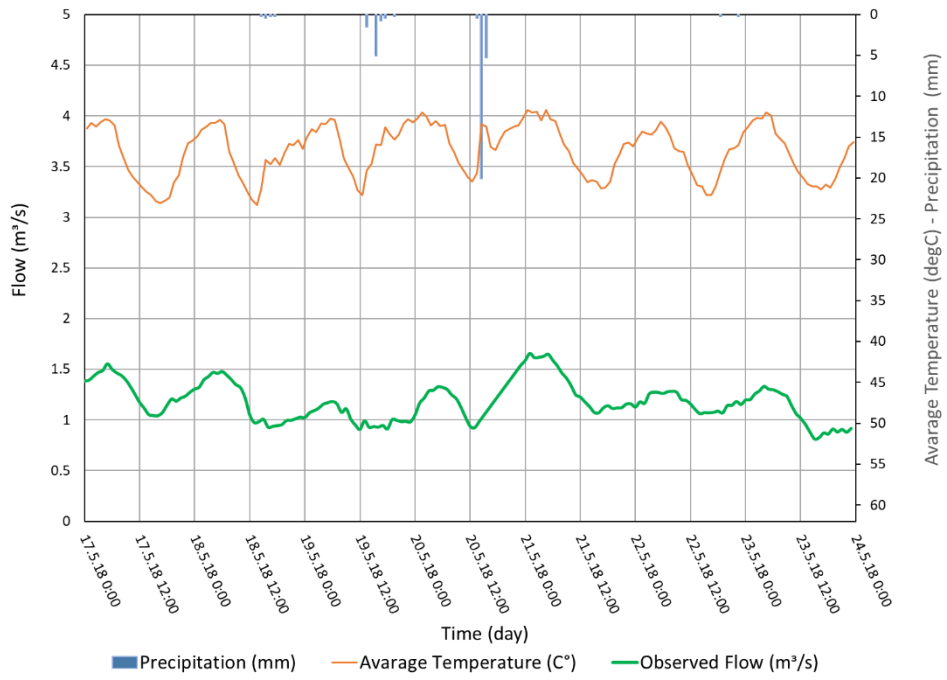


Figure 4.14. Storm event observed in between 17 May 2018 and 23 May 2018

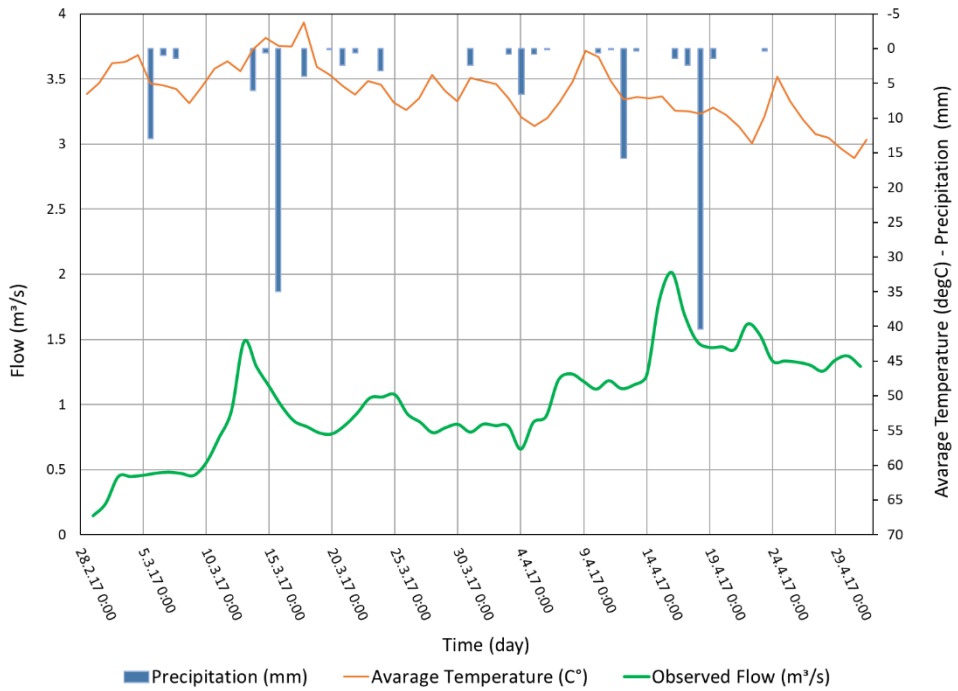


Figure 4.15. Storm events observed in between 1 March 2017 and 1 May 2017

There are some fluctuations in observed stream flow between 17 May, 2018 and 23 May, 2018 which seem to be independent of the precipitation as it can be seen in Figure 4.14. These may be due to point discharges to or withdrawals from the streamflow. These anthropogenic disturbances may result in the observed fluctuations since stream flow is already very low. Moreover, between 1 March 2017 and 1 May 2017, basin response to similar storm events is different as it can be seen in Figure 4.15. This may be due to the pressure sensor used in measuring the Çakıt Basin. For low flows pressure sensor is not so dependable. Therefore, through the whole observation period, the most consistent events are selected as the calibration and validation periods. Therefore, event-based model is calibrated for the storm event that occurred for 5-days in April 2018 and model is validated for storm event starts in May 2018. Auto-calibration is followed by manual calibration for the event-based model for fine tuning. Calibration is carried out for the selected methods using a set of performance evaluation criteria, which are *NSE*, *PBIAS*, *RMSE*, and R^2 values. Required inputs and calibrated parameters of used methods are listed in Table 4.12.

Table 4.12. Required inputs and calibrated parameters of used methods in event-based model

<i>Method</i>	<i>Input Parameters</i>	<i>Calibrated Parameters</i>
SCS CN	Initial Abstraction, Impervious Area Percent and Curve Numbers	Initial Abstraction and Impervious Area Percent
SCS UH	Lag Time	Lag Time
Recession	Ratio to The Peak Value and Recession Constant	Ratio to The Peak Value
Muskingum	Storage Constant and Weighting Factor	Storage Constant

“SCS CN” method has three inputs for simulating runoff processes, which are curve number, initial abstraction, and impervious area percent. Curve numbers are not calibrated; however, initial abstraction and impervious area percent values are calibrated to adjust rainfall runoff relationship of the basin. Also, the “SCS-UH” transform method input, lag time, is calibrated. Calibrated values are provided in Table

4.13. Moreover, the ratio to the peak value of the “Recession” baseflow method and the storage constant, K , values for “Muskingum” methods are calibrated, and they are provided in Table 4.14.

Table 4.13. Calibrated parameters used in the event-based model

<i>Sub-basin Code</i>	<i>SCS CN</i>		<i>SCS UH</i>	<i>Recession Baseflow</i>
	<i>Initial Abstraction (mm)</i>	<i>Impervious Area Percent (%)</i>	<i>Lag time (min)</i>	<i>Ratio to Peak</i>
W370	70	2.5	250	0.40
W380	35	2.0	200	0.50
W960	65	5.0	140	0.60
W250	60	4.0	220	0.70
W910	50	2.0	100	0.50
W210	55	3.0	220	0.45
W260	50	5.0	180	0.30
W900	70	4.0	120	0.30
W280	55	2.0	100	0.25
W230	60	6.0	170	0.50
W220	60	2.0	180	0.50
W240	50	1.0	180	0.40

Table 4.14. Calibrated routing parameters used in the event-based model

<i>Reach</i>	<i>Length (m)</i>	<i>Muskingum K (hour)</i>
R980	4,787	4.0
R150	250	1.0
R180	4,359	3.5
R110	1,675	2.0
R40	7,080	6.0
R90	2,552	2.0
R100	1,545	1.0
R80	5,623	5.0
R60	8,211	7.0

4.4. Case 2 - Continuous Model Setup

The continuous model is developed for simulating long term events with daily time steps for Çakıt Basin according to Çakıt SGS. Moreover, Darboğaz Basin, which is a sub-catchment of Çakıt Basin is used for model calibration as well. Specifications of continuous model simulation of Çakıt Basin is provided in Table 4.15.

Table 4.15. Continuous model specifications

<i>Basin Model Parameters</i>		<i>Meteorological Model Parameters</i>	
Loss Method	Deficit and Constant	Precipitation	Specified Hyetograph
Transform Method	SCS UH	Evapotranspiration	Specified
Routing Method	Muskingum	Snowmelt	Px Temperature
Baseflow Method	Recession	Control Specification	One day

“Deficit and Constant” method is used for loss calculations in the transferred basin model from HEC-GeoHMS. For the “Deficit and Constant” method, the initial deficit, the maximum deficit, the constant rate, and the imperviousness values are required as inputs. Initial values are assigned to these inputs based on the ranges provided in User’s Manual of HEC-HMS (2018) and similar studies conducted with “Deficit and Constant” method. For the “SCS-UH” method, lag time is required as the input. The initial value is entered according to similar studies and the manual. The default unit hydrograph PFR of 484 is selected for peak rate factor. For the “Recession” baseflow method, the ratio to the peak value and recession constant are required as inputs. Moreover, for the “Muskingum” routing method the storage constant (K) and weighting factor (x) is required as inputs. Initially values are assigned for all the inputs based on similar studies and the manual. Similarly, snowmelt parameters are initially entered according to the suggestions of User’s Manual of HEC-HMS (USACE, 2018). Elevation values are specified for each sub-basin by using the area-weighted elevation of the DEM. Since there was no snow content at the beginning of the simulation, initial snow content inputs are set to zero. Initial deficit values are entered as 15 mm, Max

storage as 30 mm, constant rate as 1 mm/hr, impervious area as 1%, lag time as 1000 minutes, recession constant as 0.9 and ratio to peak as 0.5 for all the sub-basins. Moreover, storage constant (K) parameters are entered as 2 and weighting factor (α) as 0.15 and Max storage values for surface and canopy methods are entered as 10 and 2, relatively for all sub-basins.

The meteorological model, which is prepared in HEC-GeoHMS, is transferred to HEC-HMS. For this model, observed precipitation and calculated evapotranspiration values are used as inputs. Snowmelt is simulated using Px temperature method. Parameters of the model are first initialized based on the manual and later calibrated. Initial values used for snowmelt inputs of the continuous model are illustrated in Table 4.16.

Table 4.16. Initial values used for snowmelt inputs of the continuous model

<i>Snowmelt</i>	
Px Temp. (°C)	1.0
Base Temp. (°C)	0.0
Wet Melt rate (mm/°C day)	5.0
Rain Limit (mm/day)	0.0
Meltrate Coefficient	0.9
Cold Limit	0.0
Coldrate Coefficient	0.9
Water Capacity (%)	5.0
Groundmelt (mm/day)	0.0

The continuous model is created for daily time steps. Daily precipitation data obtained from Ulukışla WS is used. Evapotranspiration values are taken from study from Akyürek et al. (2019) in which evapotranspiration is calculated by Penman-Monteith method. Daily streamflow observations of Çakıt SGS and the Darboğaz SGS are used. Simulation starts on 9 September 2016 and ends on 30 September 2018 for calibration and starts on 1 October 2018 and ends on 1 July 2019 for validation. The time interval

of mathematical calculations is defined as one day. Continuous model is calibrated by using observed flow values at Çakıt SGS. To improve the model calibration, Darboğaz Basin is used for calibration as well. For calibration, streamflow observations at Çakıt SGS and Darboğaz SGS between 9 September, 2016 and 30 September, 2018 is used. The validation is carried out for Çakıt SGS between 1 October, 2018 and 1 July, 2019.

As it is stated in section 3.2.5 auto-calibration methods provided in HEC-HMS software are inefficient with snow parameters. Therefore, manual calibration is applied for the parameters of the selected methods. Required inputs and calibrated parameters of used methods are listed in Table 4.17.

Table 4.17. Required inputs and calibrated parameters of used methods in the event-based model

<i>Method</i>	<i>Input Parameters</i>	<i>Calibrated Parameters</i>
Deficit and Constant	Initial Deficit, Maximum Storage, Constant Rate, Impervious Area Percent	Constant Rate and Impervious Area Percent
Surface	Max Storage	Max Storage
Canopy	Max Storage	Max Storage
SCS UH	Lag Time	Lag Time
Recession	Ratio to The Peak Value and Recession Constant	Ratio to The Peak Value
Muskingum	Storage Constant and Weighting Factor	Storage Constant
Snowmelt	Px Temperature, Base Temperature, Wet Meltrate, Rain Limit, Meltrate Coefficient, Cold Limit, Coldrate Coefficient, Water Capacity, Groundmelt, Elevation bands	Px Temperature, Base Temperature, Wet Meltrate, Rain Limit, Meltrate Coefficient, Cold Limit, Coldrate Coefficient, Water Capacity, Groundmelt,

Parameters of the “Deficit and Constant” method are Constant Rate, and The Impervious Area Percent which are calibrated together with parameters of “Surface” and “Canopy” methods. Also, the “SCS-UH” transform method’s input, the lag time, is calibrated. Moreover, the ratio to the peak value of the “Recession” baseflow method and *K* values for “Muskingum” methods are calibrated. Calibrated values for these parameters are provided in Table 4.18 and Table 4.19.

Table 4.18. Calibrated parameters used in the continuous model

<i>Sub-basin Code</i>	<i>Surface Method</i>	<i>Canopy Method</i>	<i>Deficit and Constant</i>		<i>SCS UH</i>	<i>Recession Baseflow</i>
	<i>Max Storage (mm)</i>	<i>Max Storage (mm)</i>	<i>Constant Rate (mm/hr)</i>	<i>Impervious Area Percent (%)</i>	<i>Lag time (min)</i>	<i>Ratio to Peak</i>
W370	25	2.0	1.2	5	3500	0.95
W380	25	2.0	1.5	3	2500	0.95
W960	18	2.0	1.5	3	1000	0.90
W250	19	1.0	1.8	3	800	0.95
W910	2	2.2	1.4	3	1300	0.90
W210	10	1.5	1.1	3	2000	0.90
W260	8	1.5	1.2	2	1300	0.80
W900	15	1.5	0.8	7	500	0.60
W280	9	1.0	1.1	6	1000	0.80
W230	13	0.5	1.8	9	1100	0.80
W220	5	0.5	2.0	8	1300	0.90
W240	2	0.5	1.4	8	1000	0.90

Table 4.19. Calibrated routing and snowmelt parameters used in the continuous model

<i>Muskingum</i>			Snowmelt	
<i>Reach</i>	<i>Length (m)</i>	<i>K (hour)</i>		
R980	4,787	4.0	Px Temp. (°C)	2.9
R150	250	1.0	Base Temp. (°C)	0.0
R180	4,359	3.5	Wet Meltrate (mm/°C day)	9.0
R110	1,675	2.0	Rain Limit (mm/day)	0.0
R40	7,080	6.0	Meltrate Coefficient	0.8
R90	2,552	2.0	Cold Limit	0.0
R100	1,545	1.0	Coldrate Coefficient	0.95
R80	5,623	5.0	Water Capacity (%)	15
R60	8,211	7.0	Groundmelt (mm/day)	0.0

4.5. Case 3 - Continuous Model without Snowmelt Setup

The continuous model is developed for simulating long term events with daily time steps for Çakıt Basin according to Çakıt SGS. In this case study calibrated model in Case 2 is used to understand importance of snowmelt mechanism for study area which is a snow affected area. In order to highlight the importance of the snowmelt in the continuous run, the hydrological model is simulated without the “Temperature Index” snowmelt method. In this case all the precipitation is assumed to be rain and partitioning between snow and rain is not applied. Specifications of model used for Case 3 is provided in Table 4.20.

Table 4.20. Continuous model without snowmelt specifications

<i>Basin Model Parameters</i>		<i>Meteorological Model Parameters</i>	
Loss Method	Deficit and Constant	Precipitation	Specified Hyetograph
Transform Method	SCS UH	Evapotranspiration	Specified
Routing Method	Muskingum	Snowmelt	Not used
Baseflow Method	Recession	Control Specification	One day

Basin model which is created during Case 2 and the same input parameters are used for this case. Once again, the same meteorological model is used. However, snowmelt method is not selected for this case; therefore, no snow calculations are included in model. Similar to Case 2, the continuous model without snowmelt is created for daily time steps. Daily precipitation and evapotranspiration data are used. Daily streamflow observations of Çakıt SGS and the Darboğaz SGS are used. Simulation is done for same time intervals of Case 2. However, both calibration and validation time intervals of Case 2 are used for validation of the Case 3. Simulations starts on 9 September 2016 and ends on 30 September 2018 and starts on 1 October 2018 and ends on 1 July 2019. The time interval of mathematical calculations is defined as one day.

CHAPTER 5

RESULTS OF CALIBRATION AND VALIDATION OF CASE STUDIES

In this chapter, results of calibration and validation of case studies are presented.

5.1. Case 1 - Event-based Model Results

The comparison of the streamflow obtained as a result of the event-based model calibration with the flow values measured at Çakıt SGS is given in Figure 5.1. As it can be seen in Figure 5.1, calibrated and observed flows are in good agreement. Timing of the simulated peak flows are well-matched with that of the observed flows. The *NSE*, *PBIAS* and R^2 values are calculated as 0.91, 3.0, and 0.92, respectively. Moreover, *RMSE* is calculated as 0.51, while the standard deviation of observed flow is 1.69. Performance qualitative ratings for the model can be classified as “very good” according to Table 2.3. The model is validated using the storm event occurred for 8-days between 28 May to 4 June 2018. The results are given in Figure 5.2. For the validation period, timing of the simulated peak flows is generally in agreement with that of the observed values. The *NSE*, *PBIAS* and R^2 values are calculated as 0.84, 3.48, and 0.94, respectively. Moreover, *RMSE* is calculated as 1.9, while standard deviation of observed flow is 4.8. Performance qualitative ratings for the model can be classified as “good” according to Table 2.3. The scatter plot of calibration period is given in Figure 5.3 and scatter plot of validation is given in Figure 5.4

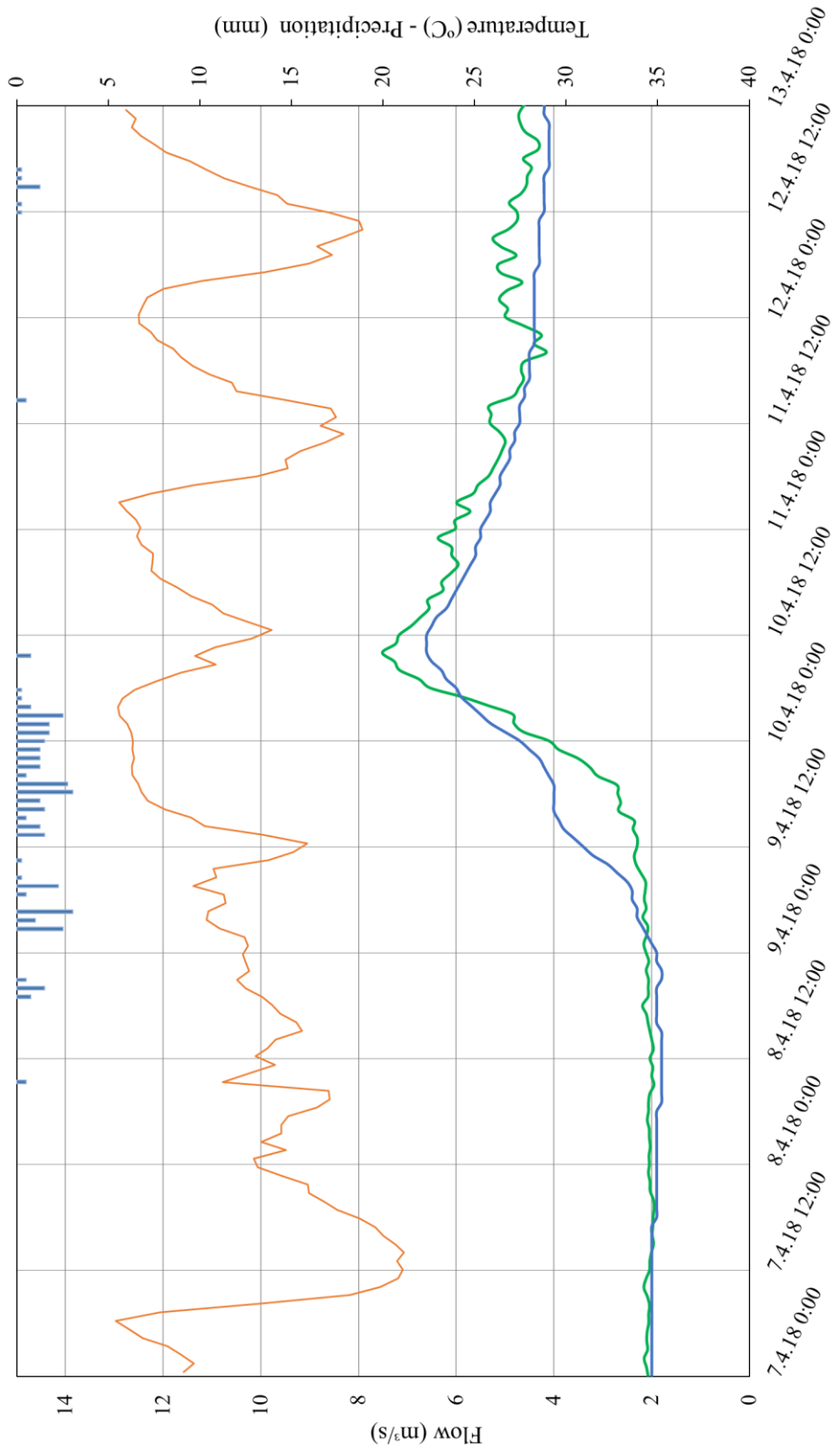


Figure 5.1.1. Event-based model calibration for Çakıt SGS between 7 April, 2018 and 13 April, 2018

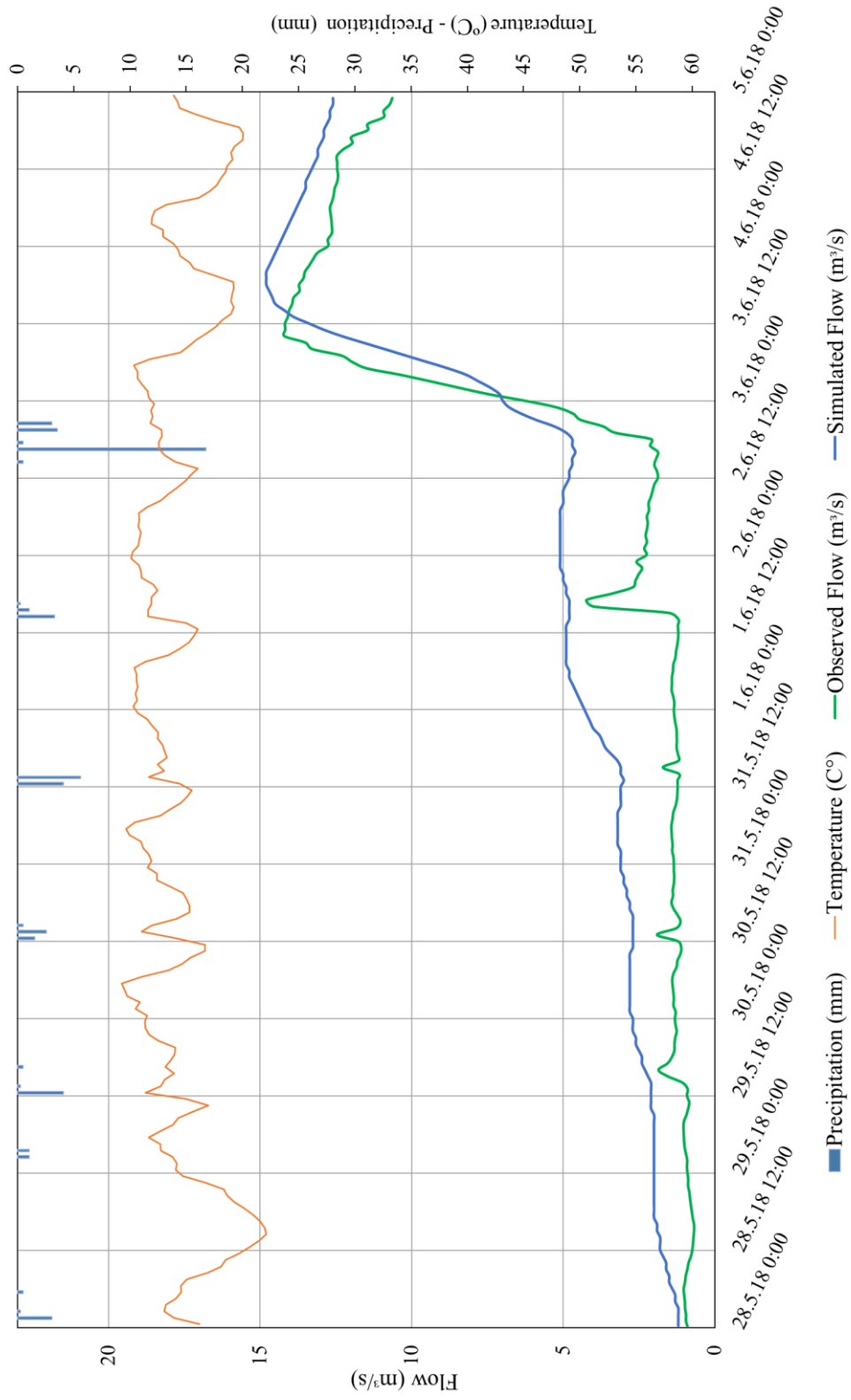


Figure 5.2. Event-based model validation for Çakıt SGS between 28 May, 2018 and 5 June, 2018

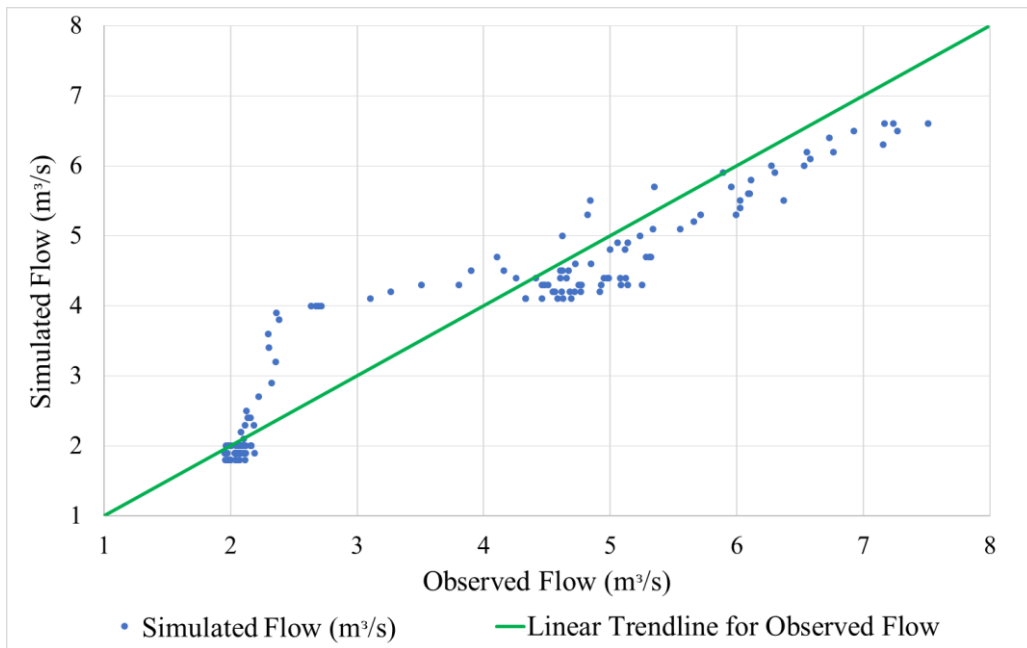


Figure 5.3. Scatter plot for event-based model calibration for Çakıt SGS in between 7 April, 2018 and 13 April, 2018

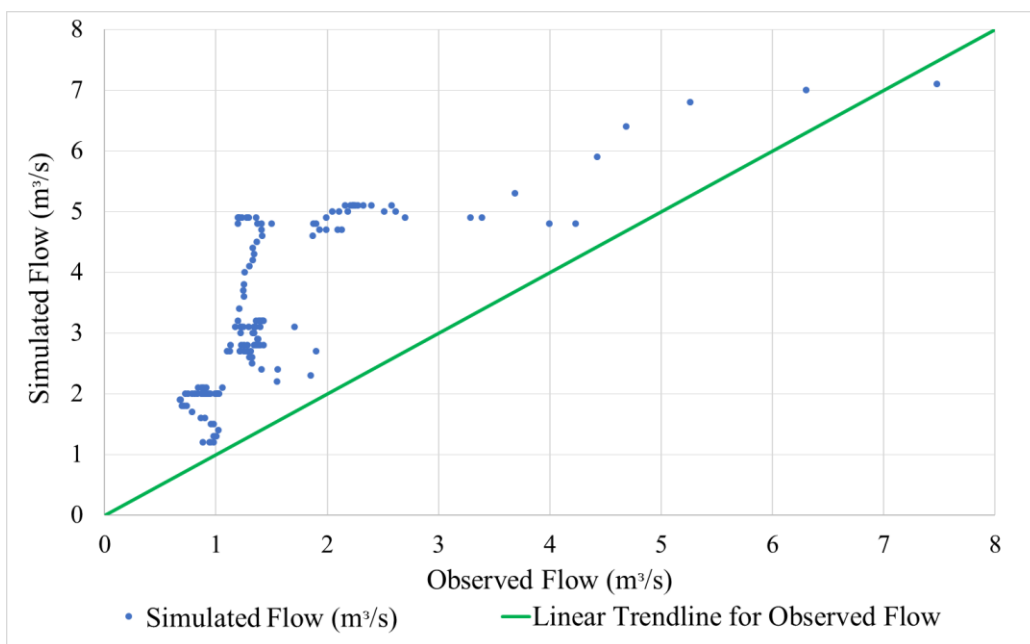


Figure 5.4. Scatter plot for event-based model validation for Çakıt SGS in between 28 May, 2018 and 5 June, 2018

These results indicate that the calibrated event-based model for Çakıt SGS is capable of simulating the storm events. Utilizing “SCS CN” method for loss, “SCS UH” method for transform, “Recession” for baseflow and “Muskingum” method for routing calculations resulted in a well calibrated hydrologic model for Çakıt Basin.

“Muskingum” method is based on the differential equation of storage. Storage is represented by 2 different parameters as linear function of inlet and outlet. These parameters are not calibrated with observation data. However, calibrated wave travel time values of sub-basins are proportional to distances of each sub-basins to outlet.

All of the studies evaluated in the literature review suggested that evapotranspiration can be ignored for the event-based model. In order to verify this suggestion, runs including and excluding evapotranspiration are carried out. To include evapotranspiration, daily observed evapotranspiration value is converted to hourly data. Results for the calibration period proved that ignoring evapotranspiration did not negatively affect the event-based model performance. The *NSE*, *PBIAS* and R^2 values are calculated as 0.91, 3.0, and 0.92, respectively for both cases (i.e., including and not including evapotranspiration). Moreover, *RMSE* is calculated as 0.51 when evapotranspiration is included, while it is 0.56 for the case without evapotranspiration.

Scatter plot of the calibration period shows that higher flow rates are simulated better with the model. Also, it is observed that the model over estimates low flows. Simulated flow values are higher than observed values for the validation period as it can be seen in scatter plot which is given in Figure 5.4. Multiple storm events in validation period are not simulated accurately by the model. In order to better calibrate the model, longer periods with multiple storms need to be used. However due to limited data, this could not be achieved in the current study.

5.2. Case 2 - Continuous Model Results

The continuous model is built for both Darboğaz and Çakıt basins. Darboğaz sub-basin is composed of five sub-basins (i.e. W370, W380, W960, W900, W910 Figure 4.12) and it has a drainage area of 179 km² (Table 4.1). In the continuous model

calibration, first Darboğaz sub-basin is calibrated, then Çakıt basin is calibrated. This eased the calibration process and resulted in improved model performance.

The calibration period is between 9 September 2016 and 30 September 2018 while the validation is between 1 October 2018 and 1 July 2019. In the continuous model, utilizing “Deficit and Constant” method for loss, “SCS UH” method for transform, “Recession” for baseflow and “Muskingum” method for routing calculations with Temperature Index method for snowmelt resulted in a well calibrated hydrologic model for Çakıt Basin. As explained in Section 4.5, for regions such as Çakıt basin where snowmelt has a considerable contribution in the streamflow, a snowmelt method has to be used while building the continuous hydrological model. The significance of the snowmelt method is demonstrated in this study through comparison of Case 2 and Case 3.

The comparison of the simulated flow and observations at Çakıt SGS for the calibration period is given in Figure 5.5, and comparison for Darboğaz SGS is given in Figure 5.6.

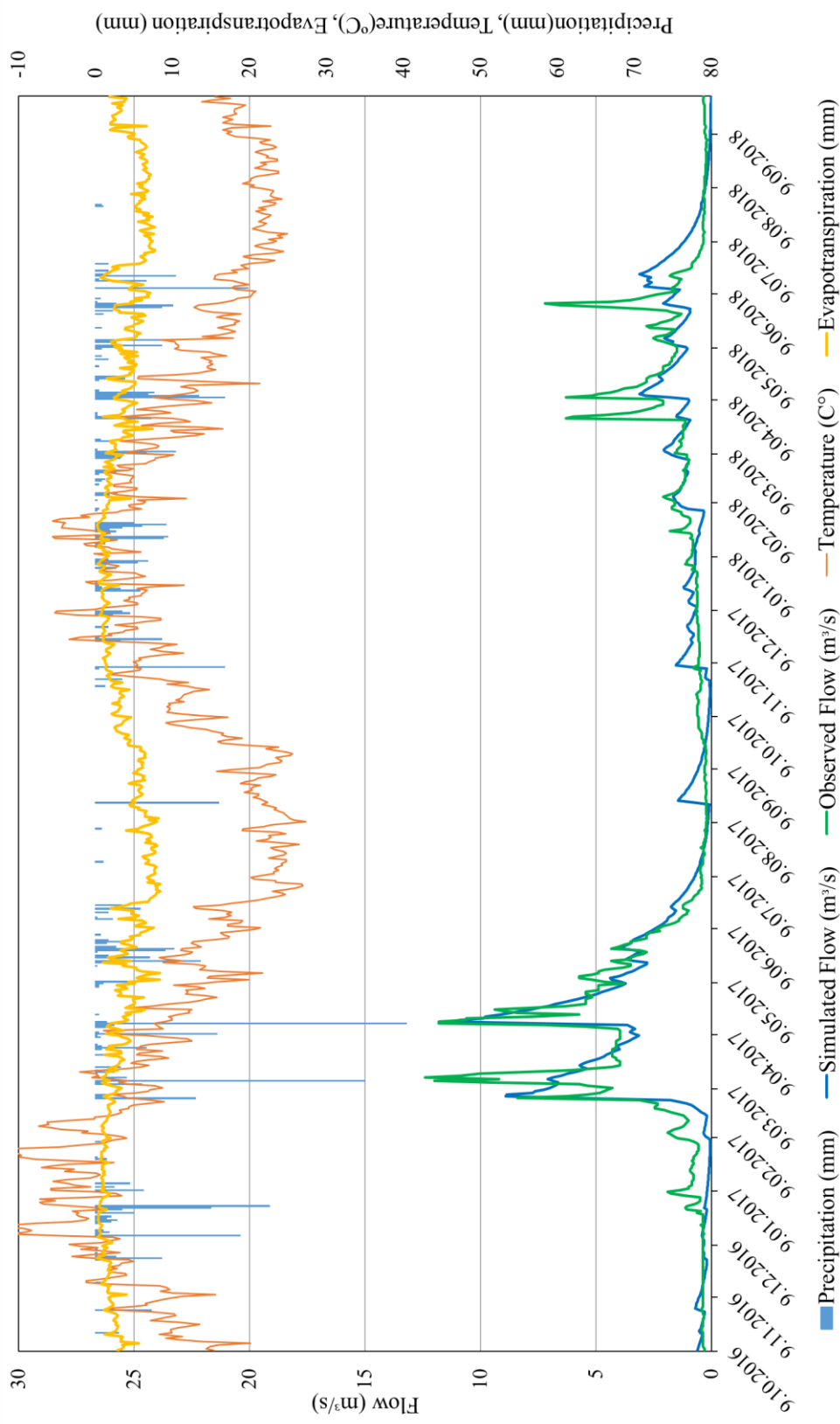


Figure 5.5. Continuous model calibration for Çakıt SGS between 9 September, 2016 and 30 September, 2018

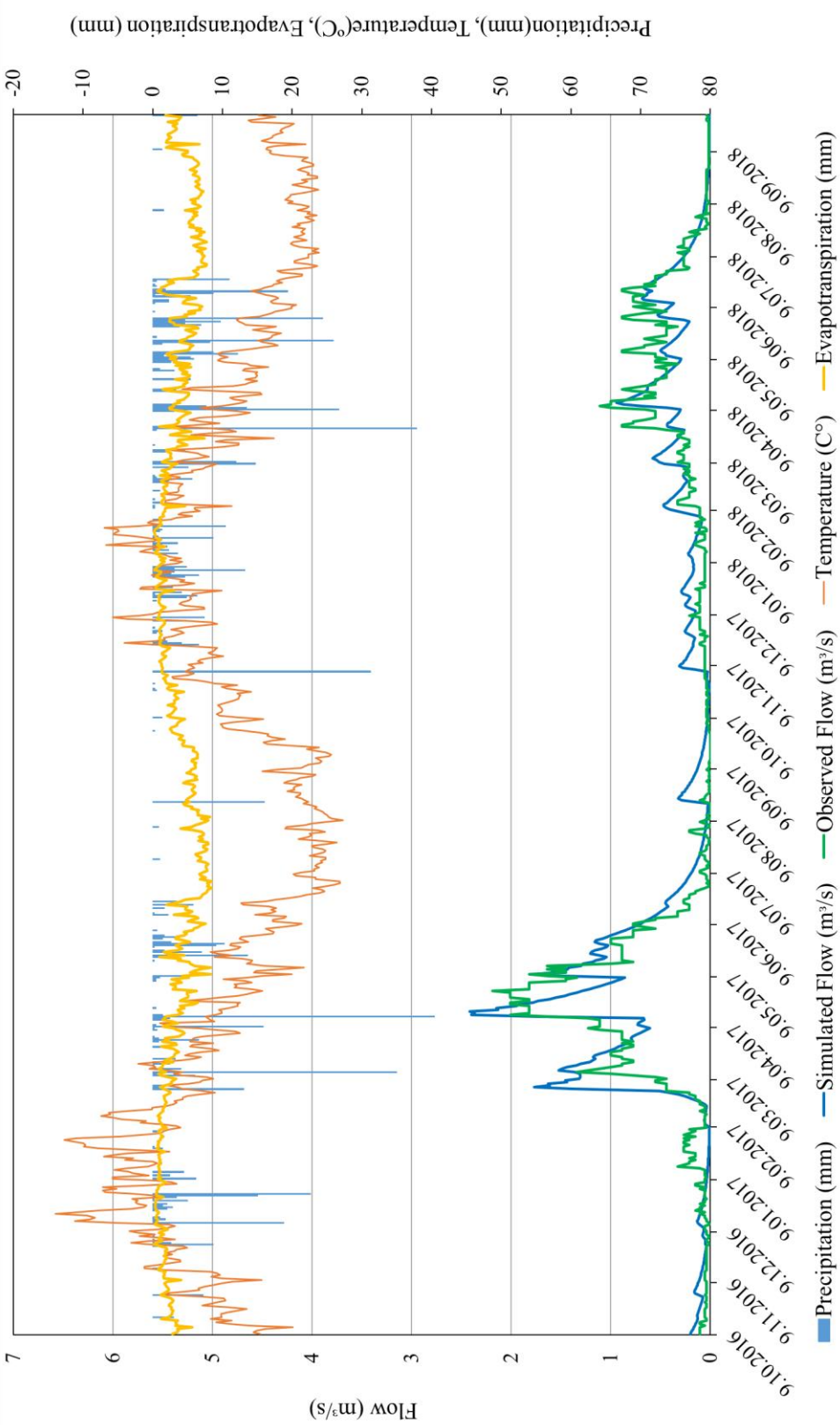


Figure 5.6. Continuous model calibration for Darboğaz SGS between 9 September, 2016 and 30 September, 2018

As can be seen from Figure 5.5 and Figure 5.6, simulated and observed flows are consistent. Timing of the simulated peak flows are generally in agreement with those of the observed flows. For Çakıt SGS, *NSE*, *PBIAS* and R^2 values are calculated as 0.78, 10.1, and 0.78, respectively. Moreover, *RMSE* is calculated as 0.91, while the standard deviation of observed flow is 1.94. For Darboğaz SGS, the *NSE*, *PBIAS* and R^2 values are calculated as 0.75, 8.46, and 0.77, respectively. Moreover, *RMSE* is calculated as 0.20, while the standard deviation of observed flow is 0.43. Performance qualitative ratings for both SGS can be classified as “good” according to Table 2.3.

Model validation for Çakıt SGS between 1 October 2018 and 1 July 2019 is illustrated in Figure 5.7. For the validation period the timing of the simulated peak flows is generally in agreement with those of the observed flows. *NSE*, *PBIAS* and R^2 values are calculated as 0.64, 15, and 0.70, respectively. Moreover, *RMSE* is calculated as 0.88, while the standard deviation of observed flow is 1.47. Performance qualitative ratings for the model can be classified as “satisfactory” according to Table 2.3. Model validation for Darboğaz SGS between 1 October 2018 and 1 July 2019 is illustrated in Figure 5.8. For the validation period the timing of the simulated peak flows is generally in agreement with those of the observed flows. *NSE*, *PBIAS* and R^2 values are calculated as 0.51, 8.7, and 0.51, respectively. Moreover, *RMSE* is calculated as 0.41, while the standard deviation of observed flow is 0.69. Performance qualitative ratings for the model can be classified as “satisfactory” according to Table 2.3.

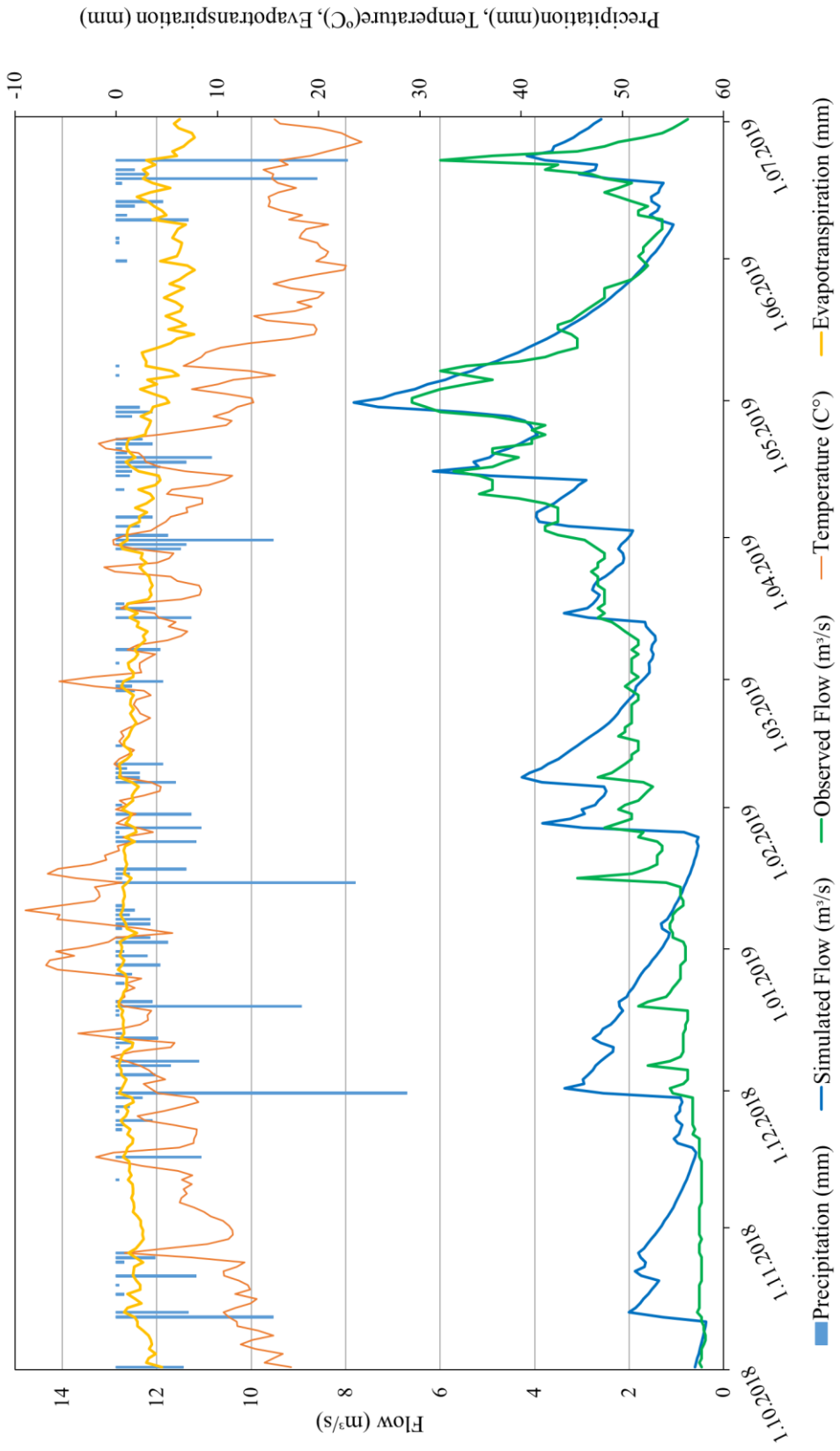


Figure 5.7. Continuous model validation for Çakıt SGS between 1 October, 2018 and 1 July, 2019

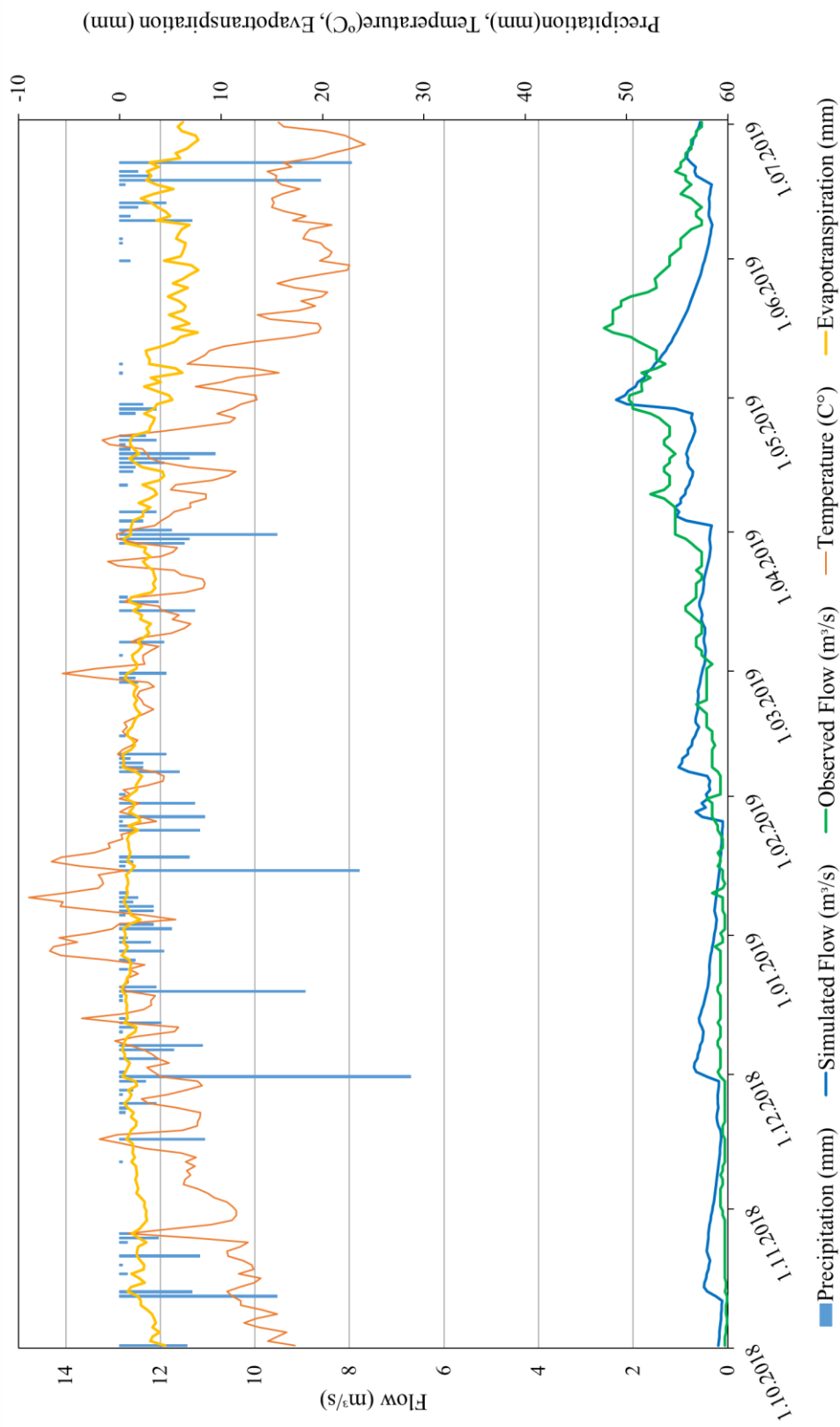


Figure 5.8. Continuous model validation for Darboğaz SGS between 1 October, 2018 and 1 July, 2019

Moreover, simulated snow water equivalent (SWE) is evaluated with respect to the observed values. SWE is not measured in study area but snow depths are measured. However, SWE can be determined by using snow depth and density of the snow according to the following formulation of USDA (2019):

$$\text{SWE} / \text{Snow Density} = \text{Snow Depth} \quad (14)$$

Typical values for snow densities are 10-20% in the winter and 20-40% in the spring (USDA, 2019). Snow density is identified as 0.18 for this study based on the field study conducted on 29 January 2018. Snow depths are measured at Darboğaz WS which is located within the boundaries of sub-basin W910. Location of the Darboğaz WS can be seen in Figure 4.1 and location of W910 can be seen in Figure 4.12. The median elevation value of the sub-basin W910 is close to 2314 meters which is presented on the hypsometric curve which is presented in Figure 4.6. Average elevation of the sub-basin W910 is 2207 meters whereas Darboğaz WS is located at an elevation of 1580 m.

Snow depths measured at Darboğaz WS are used to determine SWE by using measured snow density. These values are compared with simulated SWE in sub-basin W910 and results are represented in Figure 5.9.

Most of the W910 sub-basin is above 2000 meters which shows that it is a snow dominated basin. Therefore, including snow mechanism is important for this study area. Snowmelt algorithm of “Temperature Index” Method is provided in Figure 3.5 and parameters of this method are explained in Appendix B. According to the mechanism of this method, some part of the precipitation is assumed to be in the snow form when temperature is less than the specified value which is called Px Temperature. This value is selected as 2.9 °C during the calibration studies. Observed precipitation and temperature values are presented with Px temperature for both calibration and validation periods in Figure 5.10.

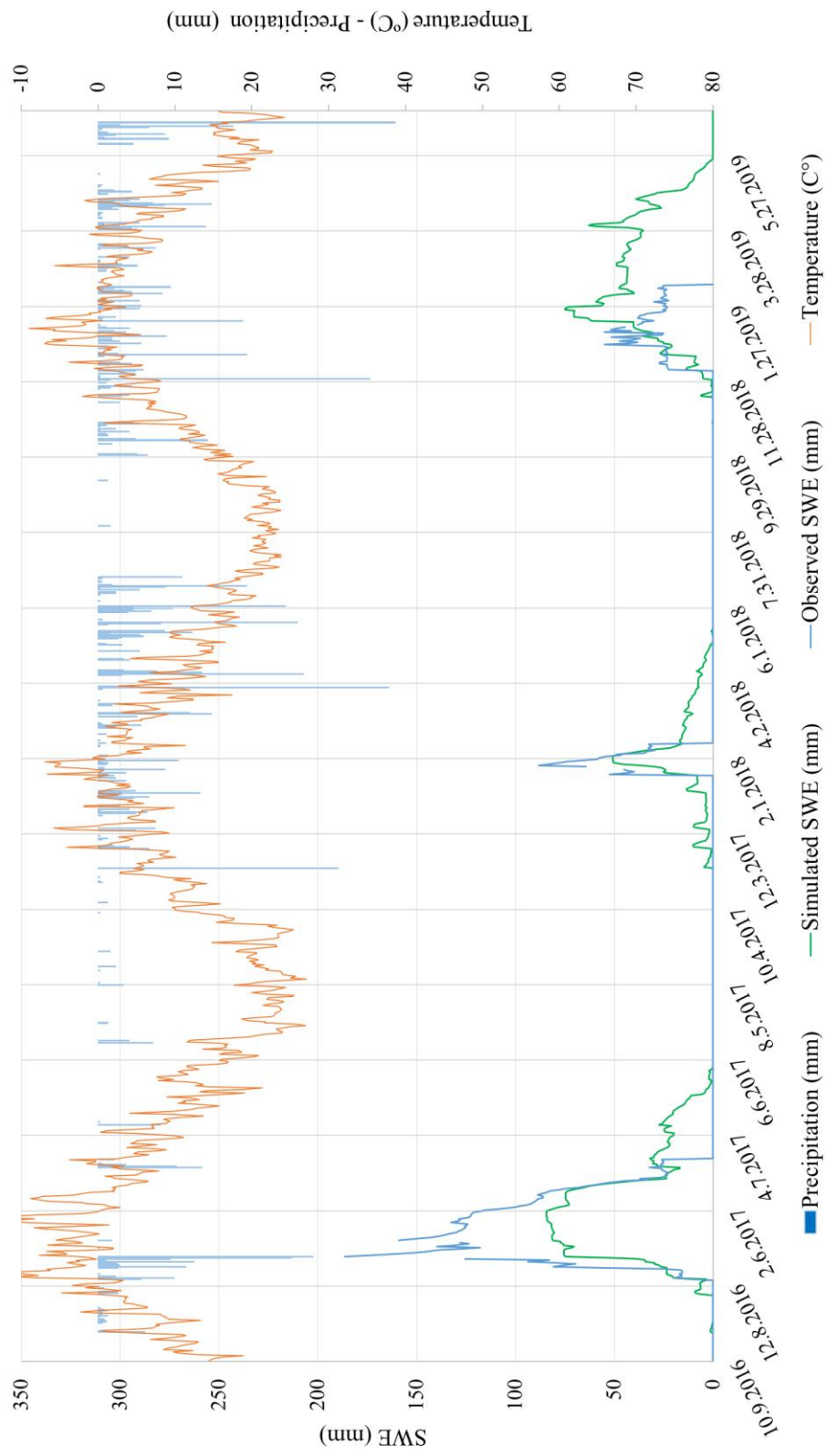


Figure 5.9. Comparison of simulated and observed SWE

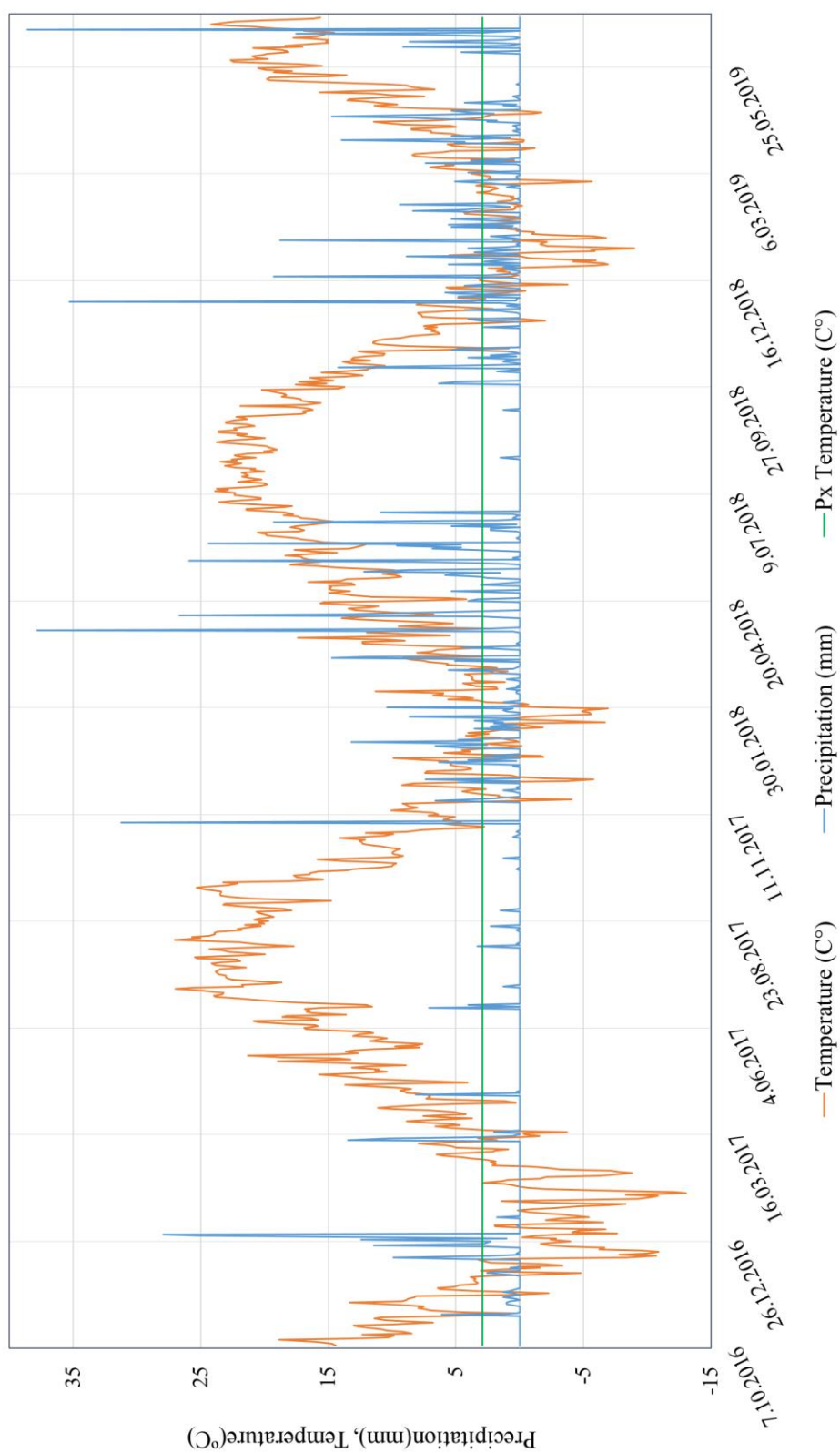


Figure 5.10. Observed temperature and precipitation values between 9 September, 2016 and 1 July, 2019.

The SWE values obtained for the basin show variation for the modelling period of years as can be seen in Figure 5.9. In 2017 snow depth observed in the area is higher than the values observed in 2018 and 2019. Not only the snow depth varies, the duration snow stays on the ground is long in 2017 compared to the other years. This situation is simulated quite well by the model, where the snow accumulation and melting timings are modelled well. It can be said that the SWE results of the model are quite successful for 2017 and 2018. The simulated and observed SWE values change in volume, the observed values are larger than the simulated values. This is due to the difference between the mean elevation of the sub-basin W910, which is 2207 m and the elevation of Darboğaz WS, which is 1580 m. Location of the Darboğaz WS can be seen in Figure 4.12. Snowmelt is expected to occur later in higher elevations and the simulation results for the sub-basin are lump values. In 2019 more rainfall is observed at Darboğaz WS, it is possible to get the snow melted by the rainfall at high elevations. It is the well know rain-on-snow problem where it is hard to model with degree-day snow melt modelling approach.

5.3. Case 3 - Continuous Model without Snowmelt Results

Çakıt basin is located in Niğde province where snow is important component of the streamflow (TSMS, 2019). In this study, as explained in the previous section, the continuous model built for Çakıt and Darboğaz basins simulates observed streamflow realistically. Case 3 is applied to show the importance of the snowmelt in the continuous run by eliminating snowmelt calculations. Basin model which is already calibrated during Case 2 is used with the same input parameters except snowmelt method. The comparison of the simulated flow and observations at Çakıt SGS for the calibration period of Case 2 without snowmelt is given in Figure 5.11.

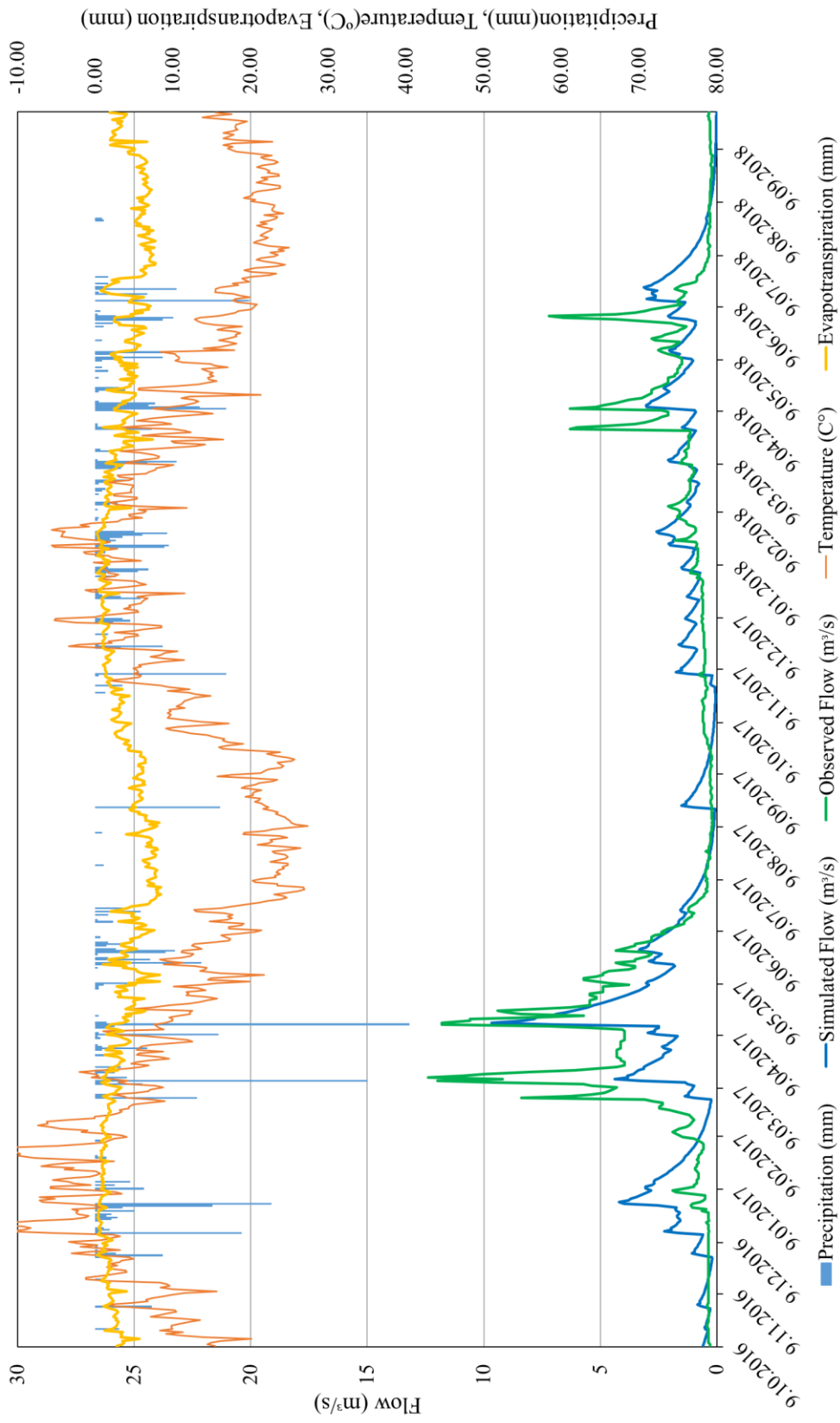


Figure 5.11. Results of continuous model without snowmelt for Çakıt SGS between 9 September, 2016 and 30 September, 2018

As can be seen from Figure 5.11, simulated flows are underestimated, especially during high flows. Timing of the simulated peak flows are generally in agreement with the observed flows but the agreement is not as good in terms of volume. For Çakıt SGS, *NSE*, *PBIAS* and R^2 values are calculated as 0.52, 14.5, and 0.54, respectively. Moreover, *RMSE* is calculated as 1.35, while the standard deviation of observed flow is 1.94. Performance qualitative ratings for both stream gauging stations can be classified as “satisfactory” according to Table 2.3.

The comparison of the simulated flow and observations at Çakıt SGS for the validation period of Case 2 without snowmelt is illustrated in Figure 5.12. For validation period the timing of the simulated peak flows is not in agreement with those of the observed flows. *NSE*, *PBIAS* and R^2 values are calculated as 0.35, 10, and 0.02, respectively. Moreover, *RMSE* is calculated as 1.71, while the standard deviation of observed flow is 1.47. Performance qualitative ratings for the model can be classified as “unsatisfactory” according to Table 2.3.

As can be seen from these results, ignoring snow effect decreases the performance of the continuous model significantly. However, for December 2018, simulated hydrograph of the continuous model without snowmelt is in slightly better agreement with observed values than the continuous model with snowmelt. This may be due to early snow melting in the simulation period than expected for areas which are located in high elevations. This is most probably due to the change of temperature with respect to altitude. Variation of temperature with elevation need to be better adjusted for the model to simulate flow with higher efficiency. This requires spatial distribution of temperature for the basin which needs meteorological stations at high altitudes. In this study mean elevation of the basin is used in the modelling.

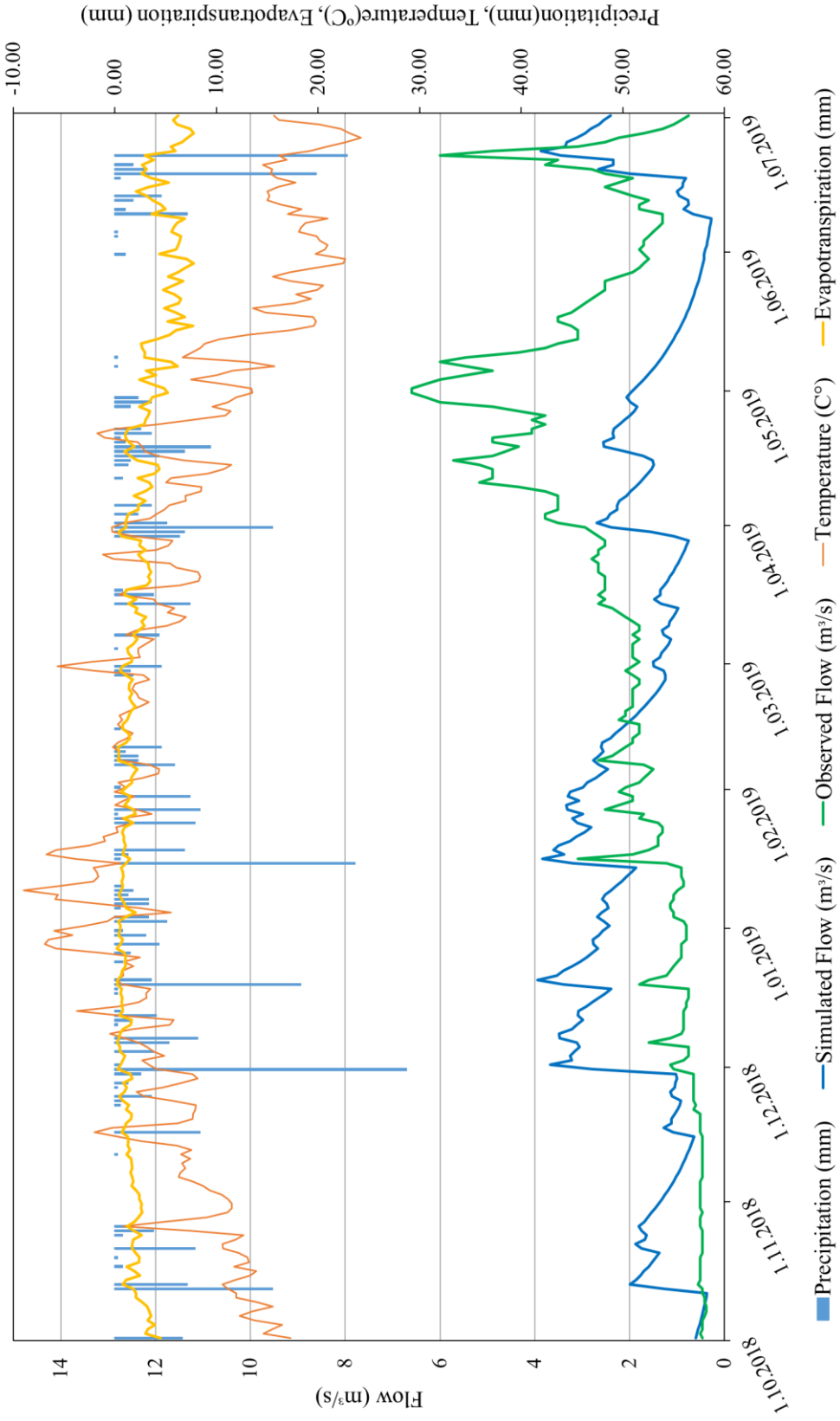


Figure 5.12. Results of continuous model without snowmelt for Çakıt SGS between 1 October, 2018 and 1 July, 2019

5.4. Comparison of Case 1 and Case 2

Performance of the event-based model (Case 1) and continuous model (Case 2) is compared in this section. Daily total flow volumes simulated in calibration and validation periods of the event-based and continuous models are compared. Average values for both observed and simulated flows are converted to the daily total volume. Results of these comparisons are given for 7 April, 2018 and 13 April, 2018 in Figure 5.13 and for 28 May, 2018 and 5 June, 2018 in Figure 5.14. These graphs prove that event-based models are more successful than continuous models especially for peak flow estimations. Utilization of event-based models is suggested for flood analysis in the literature and the findings of the current study is in line with this suggestion. For both periods provided in Figure 5.13 and Figure 5.14 event-based model simulated volumes are closer to observed volumes than continuous model simulated volumes, especially during peak discharges. Continuous model underestimates the total volume for the whole simulation period of event-based model.

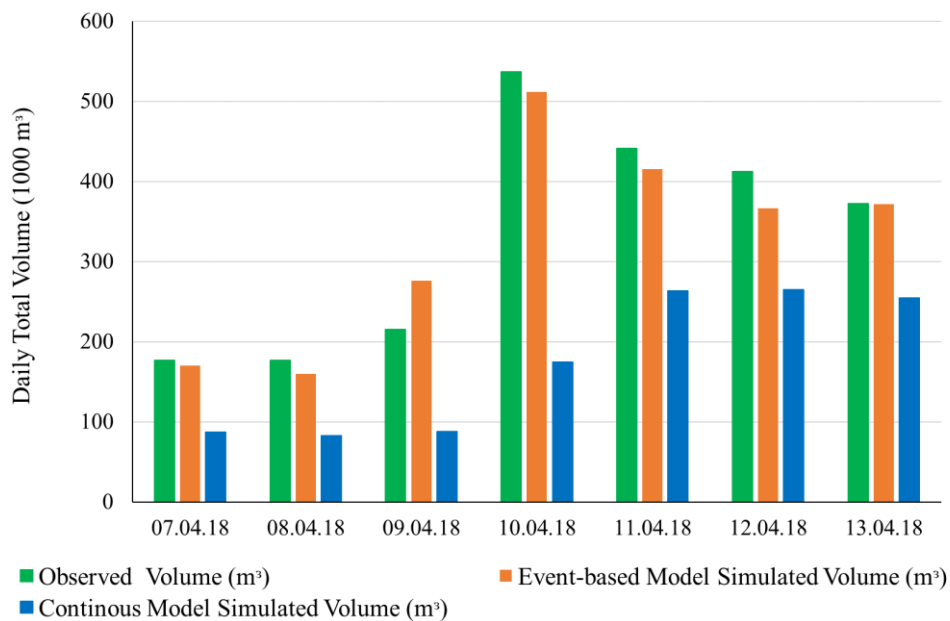


Figure 5.13. Daily total volume comparison of Case 1 and Case 2 between 7 April, 2018 and 13 April, 2018

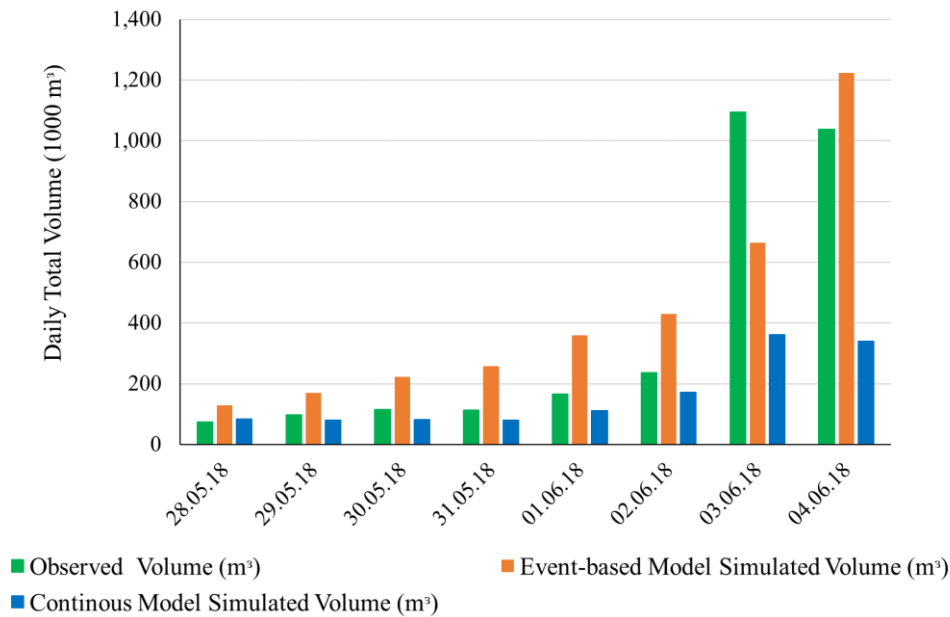


Figure 5.14. Daily total volume comparison of Case 1 and Case 2 between 28 May, 2018 and 5 June, 2018

5.5. Comparison of Case 2 and Case 3

Continuous model created with snowmelt method (Case 2) is compared with continuous model without snowmelt (Case 3) in this section. This comparison is done for better understanding of efficiency and importance of the snowmelt method for snow affected study areas. Although results of the continuous model without snowmelt are unsatisfactory, it is analyzed in more detail. For this reason, simulated flow for both models are compared with bar charts to understand deviations between these two model results and observations.

This comparison is made for dry and wet season for the duration of 2016 to 2019 which defined according to snow observed periods and climate conditions of the study area. Climate conditions of the study area is presented in Section 4.1.1. Differences with observed values for both cases are normalized according to Equation (15).

$$E_t = \frac{|Q_{o,t} - Q_{s,t}|}{Q_{o,t}} \times 100 \quad (15)$$

where E_t is the error at time t (%), $Q_{o,t}$ is the observed flow at time t , $Q_{s,t}$ is the simulated flow at time t .

Comparison of Case 2 and Case 3 with bar charts according to seasonal variation is provided for 9 September, 2016 and 9 May, 2017 in Figure 5.15, for 10 May, 2017 and 30 September, 2017 in Figure 5.16. Comparison for 1 October, 2017 and 10 May, 2018 in Figure 5.17, for the rest of the year till 30 September, 2018 in Figure 5.18. Similarly, for 1 October, 2018 and 9 May, 2019 in Figure 5.19 and for 1 October, 2018 and 9 May, 2019 in Figure 5.20.

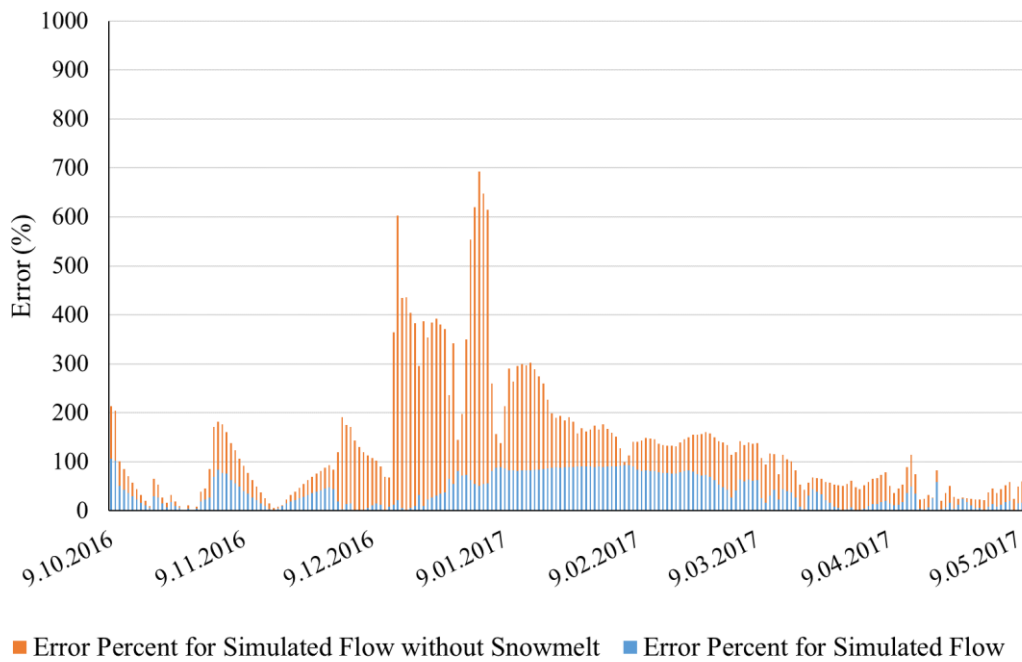


Figure 5.15. Percent errors in between 9 September, 2016 and 9 May, 2017

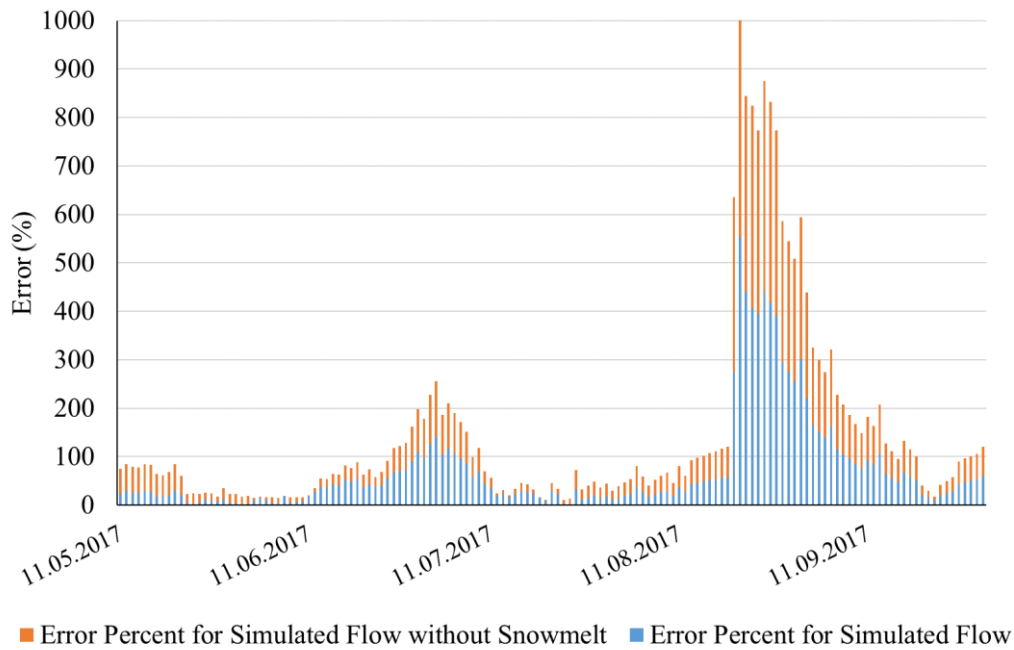


Figure 5.16. Percent errors in between 10 May, 2017 and 30 September, 2017

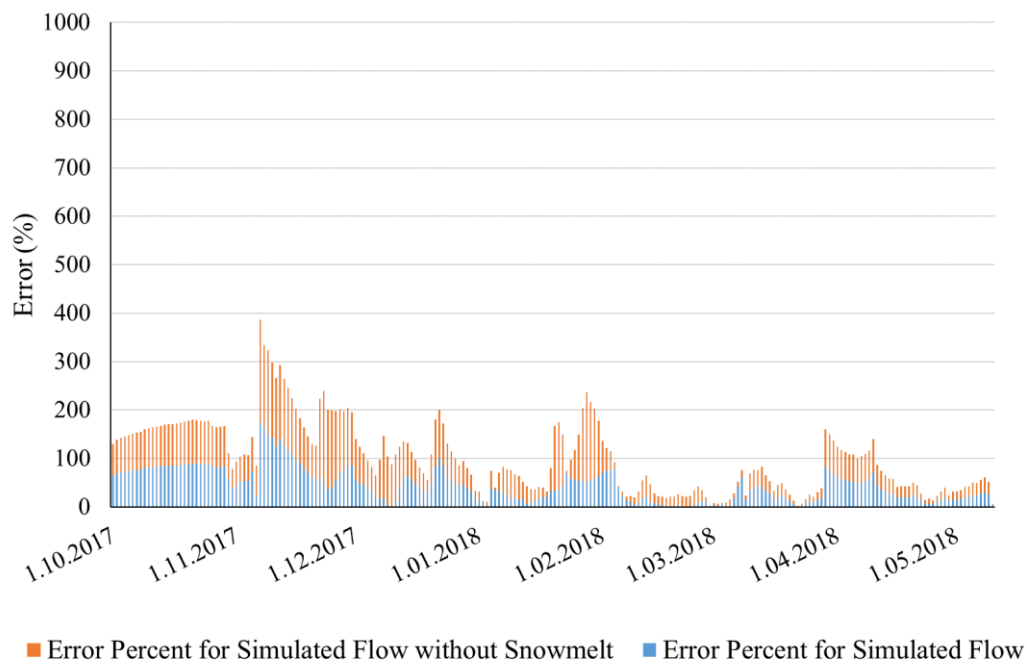


Figure 5.17. Percent errors in between 1 October, 2017 and 10 May, 2018

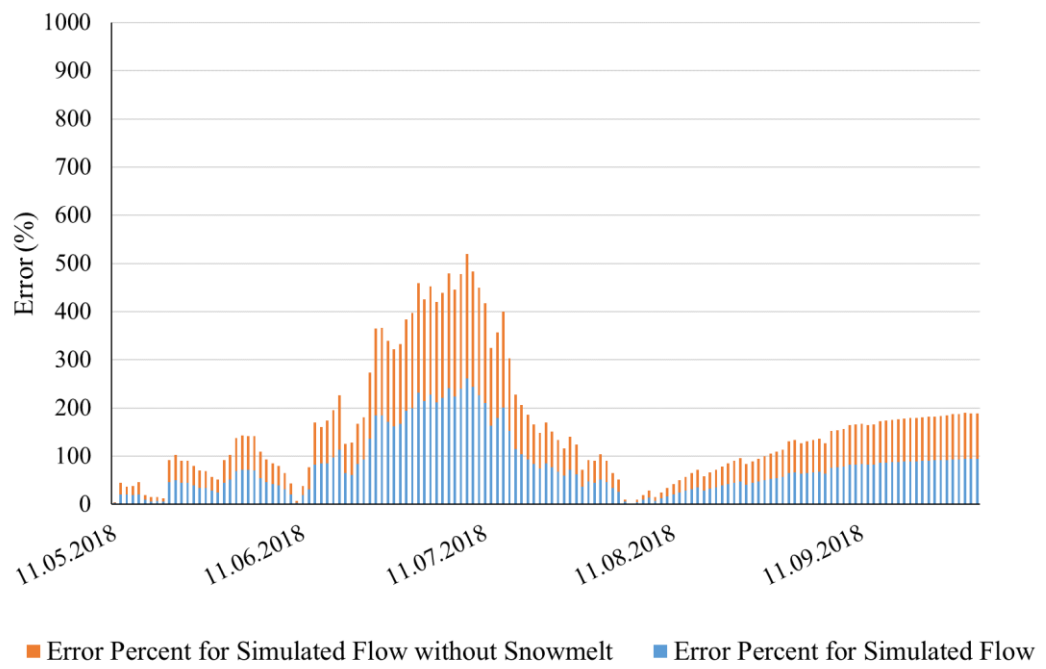


Figure 5.18. Percent errors in between 11 May, 2018 and 30 September, 2018

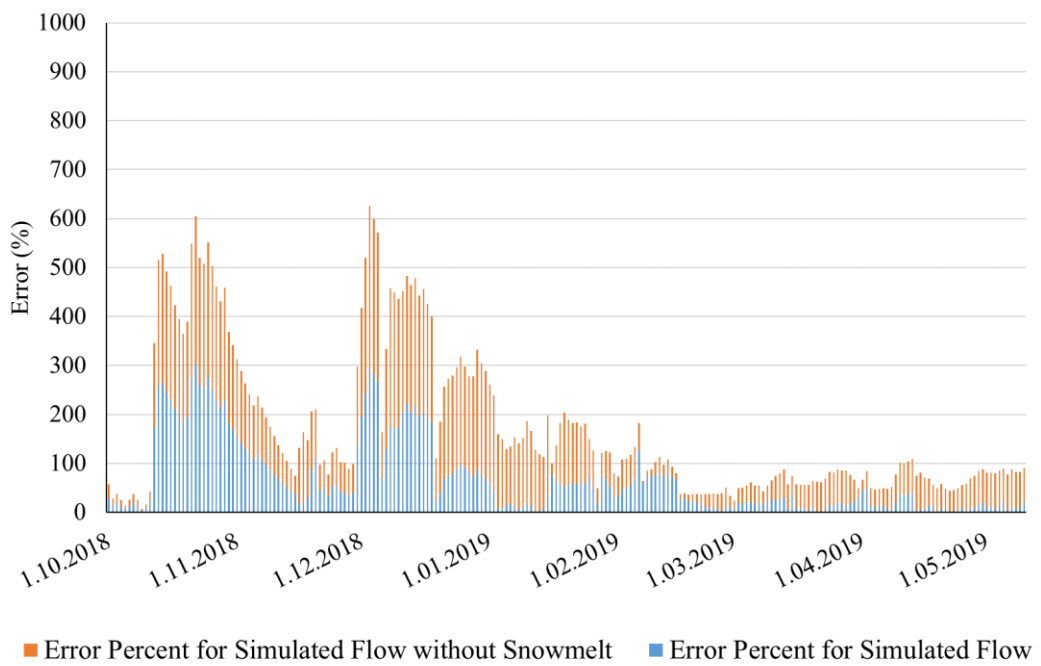


Figure 5.19. Percent errors in between 1 October, 2018 and 9 May, 2019

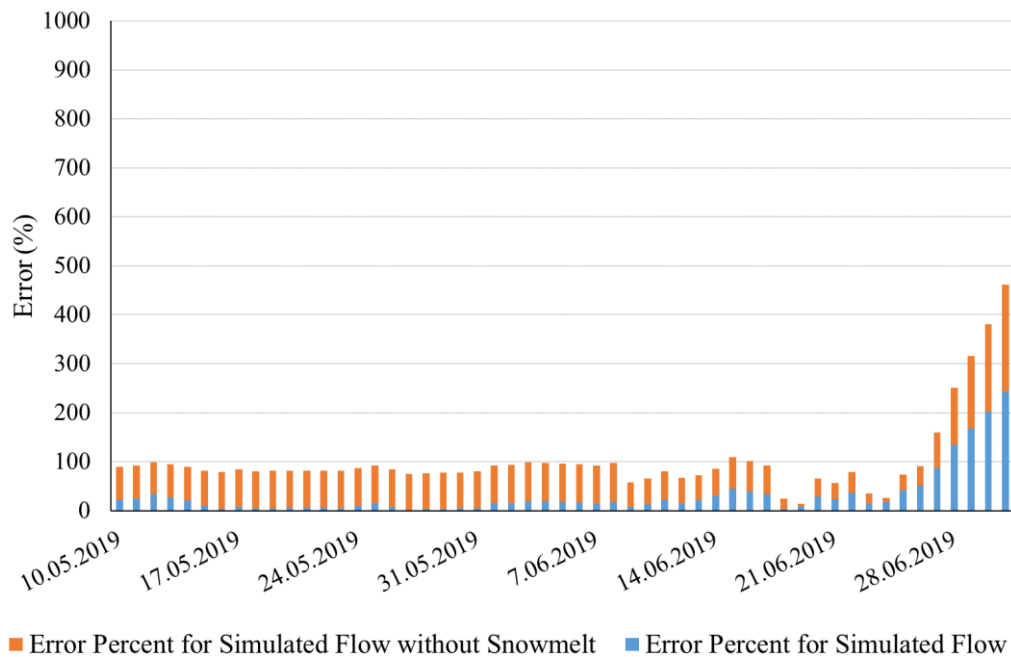


Figure 5.20. Percent errors in between 10 May, 2019 and 1 June, 2019

Percent errors are mostly higher for continuous model without snowmelt (Case 3) than continuous method (Case 2) as can be seen in Figure 5.15, Figure 5.16, Figure 5.17, Figure 5.18, Figure 5.19 and Figure 5.20. Percent errors are higher for snow affected periods which mainly starts from September and ends around May as can be seen in Figure 5.15, Figure 5.17 and Figure 5.19. Moreover, for dry periods, percent errors are very close to each other for both cases as can be seen in Figure 5.16, Figure 5.18 and Figure 5.20. These results demonstrate the importance of using snowmelt method, especially to obtain higher performance for high flow periods. Also, comparison of simulated flows is provided for Case 2 and Case 3 for Çakıt SGS between 9 September, 2016 and 30 September, 2018 in Figure 5.21 and for Case 2 and Case 3 for Çakıt SGS between 1 October, 2018 and 1 July, 2019 in Figure 5.22.

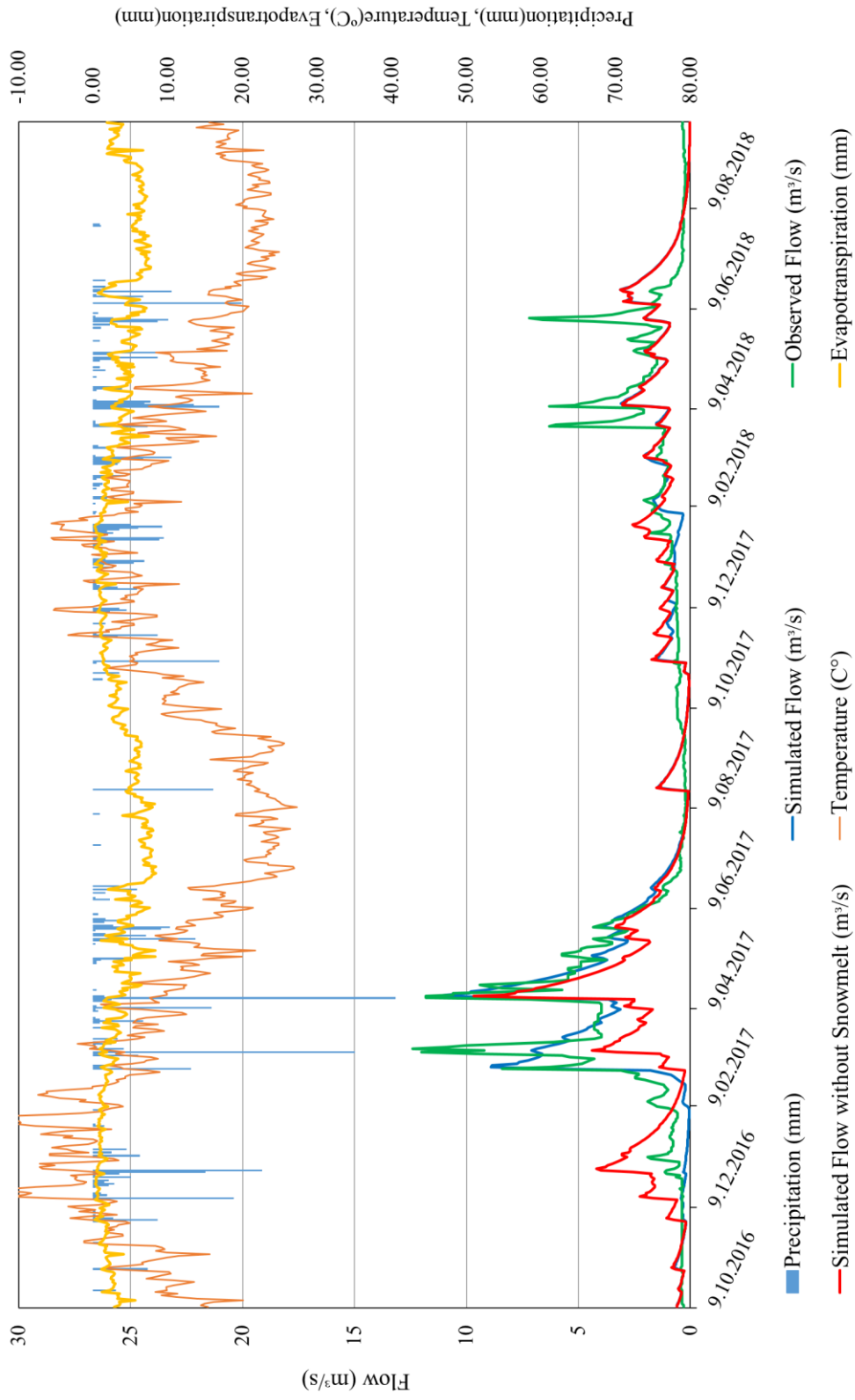


Figure 5.21. Comparison of Case 2 and Case 3 for Çakıt SGS between 9 September, 2016 and 30 September, 2018

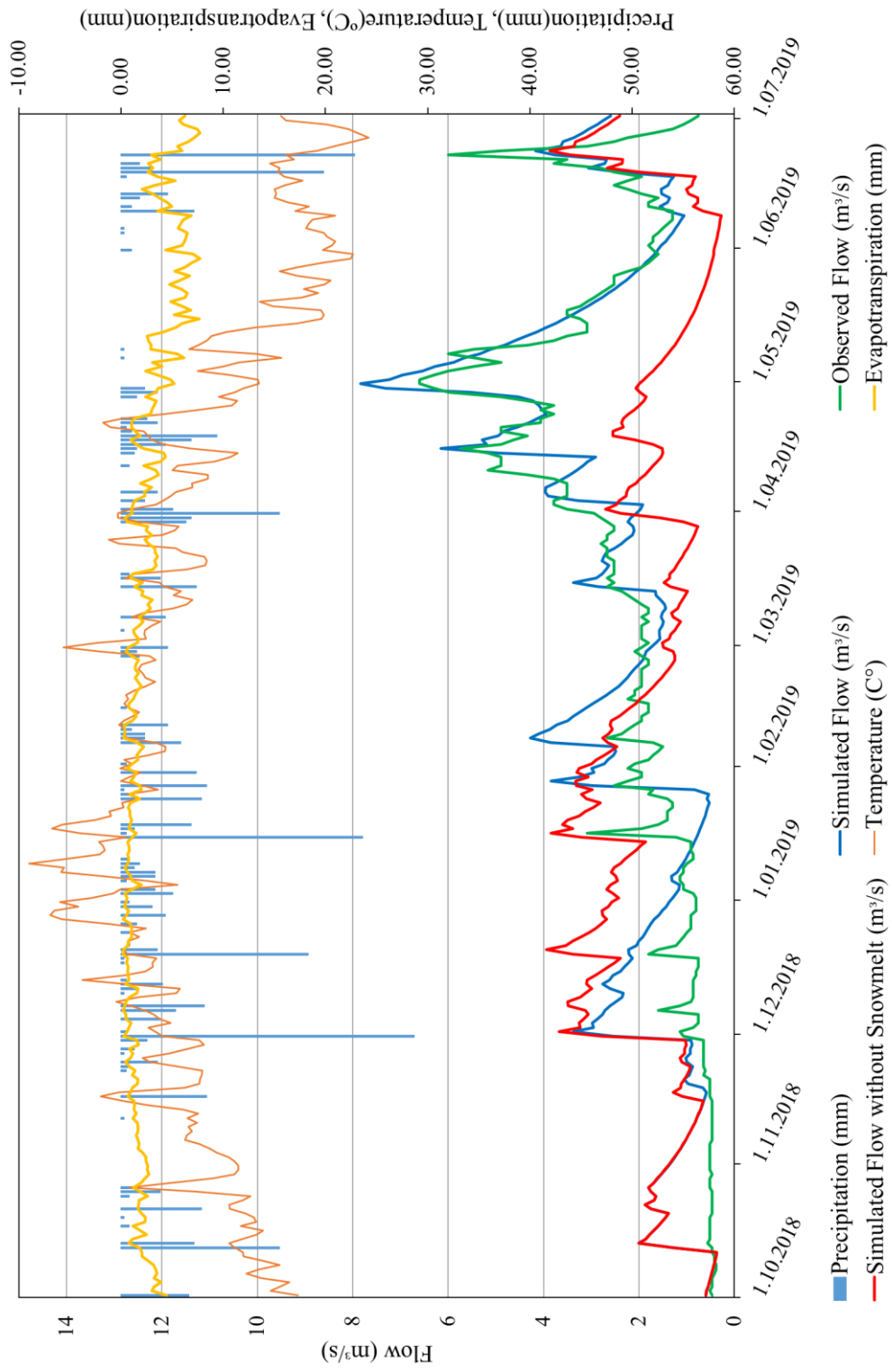


Figure 5.22. Comparison of Case 2 and Case 3 for Çakıt SGS between 1 October, 2018 and 1 July, 2019

In Case 3, “Temperature Index” snowmelt method is not used; in other words, effect of snowmelt is ignored. Since Çakıt Basin is located at a relatively high elevation, snowmelt is an important component of the streamflow. When snowmelt is not included in the continuous model, the performance of the model decreased considerably; especially the discrepancies become obvious in the peak flows. Since snow starts melting with the increase of temperatures in the spring, the contribution of snowmelt in the streamflow increases. When the snowmelt is ignored, this effect cannot be simulated by the model and the peak streamflow are underestimated.

5.6. Comparison of Low and High Flows

Performance of the continuous model is evaluated separately for observed flows less than $2 \text{ m}^3/\text{s}$ and higher than $2 \text{ m}^3/\text{s}$ in order to understand how model performs for low and high flows. The results of continuous model simulation are grouped according to the magnitudes of observed flows in order to examine performance of model for the calibration and validation periods. Observed flows in 566 days of the calibration period were less than $2 \text{ m}^3/\text{s}$ while remaining 156 days had higher flows than $2 \text{ m}^3/\text{s}$. For the validation period, in 172 days the flow was less than $2 \text{ m}^3/\text{s}$ while it was higher in 102 days. Performance evaluation results are given according to time periods in Table 5.1.

Table 5.1. Result for comparison of low and high flows

	<i>NSE</i>	<i>PBIAS</i>	R^2	<i>RMSE (SD)</i>
Low flows in calibration period	0.27	54.49	0.31	0.51 (0.45)
High flows in calibration period	0.44	15.28	0.59	1.69 (2.28)
Low flows in validation period	-0.37	-45.29	0.14	0.90 (0.55)
High flows in validation period	0.64	18.28	0.65	0.83 (1.30)

Results shows that the continuous model simulates flows higher than $2 \text{ m}^3/\text{s}$ better both for calibration and validation periods. Manual calibration of the continuous model was carried out focusing mainly on peak values. Therefore, it is expected to see

lower performance evaluation values for low flows. Better results can be obtained for low flows if calibration is carried out with high performance objective for low flows.

As it is seen in observations during the site visits and also in the measured values, streamflow of most of the tributaries in the study area are low (i.e. the base flow for Çakıt basin is less than $1 \text{ m}^3/\text{s}$ as can be seen in Figure 5.11). Potential point discharges may cause fluctuations in these low stream flows. Calibration is challenging when the streamflow is low and this is further pronounced when unnatural fluctuations occur due to point discharges. Although in general higher flow rates are estimated successfully, there are problems associated with low flows. As can be seen in Figure 5.11 there are very low flows which are very hard to measure in the Çakıt basin. These hard to measure flow rates are not accurate and they negatively affect the calibration performance as well. Moreover, it is concluded that using datasets with both low and high flowrates for calibration and validation of hydrological models may result in reducing uncertainty (Blasone, 2007).

5.7. Sensitivity Analysis

During the calibration process, it is observed that some parameters have more impact on results when compared to others. Therefore, sensitivity analysis is performed to see how the model responds to changes in model parameters and to find the most sensitive parameters. Knowledge of sensitive parameters can ease the manual calibration especially for cases like the continuous model established in this study which has many parameters to be calibrated. HEC-HMS model does not have built-in functions to do sensitivity analysis, therefore it is conducted manually. Both for event-based model and continuous model calibrated values are changed $\pm 10\%$, $\pm 15\%$ and $\pm 25\%$ to assess sensitivities of the model for the selected parameters.

5.7.1. Event-based Model Sensitivity

Required inputs and calibrated parameters for event-based model are given in Table 4.12. Along these parameters, sensitivity analysis is carried out for curve number, initial abstraction, impervious area percent parameters of “SCS CN” method, lag time

parameter of “SCS UH” method, ratio to the peak value parameter of “Recession” method and storage constant, and weighting factor parameters of “Muskingum” method. Sensitivity analysis is not done for the recession constant of “Recession” baseflow method since it is selected from a narrow interval and changes in performance evaluations were not significant as observed during the calibration process. Performance evaluations for sensitivity analysis are provided in Table 5.2. Moreover, results of sensitivity analysis according to Nash-Sutcliffe Efficiency are provided in Figure 5.23. In Figure 5.23 there is a comparison between NSE values of calibrated model and values that are achieved by changing the parameter ($\pm 10\%$, $\pm 20\%$, $\pm 25\%$) which is used for the sensitivity analysis. For example, NSE value calculated by changing CN value by $+25\%$ is compared with NSE value of the calibrated model in order to see the effect of $+25\%$ change in CN on Nash-Sutcliffe Efficiency. For better understanding, NSE relative changes are normalized according to Equation (16).

$$NSE_R = \frac{|NSE_C - NSE_S|}{NSE_C} \times 100 \quad (16)$$

where NSE_R is the relative NSE change (%) according to the parameter change which is taken as $\pm 10\%$, $\pm 20\%$, $\pm 25\%$ in this study, NSE_C is the NSE value of the calibrated model, and NSE_S is the NSE value of the model where the parameter has been changed.

Table 5.2. Results of sensitivity analysis for event-based model

<i>Parameter</i>	<i>Change</i>	<i>R</i> ²	<i>NSE</i>	<i>PBIAS</i> (%)	<i>RMSE</i> (<i>SD</i>)
Curve Number	-25%	0.87	0.78	7.29	0.67
	-15%	0.88	0.86	6.34	0.63
	-10%	0.89	0.88	5.15	0.59
	Calibrated	0.92	0.91	3.03	0.51 (1.69)
	+10%	0.92	0.92	4.02	0.49
	+15%	0.85	0.77	15.36	1.00
	+25%	0.75	0.54	29.71	1.83
Initial Abstraction	-25%	0.87	0.64	16.27	1.01
	-15%	0.91	0.88	7.23	0.58
	-10%	0.92	0.91	3.61	0.47
	Calibrated	0.92	0.91	3.03	0.51 (1.69)
	+10%	0.86	0.83	7.91	0.70
	+15%	0.85	0.80	9.09	0.76
	+25%	0.84	0.79	9.35	0.77
Impervious Area Percent	-25%	0.91	0.67	17.11	0.97
	-15%	0.91	0.80	11.59	0.74
	-10%	0.91	0.85	8.76	0.65
	Calibrated	0.92	0.91	3.03	0.51 (1.69)
	+10%	0.91	0.91	2.64	0.50
	+15%	0.91	0.89	5.62	0.55
	+25%	0.91	0.81	11.34	0.73
Lag Time	-25%	0.91	0.89	6.58	0.57
	-15%	0.91	0.91	2.06	0.49
	-10%	0.91	0.91	0.08	0.49
	Calibrated	0.92	0.91	3.03	0.51 (1.69)
	+10%	0.91	0.85	5.62	0.56
	+15%	0.91	0.83	6.76	0.59
	+25%	0.90	0.78	8.69	0.65
Ratio to the Peak Value	-25%	0.78	0.65	14.86	1.00
	-15%	0.86	0.79	10.22	0.77
	-10%	0.88	0.83	8.23	0.69
	Calibrated	0.92	0.91	3.03	0.51 (1.69)
	+10%	0.92	0.91	2.71	0.46
	+15%	0.92	0.90	5.89	0.52
	+25%	0.90	0.79	12.92	0.76

Table 5.2. Results of sensitivity analysis for event-based model (continued)

<i>Parameter</i>	<i>Change</i>	R^2	<i>NSE</i>	<i>PBIAS (%)</i>	<i>RMSE (SD)</i>
Storage Constant	-25%	0.85	0.83	1.51	0.63
	-15%	0.88	0.86	2.20	0.57
	-10%	0.89	0.87	2.41	0.54
	Calibrated	0.92	0.91	3.03	0.51 (1.69)
	+10%	0.92	0.89	3.57	0.49
	+15%	0.93	0.90	3.84	0.47
	+25%	0.94	0.90	4.47	0.47
Weighting Factor	-25%	0.91	0.91	3.02	0.52
	-15%	0.91	0.91	3.08	0.52
	-10%	0.92	0.91	3.06	0.51
	Calibrated	0.92	0.91	3.03	0.51 (1.69)
	+10%	0.92	0.91	3.06	0.50
	+15%	0.92	0.91	3.11	0.50
	+25%	0.92	0.91	3.15	0.50

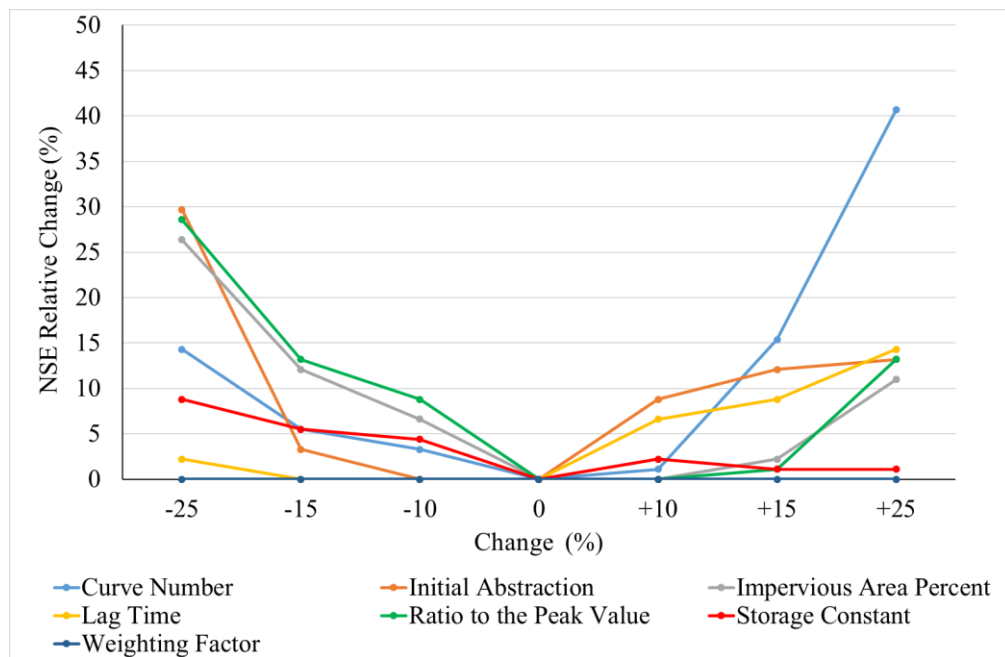


Figure 5.23. Nash-Sutcliffe Efficiency of sensitivity analysis for event-based model parameters

These results suggest that, the model is highly sensitive to curve number, ratio to peak value, initial abstraction and impervious area percent values. +25% change for the curve number results in maximum possible value for all sub-basins which causes almost all of the rainfall turn to runoff and hence simulated flow has very low NSE. The initial abstraction is a value which gives limit to accumulated rainfall to turn runoff. Therefore, having more site-specific data to define initial abstraction and impervious area percent values will be helpful in forming more robust models. Also, it can be said that better understanding of observed data to define ratio to peak value is essential.

5.7.2. Continuous Model Sensitivity

Parameter inputs and calibrated parameters for the continuous model are given in Table 4.17. Along these parameters, sensitivity analysis is done for max storage coefficient parameters of “Surface” and “Canopy” methods, constant rate, impervious area percent parameters of “Deficit and Constant” method, lag time parameter of “SCS UH” method, ratio to the peak value parameter of “Recession” method and storage constant, and weighting factor parameters of “Muskingum” method. Sensitivity analysis is not done for recession constant of “Recession” baseflow method, initial deficit and maximum storage of “Deficit and Constant” method since these parameters are selected from relatively small and changes in performance evaluations are not significant. Moreover, sensitivity analysis for Px temperature and wet meltrate parameters of “Temperature Index” snowmelt method is done but rest of the snowmelt parameters are not included in the analysis since most of these parameters have default values or narrow ranges. Performance evaluations for sensitivity analysis are provided in Table 5.3. Moreover, results of sensitivity analysis according to Nash-Sutcliffe Efficiency are provided in Figure 5.24. NSE relative changes are normalized according to Equation (16).

Table 5.3. Results of sensitivity analysis for continuous model

<i>Parameter</i>	<i>Change</i>	R^2	<i>NSE</i>	<i>PBIAS (%)</i>	<i>RMSE (SD)</i>
Canopy Max Storage	-25%	0.78	0.78	5.17	0.92
	-15%	0.78	0.78	7.47	0.92
	-10%	0.78	0.78	8.19	0.91
	Calibrated	0.78	0.78	10.07	0.91 (1.94)
	+10%	0.78	0.77	11.31	0.92
	+15%	0.78	0.77	12.25	0.92
	+25%	0.78	0.77	13.16	0.93
Surface Max Storage	-25%	0.78	0.76	4.52	0.94
	-15%	0.78	0.77	7.27	0.92
	-10%	0.78	0.78	8.29	0.91
	Calibrated	0.78	0.78	10.07	0.91 (1.94)
	+10%	0.78	0.77	11.82	0.92
	+15%	0.78	0.77	12.70	0.93
	+25%	0.78	0.77	14.38	0.94
Constant Rate	-25%	0.79	0.45	17.93	1.44
	-15%	0.79	0.72	3.90	1.03
	-10%	0.79	0.76	1.49	0.94
	Calibrated	0.78	0.78	10.07	0.91 (1.94)
	+10%	0.77	0.75	17.03	0.97
	+15%	0.76	0.71	20.19	1.04
	+25%	0.75	0.68	23.13	1.09
Impervious Area Percent	-25%	0.78	0.73	26.84	1.01
	-15%	0.78	0.76	20.13	0.96
	-10%	0.78	0.77	16.78	0.94
	Calibrated	0.78	0.78	10.07	0.91 (1.94)
	+10%	0.78	0.78	3.53	0.91
	+15%	0.78	0.77	0.01	0.92
	+25%	0.78	0.76	6.73	0.95
Lag Time	-25%	0.78	0.74	5.68	0.99
	-15%	0.78	0.77	0.71	0.93
	-10%	0.78	0.78	3.96	0.92
	Calibrated	0.78	0.78	10.07	0.91 (1.94)
	+10%	0.78	0.77	15.15	0.92
	+15%	0.78	0.77	17.14	0.93
	+25%	0.78	0.75	20.29	0.96

Table 5.3. Results of sensitivity analysis for continuous model (continued)

<i>Parameter</i>	<i>Change</i>	<i>R</i> ²	<i>NSE</i>	<i>PBIAS</i> (%)	<i>RMSE</i> (<i>SD</i>)
Ratio to the Peak Value	-25%	0.79	0.79	29.80	1.02
	-15%	0.79	0.79	21.68	0.95
	-10%	0.79	0.79	17.93	0.92
	Calibrated	0.78	0.78	10.07	0.91 (1.94)
	+10%	0.78	0.78	3.56	0.92
	+15%	0.78	0.78	2.23	0.92
	+25%	0.77	0.77	0.39	0.93
Storage Constant	-25%	0.78	0.78	10.07	0.91
	-15%	0.78	0.78	10.07	0.91
	-10%	0.78	0.78	10.07	0.91
	Calibrated	0.78	0.78	10.07	0.91 (1.94)
	+10%	0.78	0.77	10.06	0.92
	+15%	0.78	0.77	10.06	0.92
	+25%	0.78	0.77	10.06	0.92
Weighting Factor	-25%	0.78	0.78	10.06	0.92
	-15%	0.78	0.78	10.07	0.91
	-10%	0.78	0.78	10.07	0.91
	Calibrated	0.78	0.78	10.07	0.91 (1.94)
	+10%	0.78	0.78	10.06	0.91
	+15%	0.78	0.77	10.06	0.92
	+25%	0.78	0.78	10.07	0.91
Px Temperature	-25%	0.78	0.78	8.12	0.91
	-15%	0.78	0.78	8.19	0.92
	-10%	0.78	0.78	8.88	0.92
	Calibrated	0.78	0.78	10.07	0.91 (1.94)
	+10%	0.78	0.78	11.04	0.91
	+15%	0.77	0.77	12.72	0.93
	+25%	0.78	0.77	13.87	0.94
Wet Meltrate	-25%	0.77	0.73	19.61	1.00
	-15%	0.77	0.76	16.32	0.95
	-10%	0.78	0.77	14.43	0.93
	Calibrated	0.78	0.78	10.07	0.91 (1.94)
	+10%	0.78	0.77	5.57	0.93
	+15%	0.77	0.75	0.94	0.96
	+25%	0.76	0.68	3.85	1.10

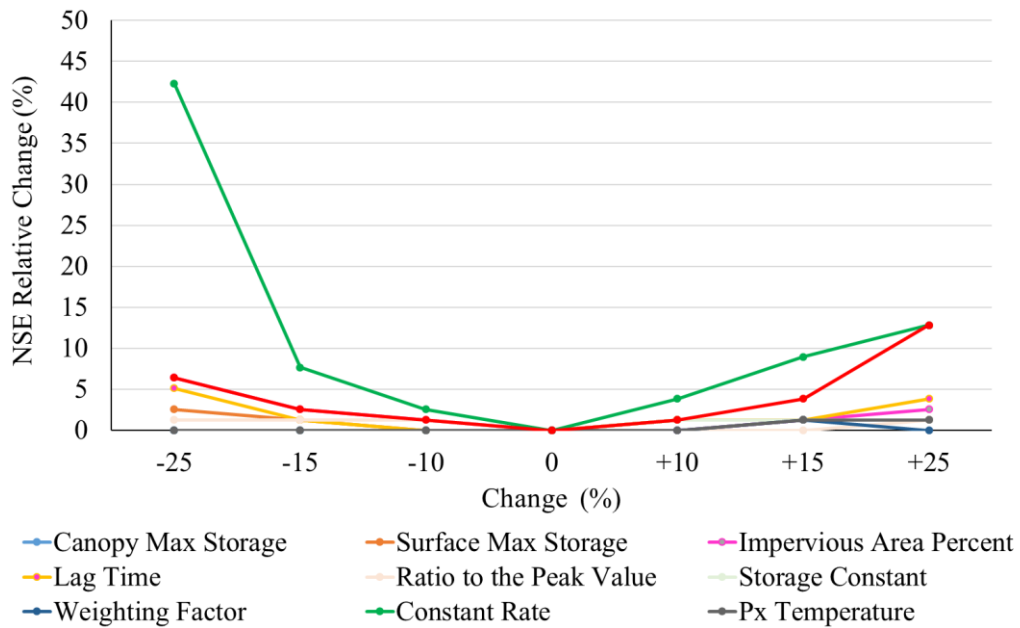


Figure 5.24. Nash-Sutcliffe Efficiency of sensitivity analysis for continuous model parameters

These results suggest that the model is relatively more sensitive to constant rate and wet meltrate values. Constant rate defines the percolation rate when the soil layer is saturated which can be better understood again with site studies. Wet meltrate represents the rate at which snowpack melts when it is raining on the pack. Therefore, it is important to understand snow mechanisms for snow affected study areas such as Çakıt Basin.

CHAPTER 6

CONCLUSIONS

In this study, the HEC-HMS model is used to simulate streamflow at Çakıt Basin. HEC-HMS model for the basin is developed using the HEC-GeoHMS module in the ArcGIS to generate spatial data inputs for the model. The following main conclusions is derived from this study:

- The model shows that HEC-HMS is a useful tool for both event-based and continuous simulations at Çakıt Basin. Event-based model demonstrates that the “SCS CN” method with “SCS UH,” “Recession,” and “Muskingum” methods can be used to simulate streamflow during short storm events in the study area. The continuous model demonstrates that the “Deficit and Constant” method with “SCS UH,” “Recession,” and “Muskingum” methods can be used to simulate streamflow for long simulation periods in the study area.
- Utilization of the snowmelt method increased the performance of the continuous model developed for snow affected study area. Therefore, it can be said that snowmelt is an important component of the streamflow and “Degree Day” method is the easiest method to estimate the snowmelt.
- Based on literature review and results of this study, daily time steps are identified to be sufficient for continuous simulations while hourly time steps are required for event-based simulations.
- Event-based model is calibrated with “SCS CN” method which reflects study area spatially, however, continuous model is developed with “Deficit and Constant” method in which loss calculations are carried out through user-assigned numerical value for each sub-basin. During calibration studies, it is seen that calibration of “Deficit and Constant” was troublous without using

any specific observations such as site studies to define exact percolation rate when the soil layer is saturated. Saturated hydraulic conductivity values of study area could be used to ease calibration and increase accuracy of model.

- The more realistic models can be obtained by simulating dependable long-term data. The pressure sensors used in measuring the water stage are not very good for streams having large seasonal variation. In Turkey, many small streams have very low streamflow at the end of summer and in the beginning of autumn, whereas flooding is observed during spring. This variation makes data collection thus modelling more challenging.

Recommendations:

- Calibration of the model where “Deficit and Constant” method is used is time consuming due to large number of parameters that need to be calibrated. Using more study area specific inputs to decrease number of other parameters to calibrate by conducting more field studies can ease calibration.
- It is seen that absence of hydrological soil group database makes event-based modelling setup with SCS CN method challenging. Experienced problems are explained in Section 4.3.1 and an alternative method is used to estimate CN in this study. Hydrological soil group of study area is created by using great soil types, erosion and depth of soil data which may cause uncertainty in CN estimation. Hence, hydrological soil groups for Turkey should be developed and made available to researchers.
- The correct hydro-meteorological data availability is very important for modelling. The automatic stations provide data but they must be checked regularly and the quality of the collected data must be checked by considering the local conditions.
- As explained in the Results of Calibration and Validation of Case Studies Section, it is recommended to use site specific data for reducing uncertainty. Thus, increasing the number of hydro-meteorological observation station in Turkey is important for establishing more reliable datasets.

REFERENCES

- Adilah, A., & Nuramirah, S. (2019). Estimating flow rate in gauged and ungauged stations in Kuantan river basin using Clark method in Hec-HMS. *Earth and Environmental Science*, 244(1). doi:10.1088/1755-1315/244/1/012014
- Akay, H., & Koçyiğit, M. (2019). Comparison of Direct Runoff Hydrographs of Two Ungauged Sub-Basins Using Instantaneous Unit Hydrograph Approach. *Journal of Natural Hazards and Environment*, 5(2), 1-8.
- Akyürek, Z., Kentel, E., Binley, A., Yanmaz, M., Merzi, N., Aksu, H., & Yakut, M. (2019). *Hydrological Cycle Parameter Estimation with Conceptual Hydrological Model*. Ankara, Turkey: TUBITAK Project Report.
- Ali, M., Khan, S., Aslam, I., & Khan, Z. (2011). Simulation of the impacts of land-use change on surface run off of Lai Nullah Basin in Islamabad, Pakistan. *Landscape and Urban Planning*, 102(4), 271– 279. doi:10.1016/j.landurbplan.2011.05.006
- Aquaveo. (2019). *Watershed Modeling System-WMS User Manual*. Retrieved November 30, 2019, from Aquaveo: <https://www.aquaveo.com/software/wms-watershed-modeling-system-introduction>
- Azam, M., Kim, H., & Maeng, S. (2017). Development of flood alert application in Mushim stream watershed Korea. *International Journal of Disaster Risk Reduction*, 21, 11-26. doi:10.1016/j.ijdrr.2016.11.008
- Azmat, M., Choi, M., Kim, T., & Liaqat, U. W. (2016). Hydrological modeling to simulate streamflow under changing climate in a scarcely gauged cryosphere catchment. *Environmental Earth Science*, 75(3), 75-186. doi:10.1007/s12665-015-5059-2

- Baumbach, T., Burckhard, S., & Kant, J. (2015). *Watershed Modeling Using Arc Hydro Tools, GeoHMS, and HEC-HMS*. Retrieved from Civil and Environmental Engineering Faculty Publications: https://openprairie.sdstate.edu/cvlee_pubs/2?utm_source=openprairie.sdstate.edu%2Fcvlee_pubs%2F2&utm_medium=PDF&utm_campaign=PDFCoverPages
- Bhuiyan, H. A., McNairn, H., & Powers, J. (2017). Application of HEC-HMS in a Cold Region Watershed and Use of RADARSAT-2 Soil Moisture in Initializing the Model. *Hydrology*, 4(1), 9. doi:10.3390/hydrology4010009
- Blasone, R. (2007). *Parameter estimation and uncertainty assessment in hydrological modelling*. DTU Environment.
- Bossard, M., Feranec, J., & Otahel, J. (2000). *CORINE land cover technical guide*. Copenhagen: EEA .
- Boughton, W., & Droop, O. (2003). Continuous simulation for design flood estimation—a review. *Environmental Modelling & Software*, 18, 309-318. doi:10.1016/S1364-8152(03)00004-5
- Büttner, G., Soukup, T., & Kosztra, B. (2012). *CLC2012 Addendum to CLC2006 Technical Guidelines*. Wien, Austria: European Topic Centre on Urban, land and soil systems, ETC/ULS.
- Chen, W., Wang, Y., Li, X., Zou, Y., Liao, Y., & Yang, J. (2016). Land use/land cover change and driving effects of water. *Environment Earth Science*, 75(1027). doi:<https://doi.org/10.1007/s12665-016-5809-9>
- Choudhari, K., Panigrahi, B., & Paul, J. (2014). Simulation of rainfall-runoff process using HEC-HMS model for Balijore Nala watershed, Odisha, India. *International Journal of Geomatics and Geosciences*, 5(2), 253-265.

- Chu, X., & Steinman, A. (2009). Event and Continuous Hydrologic Modeling with HEC-HMS. *Journal of Irrigation and Drainage Engineering*, 135(1), 119-124. doi:[https://doi.org/10.1061/\(ASCE\)0733-9437\(2009\)135:1\(119\)](https://doi.org/10.1061/(ASCE)0733-9437(2009)135:1(119))
- Corine. (2012). *European Environment Agency Corine Land Cover*. Retrieved from <https://www.eea.europa.eu/data-and-maps/data/external/corine-land-cover-2012>: <https://www.eea.europa.eu/data-and-maps/data/external/corine-land-cover-2012>
- Crawford, N., & Linsley, R. (1966). Stanford Watershed Model IV. Technical Report No. 39. *Digital Simulation in Hydrology*, 210.
- Daniel, E., Camp, J., LeBoeuf, E., Penrod, J., Dobbins, J., & Abkowitz, M. (2011). Watershed Modeling and its Applications: A State-of-the-Art Review. *The Open Hydrology Journal*, 5(1), 26-50. doi:<https://doi.org/10.2174/1874378101105010026>
- Dariane, A., Bagheri, R., Karami, F., & Javadiazadeh, M. (2019). Developing heuristic multi-criteria auto calibration method for continuous HEC-HMS in snow-affected catchment. *International Journal of River Basin Management*, 1814-2060. doi:<https://doi.org/10.1080/15715124.2019.1576696>
- Dariane, A., Javadiazadeh, M., & James, L. (2016). Developing an Efficient Auto-Calibration Algorithm for HEC-HMS Program. *Water Resources Management*, 30(6), 1923-1937. doi:10.1007/s11269-016-1260-7
- Dawdy, D., & O'Donnell, T. (1965). American Society of Civil Engineers - 91. *Mathematical models of catchment behaviour*, 123-137.
- De Silva, M., Weerakoon, S., & Herath, S. (2014). Modeling of Event and Continuous Flow Hydrographs with HEC-HMS: Case Study in the Kelani River Basin, Sri Lanka. *Journal of Hydrological Engineering*, 19(4), 800-806. doi:10.1061/(ASCE)HE.1943-5584.0000846

- Deng, Z., Zhang, X., Li, D., & Pan, G. (2015). Simulation of land use/land cover change and its effects on the hydrological characteristics of the upper reaches of the Hanjiang Basin. *Environment Earth Science*, 1119-1132. doi:<https://doi.org/10.1007/s12665-014-3465-5>
- Derdour, A., Bouanani, A., & Babahamed, K. (2018). Modelling rainfall runoff relations using HEC-HMS in a semi-arid region: Case study in Ain Sefra watershed, Ksour Mountains (SW Algeria). *Journal of Water and Land Development*, 36(1), 45-55. doi:10.2478/jwld-2018-0005
- Devia, G. K., Ganasri, B. P., & Dwarakish, G. S. (2015). A Review on Hydrological Models. *Aquatic Procedia*, 4, 1001-1007. doi:10.1016/j.aqpro.2015.02.126
- ESRI. (2015). *ArcGIS Release 10.3.1*. Redlands, CA: Environmental Systems Research Institute.
- Fang, G., Yuan, Y., Gao, Y., Huang, X., & Guo, Y. (2018). Assessing the Effects of Urbanization on Flood Events with Urban Agglomeration Polders Type of Flood Control Pattern Using the HEC-HMS Model in the Qinhuai River Basin, China. *Water*, 10(8), 2130-2138. doi:10.3390/w10081003
- FAO. (2013). *Land Degradation Assessment in Drylands - LADA*. Rome: Food and Agriculture Organization of the United Nations.
- Fleming, M., & Neary, V. (2004). Continuous Hydrologic Modeling Study with the Hydrologic. *Journal of Hydrological Engineering*, 9(3), 175-183. doi:10.1061/(ASCE)1084-0699(2004)9:3(175)
- Gebre, S. (2015). Application of the HEC-HMS Model for Runoff Simulation of Upper Blue Nile River. *Journal of Waste Water Treatment & Analysis*, 6(2), 199-207. doi:10.4172/2157-7587.1000199
- Gumindoga, W., Rwasoka, D., Nhapi, I., & Dube, T. (2017). Ungauged runoff simulation in Upper Manyame Catchment, Zimbabwe: Application of the

- HEC-HMS model. *Physics and Chemistry of the Earth*, 100, 371-382. doi:10.1016/j.pce.2016.05.002
- Gyawali, R., & Watkins, D. (2013). Continuous Hydrologic Modeling of Snow-Affected Watersheds in the Great Lakes Basin Using HEC-HMS. *Journal of Hydrological Engineering*, 18(1), 29-39. doi:10.1061/(ASCE)HE.1943-5584.0000591
- Halwatura, D., & Najim, M. (2013). Application of the HEC-HMS model for runoff simulation in a tropical catchment. *Environmental Modelling & Software*, 46, 155-162. doi:10.1016/j.envsoft.2013.03.006
- Jin, H., Liang, R., Wang, Y., & Tumula, P. (2015). Flood-Runoff in Semi-Arid and Sub-Humid Regions, a Case Study: A Simulation of Jianghe Watershed in Northern China. *Water*, 7(9), 4155-5172. doi:10.3390/w7095155
- Kaffas, K., & Hrissanthou, V. (2014). Application of a continuous Rainfall-Runoff model to the basin of Kosynthos river using the hydrological software HEC-HMS. *Global Nest Journal*, 16(1), 188-203. doi:10.30955/gnj.001200
- Kızılkaya, T. (1983). *Sulama ve Drenaj*. Ankara: General Directorate of State Hydraulic Works.
- Knebl, M., Yang, Z., Hutchison, K., & Maidment, D. (2005). Regional scale flood modeling using NEXRAD rainfall, GIS, and HEC-HMS/RAS: a case study for the San Antonio River Basin Summer 2002 storm event. *Journal of Environmental Management*, 75(4), 325-336. doi:https://doi.org/10.1016/j.jenvman.2004.11.024
- Koçyiğit, M., Akay, H., & Yanmaz, A. (2017). Estimation of Hydrologic Parameters of Kocanaz Watershed by a Hydrologic Model. *International Journal of Engineering & Applied Sciences*, 9(4), 42-50. doi:10.24107/ijeas.342039
- Koneti, S., Sunkara, S., & Roy, P. (2018). Hydrological Modeling with Respect to Impact of Land-Use and Land-Cover Change on the Runoff Dynamics in

- Godavari River Basin Using the HEC-HMS Model. *International Journal of Geo-Information*, 7(6). doi:10.3390/ijgi7060206
- McCarthy, G. (1938). *The Unit Hydrograph and Flood Routing*. Providence: U.S. Army Corps of Engineers.
- Melone, F., Barbetta, S., Diomede, T., Peruccacci, S., Rossi, M., Tassarolo, A., & Verdecchia, M. (2005). *Review and selection of hydrological models – Integration of hydrological models and meteorological inputs*. Gennaio: Istituto di Ricerca per la Protezione Idrogeologica Contract No. 12.
- Merwade, V. (2019). *Terrain Processing and HMS-Model Development Using GeoHMS*. Retrieved November 11, 2019, from White Paper, Purdue University: <https://web.ics.purdue.edu/~vmerwade/education/geohms.pdf>
- Moraes, T., Santos, V., Calijuri, M., & Torres, F. (2018). Effects on runoff caused by changes in land cover in a Brazilian southeast basin: evaluation by HEC-HMS and HEC-GEOHMS. *Environmental Earth Sciences*, 77(6). doi:10.1007/s12665-018-7430-6
- Moriasi, D., Arnold, J., Van Liew, M., & Bingner, R. (2007). Model Evaluation Guidelines for Systematic Quantification of Accuracy in Watershed Simulations. *American Society of Agricultural and Biological Engineers*, 50(3), 885–900. doi:10.13031/2013.23153
- Moriasi, D., Gitau, M., Pai, N., & Daggupati, P. (2015). Hydrologic and Water Quality Models: Performance Measures and Evaluation Criteria. *American Society of Agricultural and Biological Engineers*, 58, 1763-1785.
- National Soil Database. (2017). Retrieved from Republic of Turkey Ministry Of Agriculture And Forestry: <http://85.25.185.76/tgskmae/starter.aspx#dashboard>

- Oleyiblo, J. O., & Li, Z. (2010). Application of HEC-HMS for flood forecasting in Misai and Wan'an catchments in China. *Water Science and Engineering*, 3(1), 14-22. doi:10.3882/j.issn.1674-2370.2010.01.002
- Özkaya, A., & Akyürek, Z. (2019). Evaluating the use of bias-corrected radar rainfall data in three flood events in Samsun, Turkey. *Natural Hazards* 98, 643–674.
- Santhi, C., Arnold, J., Williams, J., Dugas, W., Srinivasan, R., & Hauck, L. (2001). Validation of the SWAT Model on a Large River Basin with Point and Nonpoint Sources. *Journal of the American Water Resources Association* 37(5), 37(5), 1169-1188. doi:10.1111/j.1752-1688.2001.tb03630.x
- Scharffenberg, B. (2008, May 28). Introduction to HEC-HMS - Watershed Modeling with HEC-HMS. Sacramento, CA.
- Singh, J., Knapp, , H., & Demissie, M. (2004). Hydrologic modeling of the Iroquois River watershed using HSPF and SWAT. *Journal of the American Water Resources Association*, 41(2), 343-360. doi:10.1111/j.1752-1688.2005.tb03740.x
- Singh, N., Kumar, M., & Kumar, A. (2019). Hydrological Modeling of Ravi River Catchment Area Using HEC-HMS. *International Journal of Engineering Technology Science and Research*, 6(7), 30-41.
- Singh, V., & Frevert, D. (2006). *Watershed Models*. Boca Raton: Taylor & Francis. doi:10.1016/b978-0-12-409548-9.11165-0
- Singh, V., & Woolhiser, D. (2002). Mathematical Modeling of Watershed Hydrology. *Journal of Hydrological Engineering*, 7(4), 270-292. doi:10.1061/(ASCE)1084-0699(2002)7:4(270)
- Sitterson, J., Knightes, C., Parmar, R., Wolfe, K., Muche, M., & Avant, B. (2017). *An Overview of Rainfall-Runoff Model Types*. Athens: United States Environmental Protection Agency.

- Song, X., Kong, F., & Zhu, Z. (2011). Application of Muskingum routing method with variable parameters in ungauged basin. *Water Science and Engineering*, 4, 4(1), 1-12. doi:10.3882/j.issn.1674-2370.2011.01.001
- Sorooshian, S., Wheater, H., & Sharma, K. (2007). *Hydrological Modelling in Arid and Semi-Arid Areas (International Hydrology Series)*. Cambridge: Cambridge University Press. doi:https://doi.org/10.1017/CBO9780511535734
- Tassew, B., Belete, M., & Miegel, K. (2019). Application of HEC-HMS Model for Flow Simulation in the Lake Tana Basin: The Case of Gilgel Abay Catchment, Upper Blue Nile Basin, Ethiopia. *Hydrology*, 6(1). doi:10.3390/hydrology6010019
- TSMS. (2019). *Turkish State Meterological Service*. Retrieved December 15, 2019, from Average Temperatures Measured in Long Period: <https://www.mgm.gov.tr/veridegerlendirme/il-ve-ilceler-istatistik.aspx?m=NIGDE>
- USACE. (1968). *HEC-1 Flood Hydrograph Package, User's Manual*. CA,USA: Hydrologic Engineering Center: Davis.
- USACE. (2000). *Hydrologic Modeling System (HEC-HMS) Technical Reference Manuel*. CA, USA: Hydrologic Engineering Center: Davis.
- USACE. (2010). *Hydrologic Modeling System (HEC-HMS) User's Manual: Version 3.1.0*. CA, USA: Hydrologic Engineering Center: Davis.
- USACE. (2013). *Geospatial Hydrological Modeling Extension (HEC-GeoHMS) User's Manual: Version 10.1*. CA, USA: Hydrologic Engineering Center: Davis.
- USACE. (2018). *Hydrologic Modeling System (HEC-HMS) User's Manual: Version 4.3.0*. CA, USA: Hydrologic Engineering Center: Davis.

- USDA. (1986). *Urban Hydrology for Small Watersheds, Technical Release-55*. Washington D.C.: U.S. Department of Agriculture - Natural Resources Conversation Service.
- USDA. (2007). *Hydrology National Engineering Handbook*. Washington D.C.: U.S. Department of Agriculture - Natural Resources Conversation Service.
- USDA. (2019, December 10). *Snow Survey*. Retrieved from National Water and Climate Center: <http://www.wcc.nrcs.usda.gov/snow>
- Van Liew, M., Arnold, J., & Garbrecht, J. (2003). Hydrologic simulation on agricultural watersheds: Choosing between models. *Transactions of the American Society of Agricultural Engineers*, 46(6), 1539-1551. doi:10.13031/2013.15643
- Verdhen, A., Chahar, B., & Sharma, O. (2013). Snowmelt Runoff Simulation using HEC-HMS in a Himalayan Watershed. *World Environmental and Water Resources Congress* (s. 3206-3215). Ohio: ASCE. doi:10.1061/9780784412947.317
- Verma, A., Jha, M., & Mahana, R. (2010). Evaluation of HEC-HMS and WEPP for simulating watershed runoff using remote sensing and geographical information system. *Paddy Water Environment*, 8(2), 131-144. doi:10.1007/s10333-009-0192-8
- Yang, W., Li, D., Sun, T., & Ni, G. (2015). Saturation-excess and infiltration-excess runoff on green roofs. *Ecological Engineering*, 74, 327-336. doi:10.1016/j.ecoleng.2014.10.023
- Yilmaz, A., Imteaz, M., & Ogwuda, O. (2012). Accuracy of HEC-HMS and LBRM Models in Simulating Snow Runoffs in Upper Euphrates Basin. *Journal of Hydrologic Engineering*, 17(2), 342-347. doi: 10.1061/(ASCE)HE.1943-5584.0000442

- Zare, M., Samani, A., & Mohammady, M. (2016). The impact of land use change on runoff generation in an urbanizing watershed in the north of Iran. *Environment Earth Science*, 75(18). doi:10.1007/s12665-016-6058-7
- Zeckoski, R., Smolen, M., Moriasi, D., Frankenberger, J., & Feyereisen, G. (2015). Hydrologic and water quality terminology as applied to modeling. *American Society of Agricultural and Biological Engineers*, 1619-1635. doi:10.13031/trans.58.10713
- Zezelew, D., & Melesse, A. (2018). Applicability of a Spatially Semi-Distributed Hydrological Model for Watershed Scale Runoff Estimation in Northwest Ethiopia. *Water*, 10(7). doi:10.3390/w10070923
- Zema, D., Labate, A., Martino, D., & Zimbone, S. (2016). Comparing Different Infiltration Methods of the HEC-HMS Model: The Case Study of the Mésima Torrent (Southern Italy): Infiltration Methods of the HEC-HMS Model in Torrents of South Italy. *Land Degradation and Development*, 28(1), 294-308. doi:10.1002/ldr.2591
- Zheng, C., Hill, M., Cao, G., & Ma, R. (2012). MT3DMS: Model use, calibration, and validation. *American Society of Agricultural and Biological Engineers*, 55, 1549-1559. doi: 10.13031/2013.42263

APPENDICES

A. DATA USED IN GENERATING CN

Table A.1. Hydrological soil types (USDA, 2007)

Soil Property	<i>Hydrologic Soil Group A</i>	<i>Hydrologic Soil Group B</i>	<i>Hydrologic Soil Group C</i>	<i>Hydrologic Soil Group D</i>
Saturated hydraulic conductivity	>40.0 $\mu\text{m/s}$	≤ 40.0 to >10.0 $\mu\text{m/s}$	≤ 10.0 to >1.0 $\mu\text{m/s}$	≤ 1.0 $\mu\text{m/s}$
Depth to water-impermeable layer	50 to 100 cm	50 to 100 cm	50 to 100 cm	≤ 50 cm
Depth to high water table	60 to 100 cm	60 to 100 cm	60 to 100 cm	≤ 60 cm

Table A.2. CORINE Land Cover (CLC) nomenclature (Büttner, Soukup, & Kosztra, 2012)

Level 1	<i>Level 2</i>	<i>Level 3</i>
1 Artificial surface	11 urban fabric	111 Continuous urban fabric
		112 Discontinuous urban fabric
	12 industrial, commercial and transport units	121 Industrial or commercial units
		122 Road and rail networks and associated land
		123 Port areas
		124 Airports
	13 Mine, dump and construction sites	131 Mineral extraction sites
132 Dumpsites		
133 Construction sites		
14 Artificial, non-agricultural vegetated areas	141 Green urban areas	
	142 Sport and leisure facilities	
2 Agricultural areas	21 Arable land	211 Non-irrigated arable land
		212 Permanently irrigated land
		213 Rice fields

Table A.2. CORINE Land Cover (CLC) nomenclature (Büttner, Soukup, & Kosztra, 2012)(continued)

<i>Level 1</i>	<i>Level 2</i>	<i>Level 3</i>
2 Agricultural areas	22 Permanent crops	221 Vineyards
		222 Fruit trees and berry plantations
		223 Olive groves
	23 Pastures	231 Pastures
		24 Heterogeneous agricultural areas
	241 Annual crops associated with permanent crops	242 Complex cultivation patterns
		243 Land principally occupied by agriculture, with significant areas of natural vegetation
244 Agroforestry areas		
<hr/>		
3 Forest and semi-natural areas	31 Forests	311 Broad-leaved forest
		312 Coniferous forest
		313 Mixed forest
	32 Scrub and herbaceous vegetation associations	321 Natural grasslands
		322 Moors and heathland
		323 Sclerophyllous vegetation
		324 Transitional woodland-shrub
	33 Open spaces with little or no vegetation	331 Beaches, dunes, sands
		332 Bare rocks
		333 Sparsely vegetated areas
		334 Burnt areas
		335 Glaciers and perpetual snow
		<hr/>
4 Wetlands	41 Inland wetlands	411 Inland marshes
		412 Peat bogs
	42 Maritime wetlands	421 Salt marshes
		422 Salines
		423 Intertidal flats
<hr/>		
5 Water bodies	51 Inland waters	511 Water courses
		512 Waterbodies
	52 Marine waters	521 Coastal lagoons
		522 Estuaries
		523 Sea and ocean

Table A.3. Runoff curve numbers for urban areas (USDA, 1986)

Cover Type	<i>Curve Numbers for Hydrologic Soil Group</i>			
	<i>A</i>	<i>B</i>	<i>C</i>	<i>D</i>
Fully developed urban areas				
Open space (lawns, parks, golf courses, cemeteries, etc.)				
Poor condition (grass cover < 50%)	68	79	86	89
Fair condition (grass cover 50% to 75%)	49	69	79	84
Good condition (grass cover > 75%)	39	61	74	80
Impervious areas:				
Paved parking lots, roofs, driveways, etc.	98	98	98	98
Streets and roads:				
Paved; curbs and storm sewers	98	98	98	98
Paved; open ditches	83	89	92	93
Gravel	76	85	89	91
Dirt	72	82	87	89
Western desert urban areas:				
Natural desert landscaping	63	77	85	88
Artificial desert landscaping	96	96	96	96
Urban districts				
Commercial and business	89	98	94	95
Industrial	81	88	91	93
Residential districts by average lot size				
1/8 acre or less	77	85	90	92
1/4 acre	61	75	83	87
1/3 acre	57	72	81	86
1/2 acre	54	70	80	85
1 acre	51	68	79	84
2 acres	46	65	77	82
Developing urban areas				
Developing urban areas	77	86	91	94

Table A.4. Runoff curve numbers for cultivated agricultural lands (USDA, 1986)

Cover Type	Hydrologic Condition	Curve Numbers for			
		Hydrologic Soil Group			
		A	B	C	D
Fallow					
Bare soil	-	77	86	91	94
Crop residue cover (CR)	Poor	76	85	90	93
	Good	74	83	88	90
Row crops					
Straight row (SR)	Poor	72	81	88	91
	Good	67	78	85	89
SR+CR	Poor	71	80	87	90
	Good	64	75	82	85
Contoured (C)	Poor	70	79	84	88
	Good	65	75	82	86
C+CR	Poor	69	78	83	87
	Good	64	74	81	85
Contoured & terraced (C&T)	Poor	66	74	80	82
	Good	62	71	78	81
C&T + CR	Poor	65	73	79	81
	Good	61	70	77	80
Small grain					
SR	Poor	65	76	84	88
	Good	63	75	83	87
SR+CR	Poor	64	75	83	86
	Good	60	72	80	84
C	Poor	63	74	82	85
	Good	61	73	81	84
C+CR	Poor	62	73	81	84
	Good	60	72	80	83
C&T	Poor	61	72	79	82
	Good	59	70	78	81
C&T + CR	Poor	60	71	78	81
	Good	58	69	77	80
Close-seeded or broadcast legumes or rotation meadow					
SR	Poor	66	77	85	89
	Good	58	72	81	85
C	Poor	64	75	83	85
	Good	55	69	78	83
C&T	Poor	63	73	80	83
	Good	51	67	76	80

Table A.5. Runoff curve numbers for other agricultural lands (USDA, 1986)

Cover Type	<i>Hydrologic Condition</i>	<i>Curve Numbers for Hydrologic Soil Group</i>			
		<i>A</i>	<i>B</i>	<i>C</i>	<i>D</i>
Pasture, grassland, or range—continuous forage for grazing	Poor	68	79	86	89
	Fair	49	69	79	84
	Good	39	61	74	80
Meadow—continuous grass, protected from grazing and generally mowed for hay.	-	30	58	71	78
Brush-brush-weed-grass mixture with a brush the major element	Poor	48	67	77	83
	Fair	35	56	70	77
	Good	30	48	65	73
Woods-grass combination (orchard or tree farm)	Poor	57	73	82	86
	Fair	43	65	76	82
	Good	32	58	72	79
Woods	Poor	45	66	77	83
	Fair	36	60	73	79
	Good	30	55	70	77
Farmsteads-buildings, lanes, driveways, and surrounding lots	Poor	59	74	82	86

Table A.6. Runoff curve numbers for arid and semiarid rangelands (USDA, 1986)

Cover Type	<i>Hydrologic Condition</i>	<i>Curve Numbers for Hydrologic Soil Group</i>			
		<i>A</i>	<i>B</i>	<i>C</i>	<i>D</i>
Herbaceous—a mixture of grass, weeds, and low-growing brush, with a brush the minor element	Poor	-	80	87	93
	Fair	-	71	81	89
	Good	-	62	74	85
Oak-aspen-mountain brush mixture of oak brush, aspen, mountain mahogany, bitterbrush, maple, and other brush	Poor	-	66	74	79
	Fair	-	48	57	63
	Good	-	30	41	48
Pinyon-juniper—pinyon, juniper, or both; grass understory.	Poor	-	75	85	89
	Fair	-	58	73	80
	Good	-	41	61	71
Sagebrush with a grassy understory.	Poor	-	67	80	85
	Fair	-	51	63	70
	Good	-	35	47	55
Desert shrub—major plants include saltbush, greasewood, creosote bush, black bush, bur sage, palo verde, mesquite, and cactus.	Poor	63	77	85	88
	Fair	55	72	81	86
	Good	49	68	79	84

B. SNOWMELT METHOD PARAMETER DEFINITIONS

- **PX temperature:** It is used to discriminate between precipitation falling as rain or snow. When the air temperature is less than the specified temperature, the precipitation is assumed to be in the form of snow, and when the air temperature is above the specified temperature, it is assumed to be in the form of rain. This discrimination temperature is usually one to two degrees above freezing temperature.
- **Base Temperature:** The difference between the base temperature and the air temperature defines the temperature index used in calculating the snowmelt. The meltrate is multiplied by the difference between the air temperature and the base temperature to estimate the snowmelt amount. If the air temperature is less than the base temperature, then the amount of melt is assumed to be zero. Typically, base temperature should be 0 °C or close to it.
- **Wet Meltrate:** This parameter is used during periods of precipitation when the precipitation is falling as rain, at rates the higher than the rain rate limit. It represents the rate at which snowpack melts when it is raining on the pack.
- **Rain Rate Limit:** Discriminates between dry and wet melt. The wet meltrate is applied as the meltrate when it is raining at rates higher than the rate limit. If the rain rate is less than the rate limit, the meltrate is computed as if there were no precipitation.
- **ATI-Meltrate Coefficient:** A meltrate must be calculated for time intervals when the precipitation rate is less than the rain rate limit. The calculation starts with the meltrate antecedent temperature index. A coefficient is used to update the antecedent meltrate index from one interval to the next. This index generally ranges from 0.015 to 0.550 and is separate from the cold content index. A typical value for the coefficient is 0.98.
- **ATI-Meltrate Function:** An antecedent temperature index meltrate function is used to calculate a meltrate from the current meltrate index. This function

should define appropriate meltrates to use over the range of meltrate index values that will be encountered during a simulation.

- **Meltrate Pattern:** a meltrate pattern may be specified that defines the percentage adjustment as a function of the time of year. If no meltrate pattern is selected, the meltrate will be computed only from the antecedent temperature index and the meltrate function.
- **Cold limit:** The cold limit amounts for the rapid changes in temperature that the snowpack undergoes during high precipitation rate. When the precipitation rate exceeds the specified cold limit, the antecedent cold content index is set to the temperature of the precipitation. If the temperature is above the base temperature, the cold content index is set to base temperature. If the temperature is below the base temperature, the cold content index is set to the actual temperature. If the precipitation rate is less than the cold limit, the cold content index is computed as the antecedent index. A typical value is 20 mm/day.
- **ATI-Meltrate Coefficient:** It is used to update the antecedent cold content index from one interval to the next. A typical value is 0.5.
- **ATI-Meltrate Function:** It is used to calculate a cold content from the current cold content index. A typical value ranges from 1.22 to 1.32 mm/°C-day.
- **Water Capacity:** It specifies the amount of melted water that must accumulate in the snowpack before liquid becomes available at the soil surface for infiltration or runoff. Typically, the maximum liquid water held in the snowpack is on the order of 3%-5% of the SWE.
- **Groundmelt:** Heat from the warm ground that is partially frozen or unfrozen can cause snowmelt. This process can be included by fix value or pattern.

Moreover, elevation bands of sub-basins and lapse rate are required for adjusting the temperature according to elevation bands which has default value of 6.5 °C per kilometer. Typically, elevation value can be specified for sub-basin by using the area-weighted elevation of the band or the average of the highest and lowest point in the

band. Also, initial SWE, initial cold content, initial liquid water, initial melt ATI, and initial cold content ATI for sub-basins should be included according to model run dates, which are defined in control specifications. Cold content represents the heat required to raise the temperature of the snow pack to 0°C. The liquid water which can occur in 0°C can be defined as 0 when no snowpack or temperature has been continually below freezing for several days. Initial ATI meltrate can be set to 0 in similar conditions, but otherwise, it must be calculated as the accumulation of degree-days since the last period of sustained air temperature below freezing. Initial cold content ATI is an index to the snow temperature near the surface of the snowpack, which should be set to the approximate snowpack temperature at the beginning of the simulation. It can also be set to 0 if the conditions are not known.

C. PREPROCESSING STEPS

Terrain Preprocessing

Hydrological models require DEM and its derivatives as input. The DEM of the study area (see Figure 4.1) is obtained from ASTER Global Digital Elevation Map with a resolution of 30 m, and it is used to find the direction and accumulation of flow, stream segmentation, catchment grid delineation, and drainage lines. The preprocessing tool of HEC-GeoHMS provides step-by-step commands to delineate the basin. These steps are explained in the following sections

Fill Sinks

This function fills the sinks in the DEM. If cells with higher elevation surround a cell, the water is trapped in that cell and cannot flow. The Fill Sinks function modifies the elevation to eliminate this problem. The role of Fill Sink command is described in Figure C.1. DEM of the study area after applying the Fill Sinks command in HEC-GeoHMS is illustrated in Figure C.2.

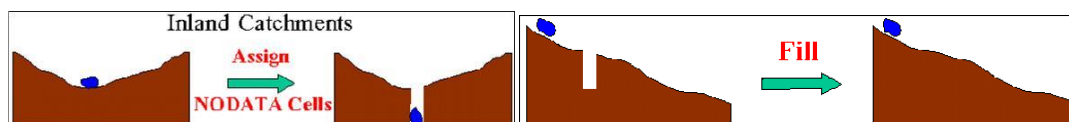


Figure C.1. Fill Sinks command in HEC-GeoHMS (USACE, 2013)

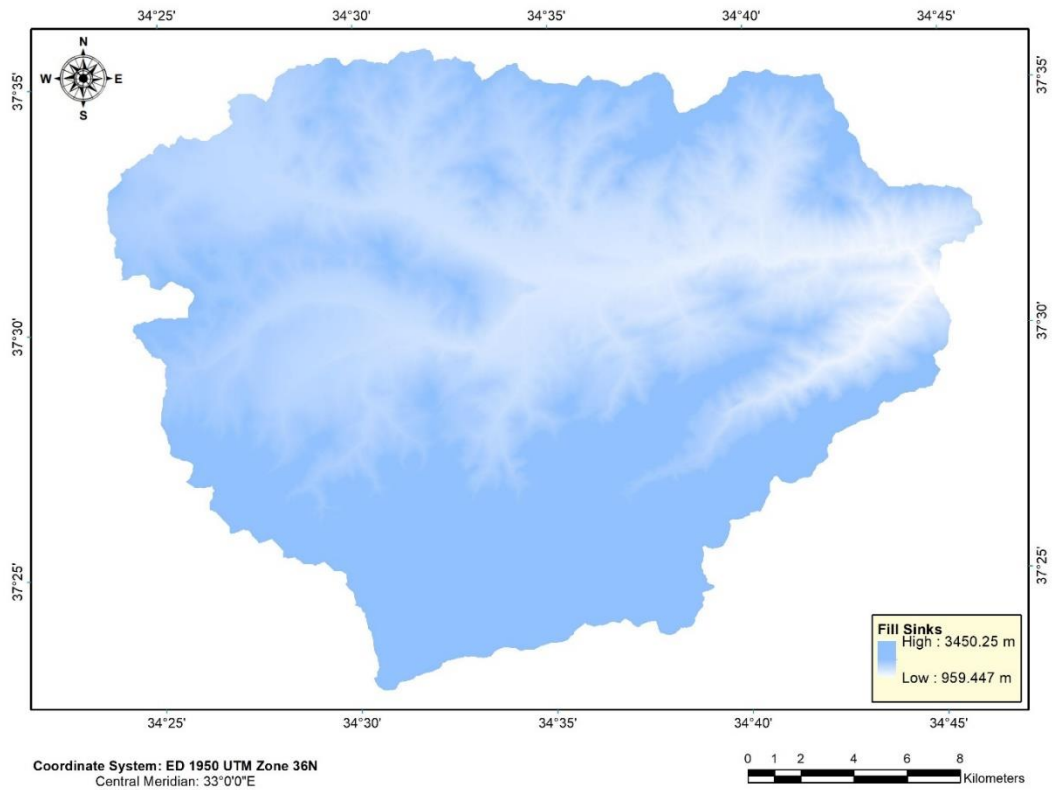
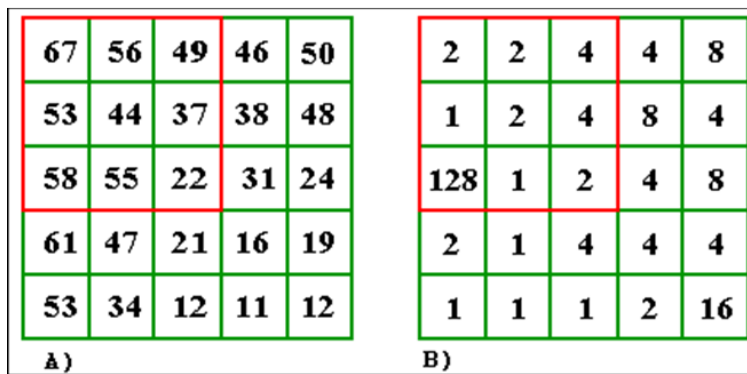


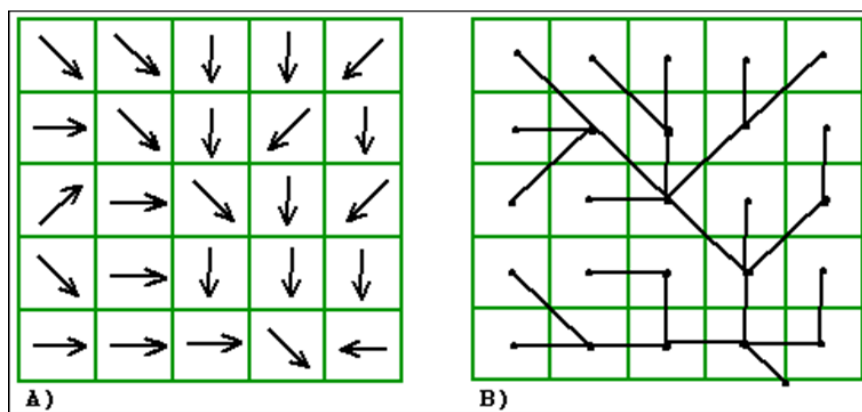
Figure C.2. DEM of the study area after applying the Fill Sinks command in HEC-GeoHMS

Flow Direction

The study area is divided into grids and Flow Direction function is used to determine the flow direction (i.e., flow direction from each grid). The values in the cells of the flow direction grid indicate the direction of the steepest descent from that cell. An example of a flow direction command is given in Figure C.3. The study area after applying the Flow Directions command in HEC-GeoHMS is illustrated in Figure C.4.



Grid Operations – A) DEM Grid; B) Flow Direction Grid



Physical Representation a Flow Direction Grid –A) with directional arrows; B) As a flow network

Figure C.3. Flow direction command in HEC-GeoHMS (USACE, 2013)

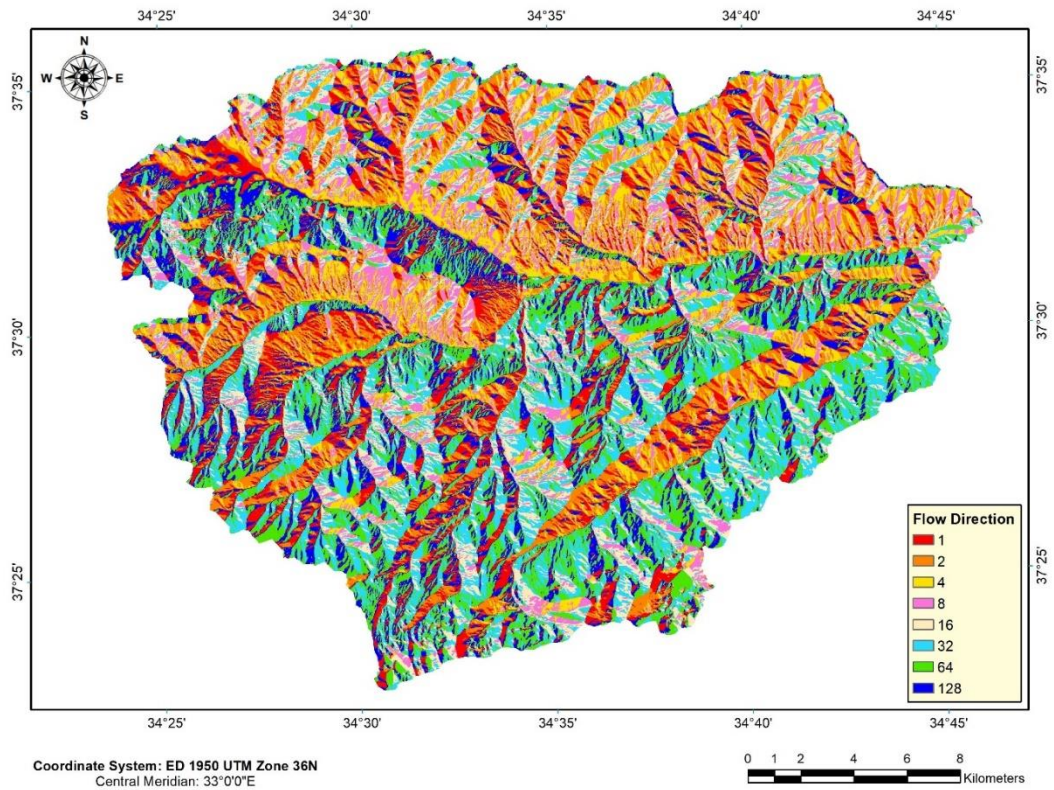
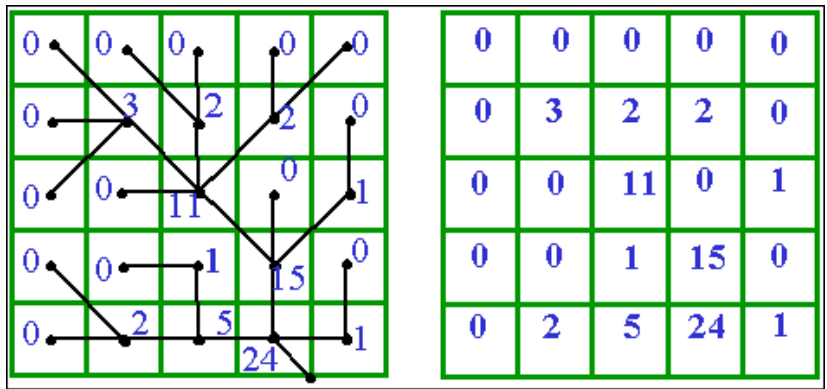


Figure C.4. The study area after applying the Flow Directions command in HEC-GeoHMS

Flow Accumulation

This step determines the number of upstream cells draining to a given cell. An example of Flow Accumulation command is given in Figure C.5. Study area after applying the Flow Accumulation command in HEC-GeoHMS is illustrated in Figure C.6.



Flow Accumulation – number of cells draining to a given cell along the flow network

Figure C.5. Flow accumulation command in HEC-GeoHMS (USACE, 2013)

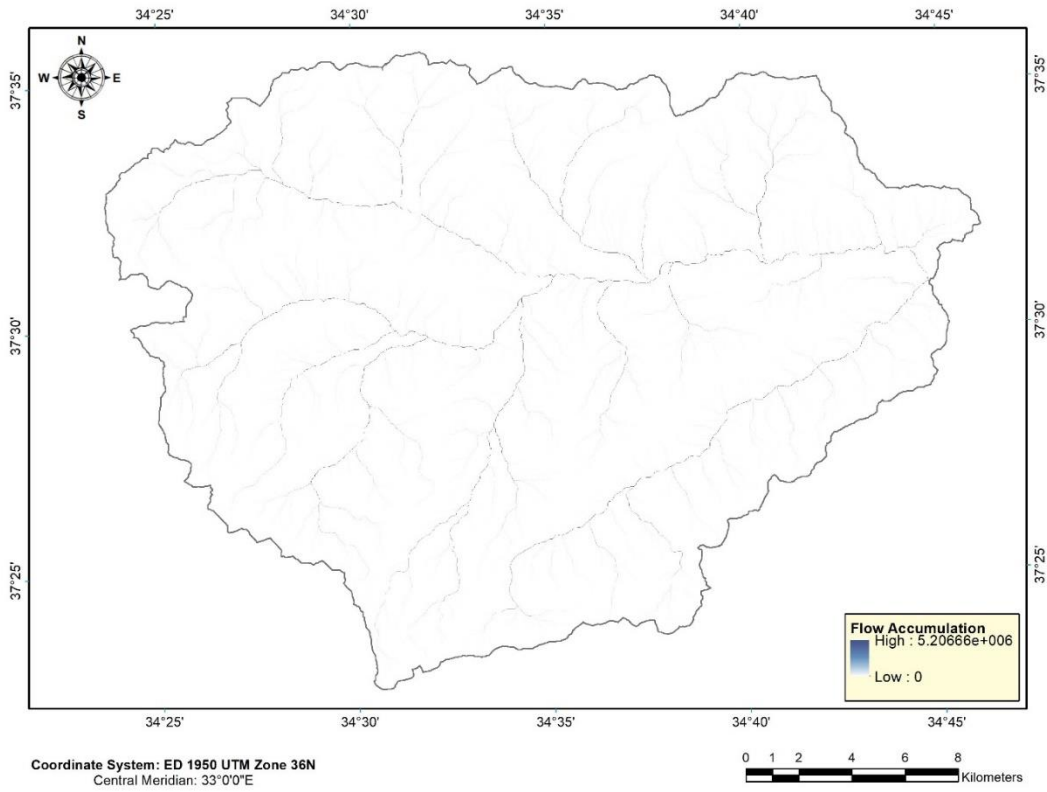
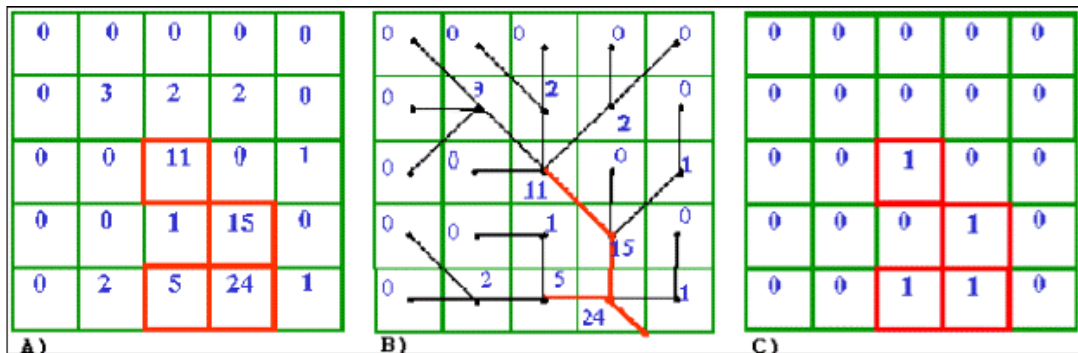


Figure C.6. The study area after applying the Flow Accumulation command in HEC-GeoHMS

Stream Definition

This command defines streams with a flow accumulation grid through the use of a threshold flow accumulation value. For example, if a value of five is set as the threshold, then any cell with a flow accumulation greater than five will be considered as a stream. This function computes a stream grid that contains a value of "1" for all the cells in the input flow accumulation grid that have a value higher than the given threshold. All other cells in the stream grid contain no data. An example of Stream Definition command is given in Figure C.7.



Stream Definition from the Flow Accumulation Grid and a threshold value – A) Grid cells with accumulation greater than or equal to 5 are considered stream cells (red); B) Streams identified on the flow network (red); C) Stream Grid

Figure C.7. Flow accumulation command in HEC-GeoHMS (USACE, 2013)

For the study area, a threshold of 25 km² is used. This value is selected according to the best reflection of observed water flows in the study area which is obtained through site studies conducted in TUBITAK Project 115Y041. Streams of the study area after applying the Stream Definition command in HEC-GeoHMS with a threshold of 25 km² is illustrated in Figure C.8.

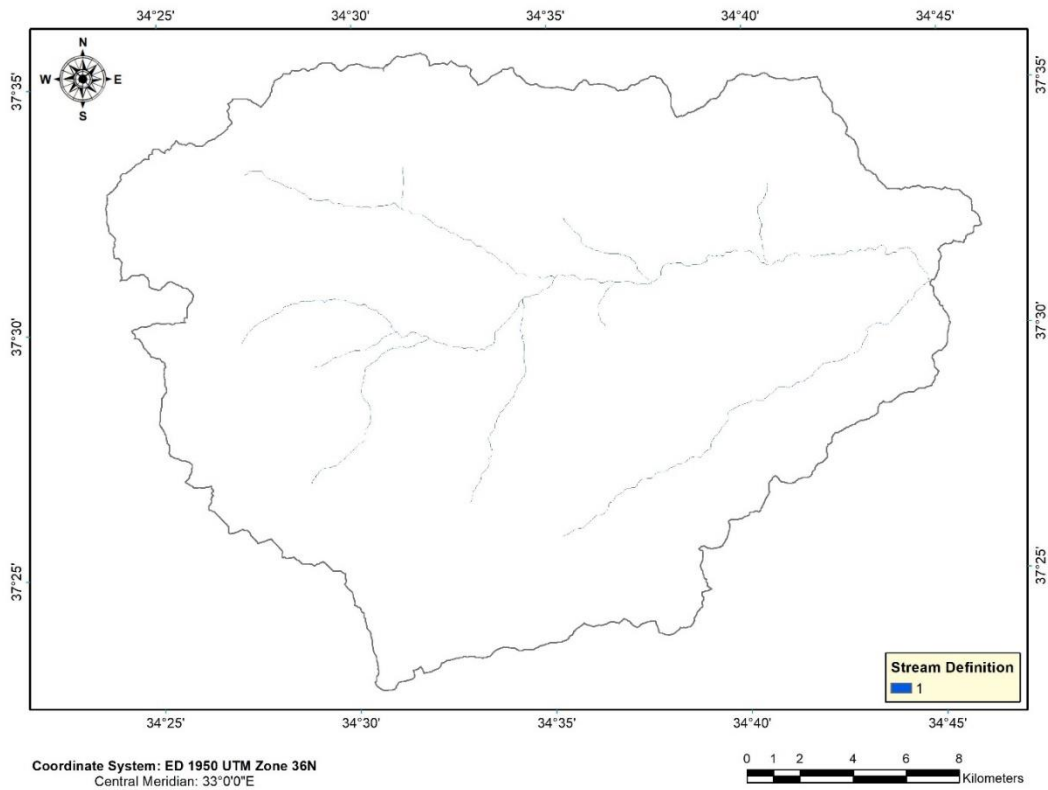
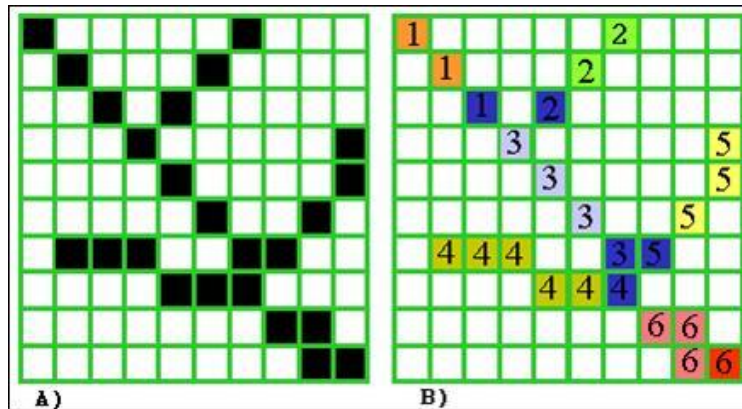


Figure C.8. Streams of the study area after applying the Stream Definition command in HEC-GeoHMS with a threshold of 25 km²

Stream Segmentation

This command is used to divide the stream network into distinct stream segments. Stream Segmentation breaks the waterway into stream segments that connect junctions to each other and to the outlets. This function creates a grid of stream segments that have a unique identification. An example of Stream Definition command is given in Figure C.9. Study area after applying Stream Segmentation command in HEC-GeoHMS is illustrated in Figure C.10.



Stream Links defined – A) Stream Grid representation, B) Stream Links (numbers) defined, link outlets (blue), watershed outlet (red)

Figure C.9. Stream Segmentation command in HEC-GeoHMS (USACE, 2013)

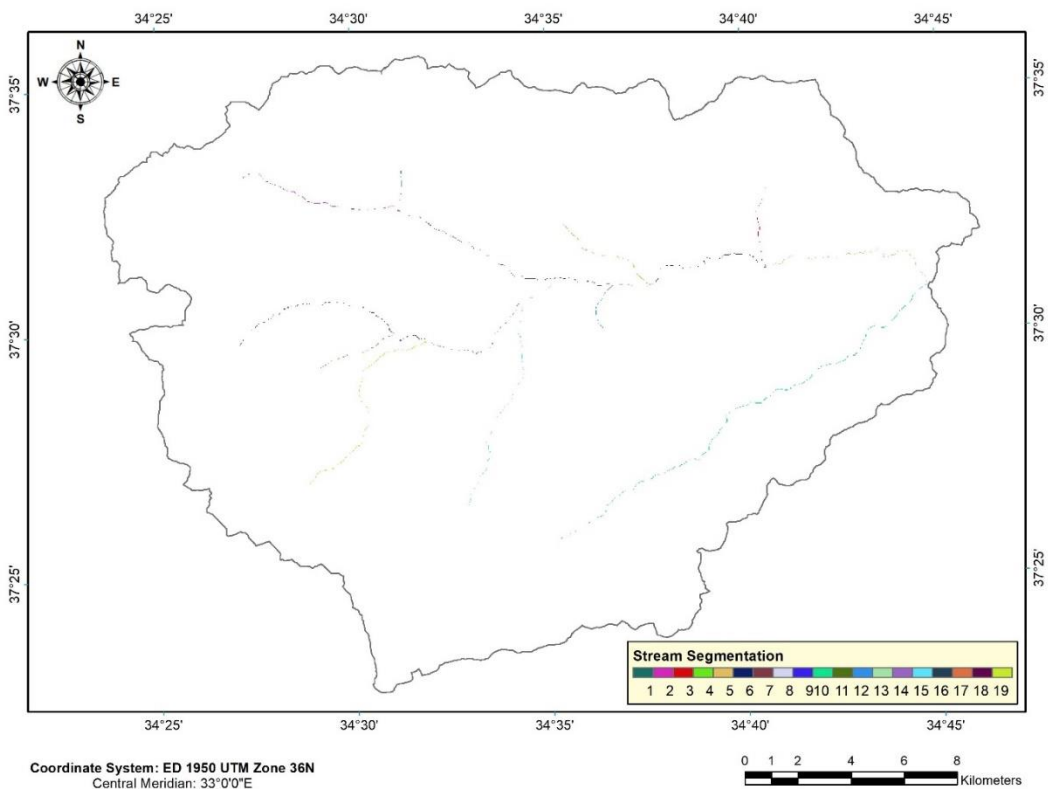


Figure C.10. The study area after applying Stream Segmentation command in HEC-GeoHMS

Catchment Grid Delineation

This command creates a grid in which each cell carries a value (grid code), indicating which catchment that cell belongs. The grid code corresponds to the value carried by the stream segment that drains that area, defined in the stream segment link grid. Study area after applying the Catchment Grid Delineation command in HEC-GeoHMS is illustrated in Figure C.11.

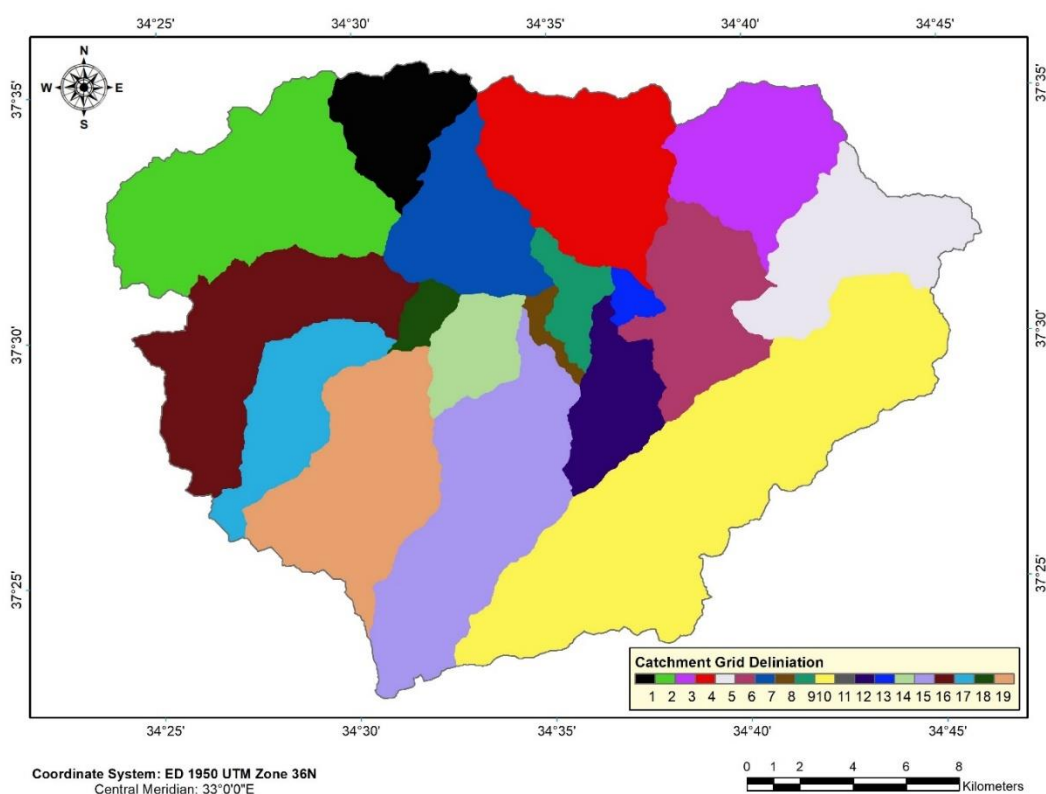


Figure C.11. The study area after applying the Catchment Grid Delineation command in HEC-GeoHMS

Catchment Polygon Processing

This command is for converting the raster data developed so far to vector format Study area after applying the Catchment Polygon Processing command in HEC-GeoHMS is illustrated in Figure C.12.

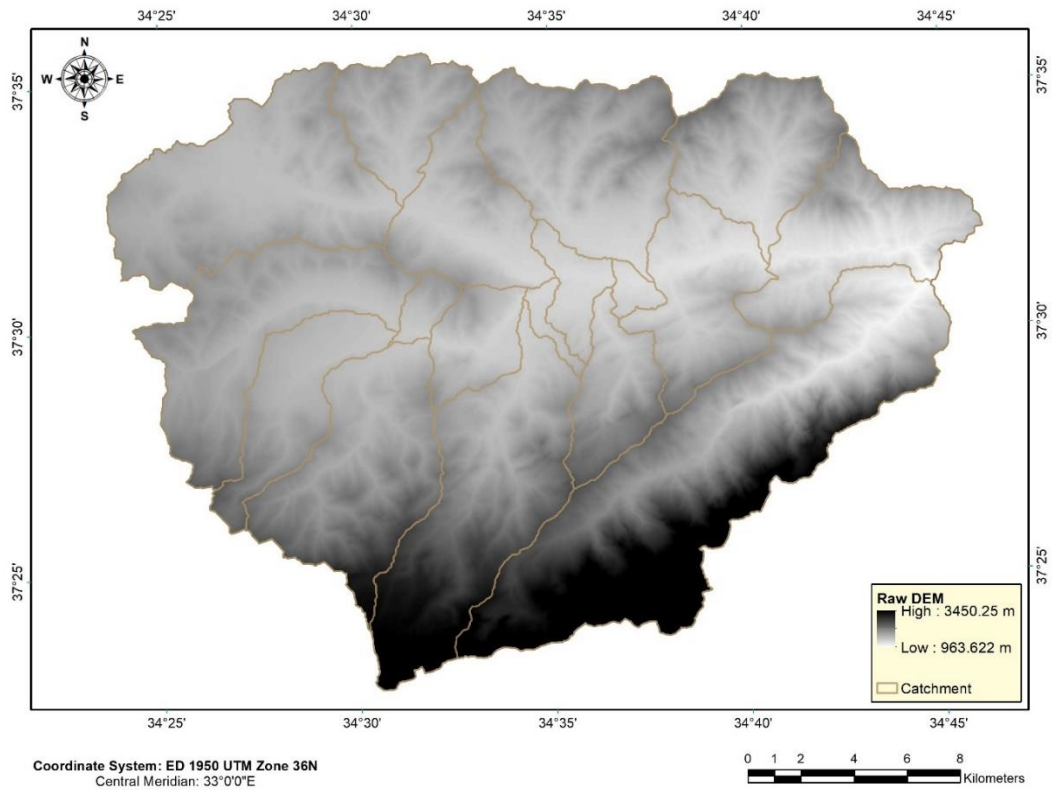


Figure C.12. The study area after applying the Catchment Polygon Processing command in HEC-GeoHMS

Drainage Line Processing

Drainage Line Processing converts the raster data for stream segments into a vector format. This command converts the input stream link grid into a “Drainage Line” feature class. Each line in the feature class carries the identifier of the catchment in which it resides. Study area after applying Drainage Line Processing command in HEC-GeoHMS is illustrated in Figure C.13.

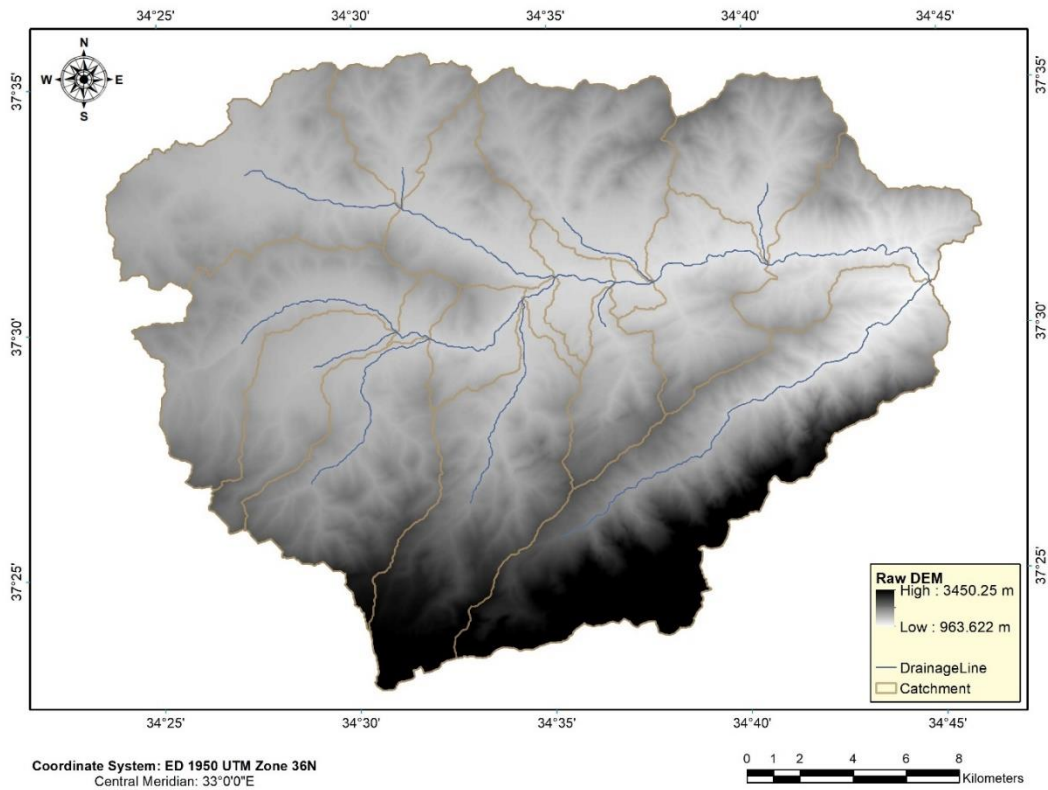


Figure C.13. The study area after applying Drainage Line Processing command in HEC-GeoHMS

Adjoint Catchment

This command generates the aggregated upstream catchments from the "Catchment" feature class. For each catchment that is not a head catchment, a polygon representing the whole upstream area draining to its inlet point is constructed and stored in a feature class that has an "Adjoint Catchment" tag. This feature class is used to speed up the point delineation process.

Drainage Point Processing

Drainage Point Processing calculates drainage outlets for each catchment. Study area after applying Drainage Point Processing command in HEC-GeoHMS is illustrated in Figure C.14.

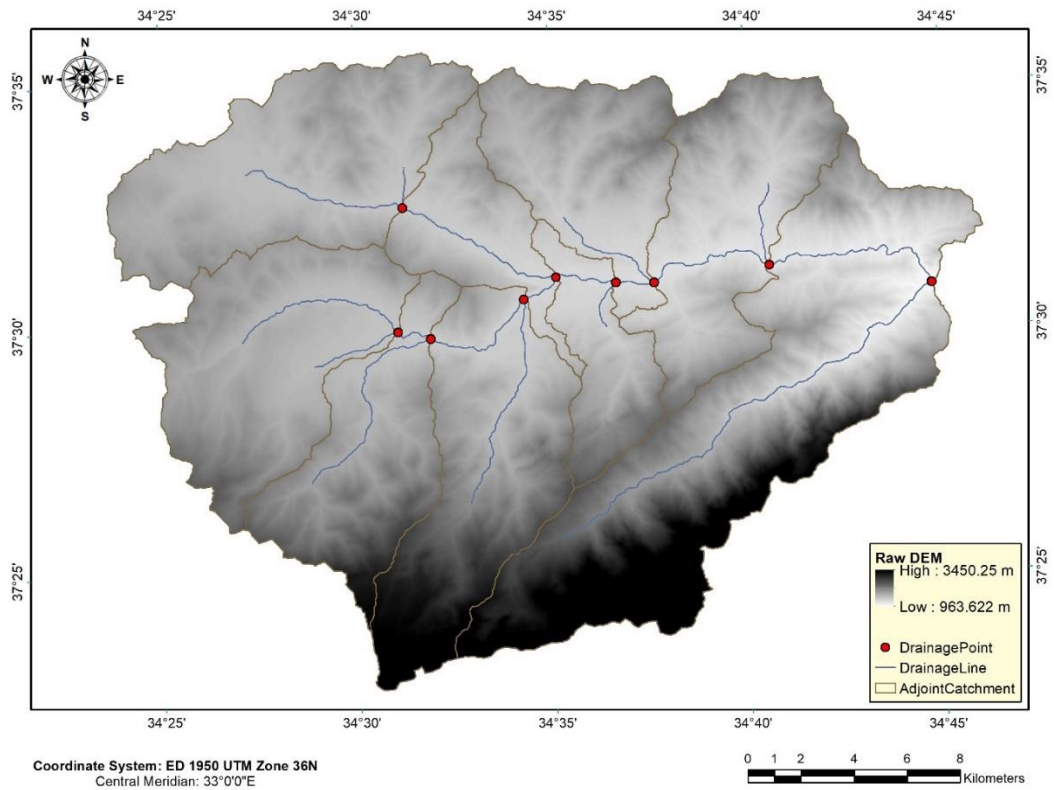


Figure C.14. The study area after applying Drainage Point Processing command in HEC-GeoHMS

Slope

This command allows generating a slope grid in percent or degree for a given DEM. Slope processing interpolates a slope grid that will be used for HEC-GeoHMS processing. Study area after applying Slope command is illustrated in Figure C.15.

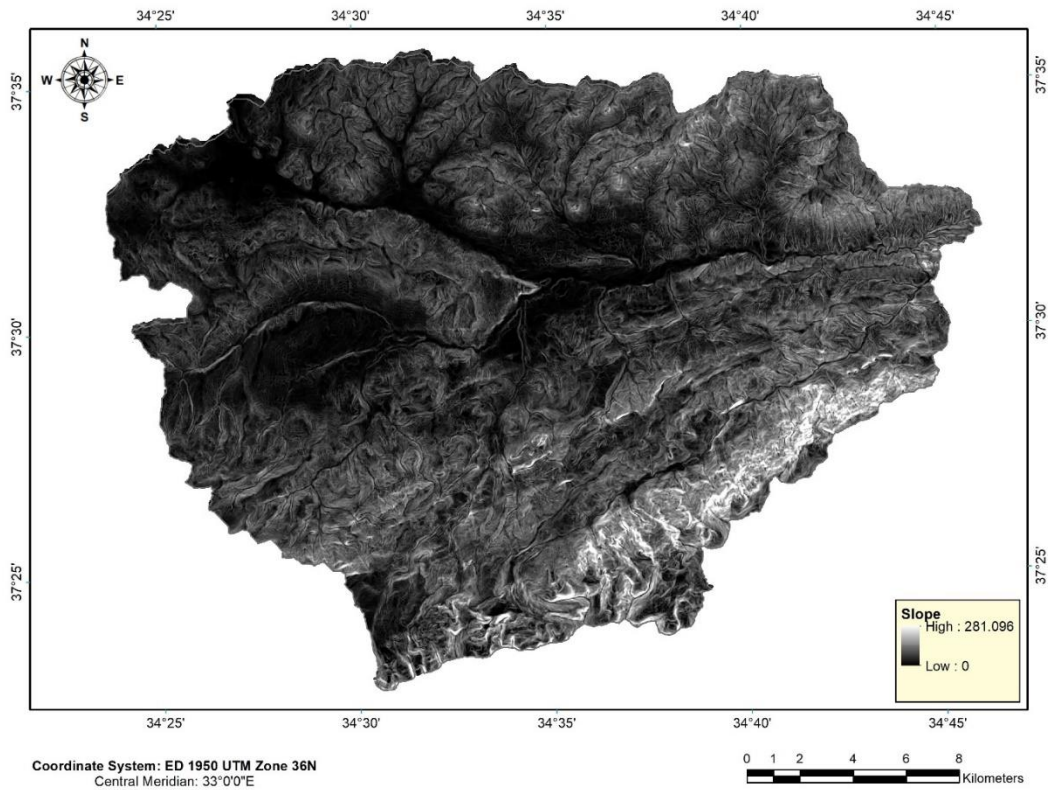


Figure C.15. The study area after applying Slope command in HEC-GeoHMS

Project Setup

The project setup tool of the HEC-GeoHMS is for creating a new project with preprocessed data. Inlet and outlet points are defined with this tool as well.

Basin Processing

Basin processing is a tool of the HEC-GeoHMS for modifying sub-basin delineations. By using Basin Processing commands, small subbasins can be merged, or large subbasin can be divided into smaller subbasins according to the purpose and characteristics of the basin. In this study, some subbasins are reshaped according to the locations of stream gauge stations. Reshaped subbasins of the study area are illustrated in Figure C.16, where changes are shown with red lines. After these

modifications' drainage area of Darboğaz SGS is reflected precisely according to sub-basin boundaries.

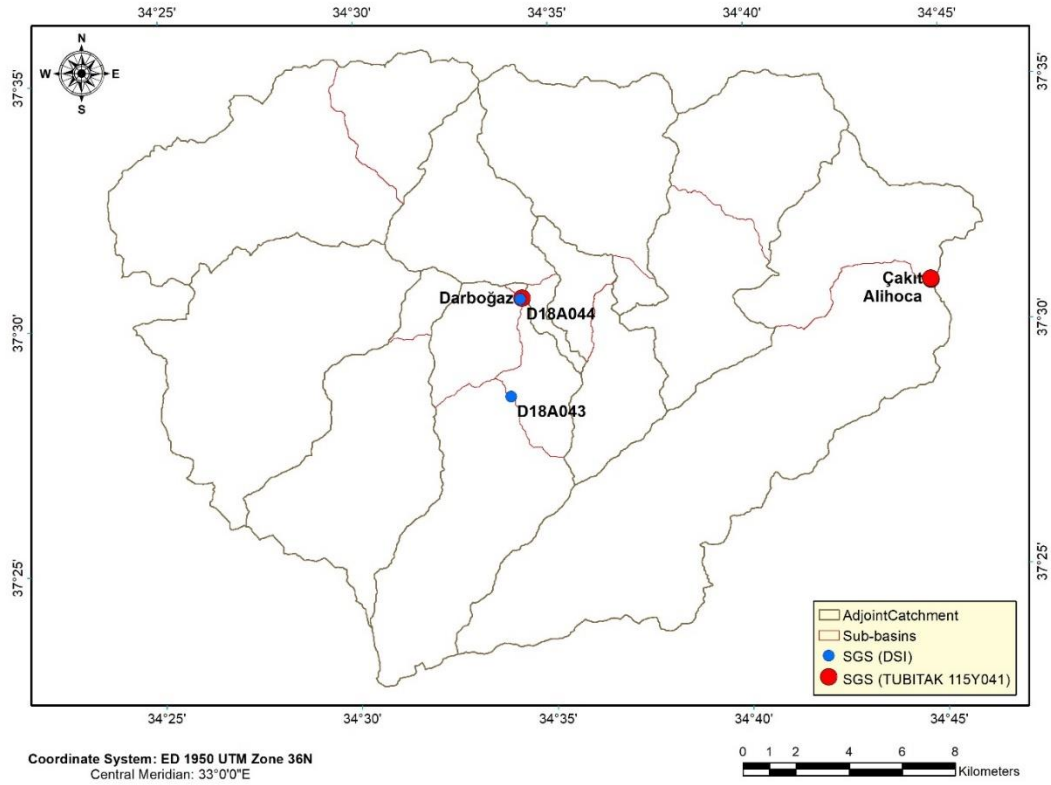


Figure C.16. The study area after applying Basin Processing commands in HEC-GeoHMS

Characteristics

The characteristics tool of the HEC-GeoHMS is for extracting the topographic characteristics of delineated streams and subbasins in order to be used in hydrological parameter calculations. River Length, River Slope, Basin Slope, Longest Flow Path, Basin Centroid, Centroid Elevation, and Centroidal Longest Flowpath commands are used for storing stream and sub-basin characteristics that are used for estimating hydrologic parameters, in attribute tables. Result of these commands for the study area is illustrated in Figure C.17.

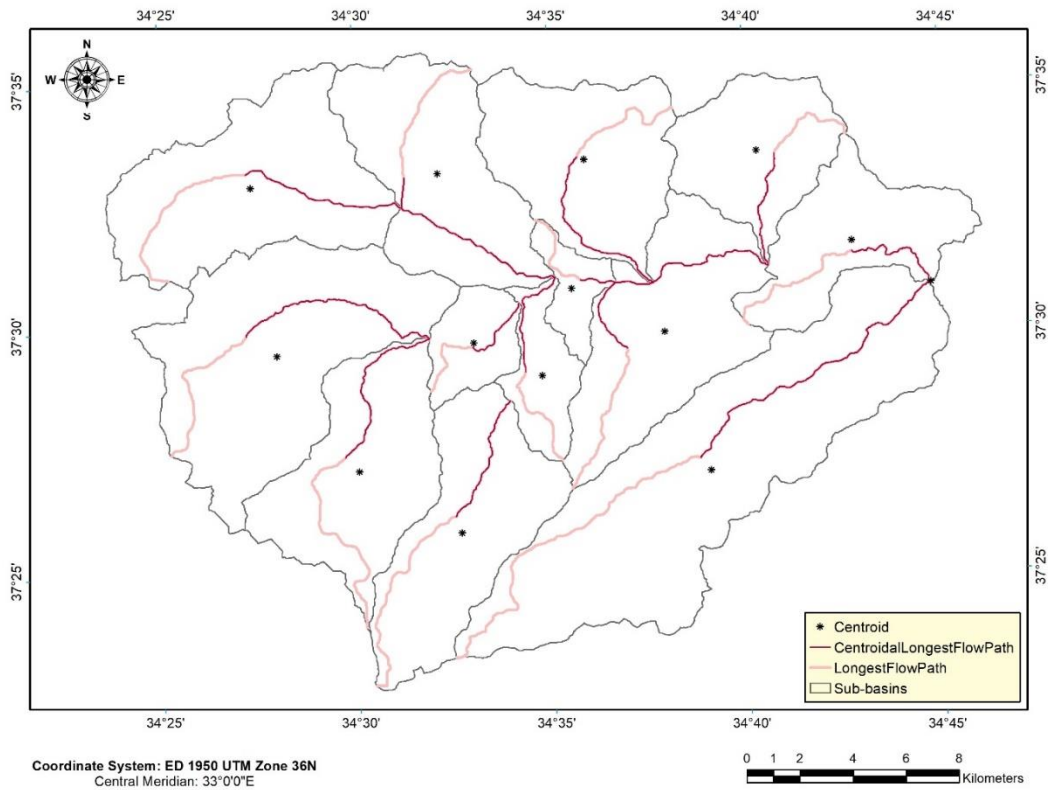


Figure C.17. The study area after applying Characteristic commands in HEC-GeoHMS

Parameters

Parameters tool of HEC-GeoHMS has commands for assigning particular names for rivers and sub-basins and for specifying HEC-HMS modelling methods. HMS Process Selection, River Auto Name, and Basin Auto Name commands are applied after the extraction of physical characteristics of streams and sub-basins with the characteristic's tools. Methods that are explained in HEC-HMS modelling section, are selected, and required inputs are added to the attribute tables. River and Basin Auto Name commands are used to allocate unique names and definitions for each sub-basin and river tributaries. Study area after applying these commands is illustrated in Figure C.18.

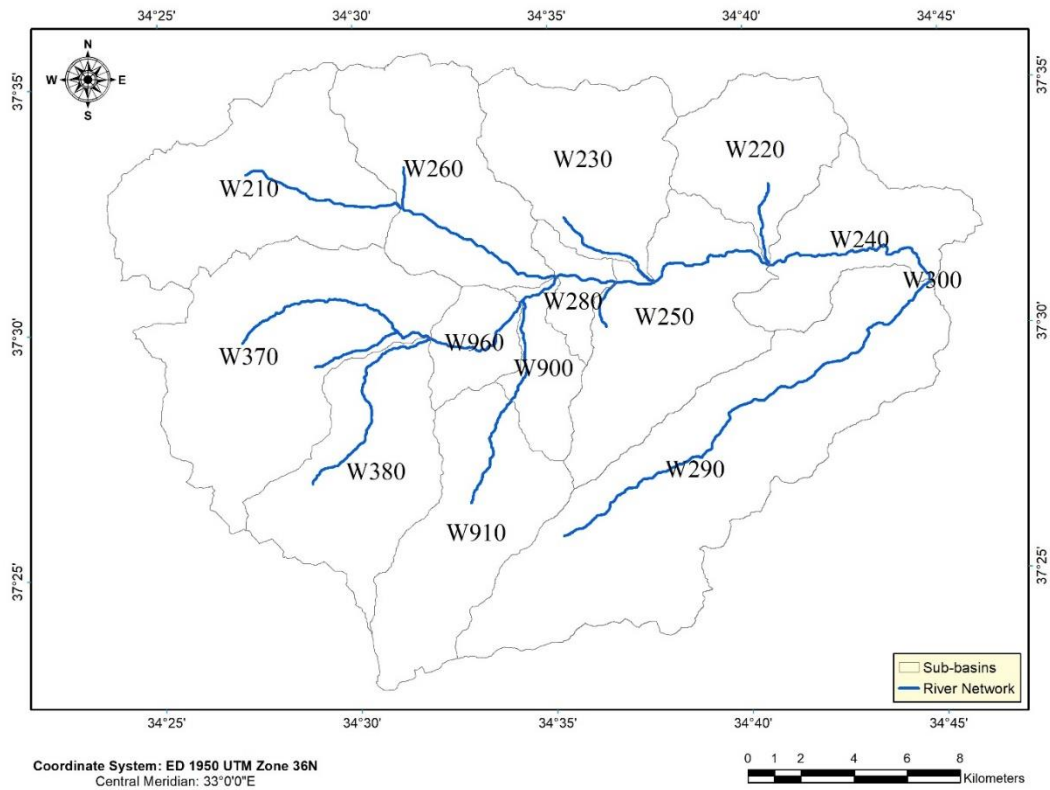


Figure C.18. The study area after applying Parameter commands in HEC-GeoHMS

Moreover, Sub-basin Parameters From Raster and Grid Cell Processing commands can be used according to the requirements of the selected method. In this study, the curve numbers are created with these commands.

HEC-HMS Transfer

The background shapefiles, basin model files, grid-cell parameter files, and meteorological model files are developed for transferring preprocessed data to HEC-HMS by using HEC-HMS toolbox of HEC-GeoHMS. In order to create necessary databases from preprocessed data, Map To HMS Units, Check Data, HMS Schematic, Add Coordinate, Prepare Data For Model, Background Shapefile, Basin Model File, and Met Model File commands are applied. As a result of these commands preprocessed basin becomes ready to be used in HEC-HMS.

Study area after preprocessing in HEC-GeoHMS is illustrated in Figure C.19. Finally, HEC-HMS project command is used for generating database file which is later used in HEC-HMS software for calibration and validation.

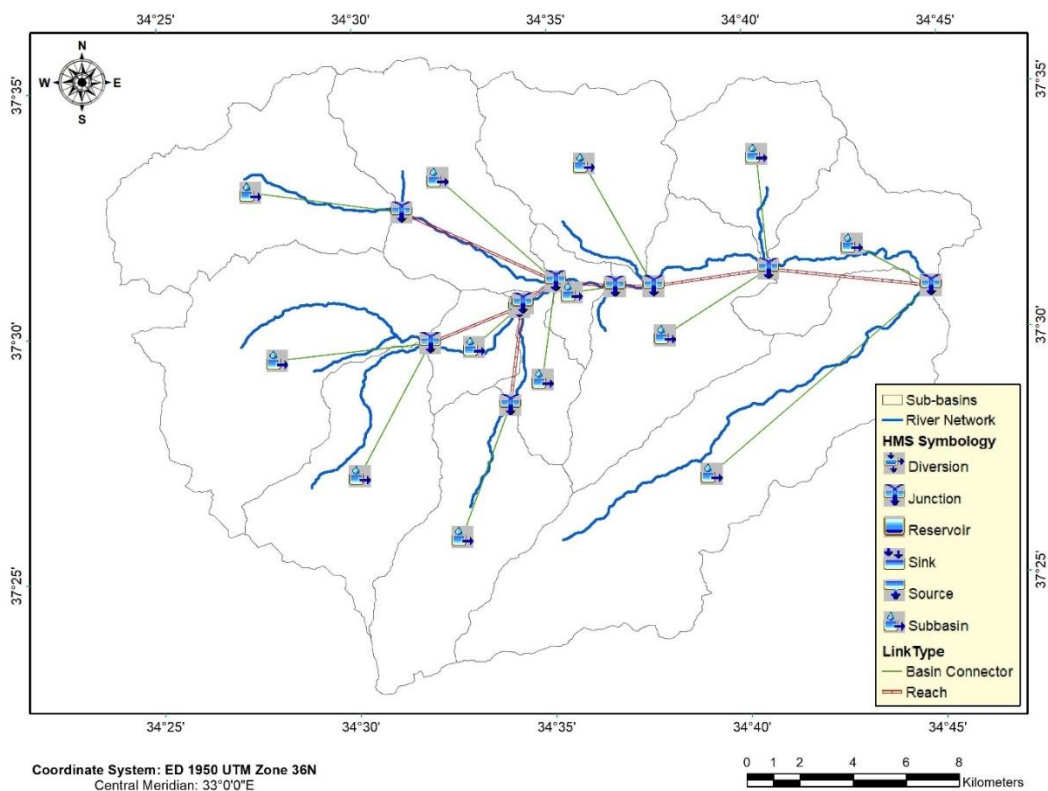


Figure C.19. The study area after preprocessing in HEC-GeoHMS